

A Appendix

I Atomic data

Section 2.1 deals with the analysis of absorbed spectra. For the investigation of this absorption, some atomic data is necessary, which is compiled in this section.

A more detailed list can be found in form of S-Lang data structures in the `atomicData`-feature of the module `lineProfile`, which is available online at <http://pulsar.sternwarte.uni-erlangen.de/hanke/diplomathesis/code/>.

I.1 Bound-free transition edge-energies and ISM abundances

Photoionization processes as described in Sect. 2.1.1 can only occur for photon-energies above the ionization threshold of the specific atom. The latter is listed for the first 30 elements in Table A I.1. The K-edge (ionization energy for a $1s$ electron) is given as well as both L-edges (L_1 for the ionization of a $2s$ electron, L_2 for a $2p$ electron). Not every element produces a strong photoabsorption edge, as the optical thickness depends also on the atomic abundance (cf. Eqs. 2.3 and 5.1). To find the astrophysically relevant atoms, the abundances in the interstellar medium (as well as the solar abundances for comparison) are also included:

Table A I.1: Neutral K- and L-edge energies and wavelengths (Verner & Yakovlev, 1995) and relative abundances A_Z^{ISM} in the interstellar medium (Wilms et al., 2000), compared with the solar abundances A_Z^{\odot} (reviewed by Asplund et al., 2005).

z (element)	${}_1\text{H}$	${}_2\text{He}$	${}_3\text{Li}$	${}_4\text{Be}$	${}_5\text{B}$	${}_6\text{C}$	${}_7\text{N}$	${}_8\text{O}$	${}_9\text{F}$	${}_{10}\text{Ne}$
E_K/keV	0.014	0.025	0.064	0.119	0.194	0.29	0.40	0.54	0.69	0.87
$\lambda_K/\text{\AA}$	912	504	193	104	63.9	42.6	30.6	23.0	17.9	14.25
E_{L_1}/keV			0.005	0.009	0.014	0.019	0.025	0.029	0.038	0.049
$\lambda_{L_1}/\text{\AA}$			2300	1330	882	639	488	435	327	256
E_{L_2}/keV					0.008	0.011	0.015		0.017	0.022
$\lambda_{L_2}/\text{\AA}$					1494	1101	853		712	575
$12 + \log A_Z^{\odot}$	12.0	10.93	1.05	1.38	2.70	8.39	7.78	8.66	4.56	7.84
$12 + \log A_Z^{\text{ISM}}$	12.0	10.99				8.38	7.88	8.69		7.94
$A_Z^{\text{ISM}}/A_{28}^{\text{ISM}}$	891 000	87 100				214	67.6	437		77.6

z (element)	${}_{11}\text{Na}$	${}_{12}\text{Mg}$	${}_{13}\text{Al}$	${}_{14}\text{Si}$	${}_{15}\text{P}$	${}_{16}\text{S}$	${}_{17}\text{Cl}$	${}_{18}\text{Ar}$	${}_{19}\text{K}$	${}_{20}\text{Ca}$
E_K/keV	1.08	1.31	1.57	1.85	2.15	2.48	2.83	3.20	3.61	4.04
$\lambda_K/\text{\AA}$	11.49	9.46	7.91	6.72	5.76	5.01	4.38	3.87	3.43	3.07
E_{L_1}/keV	0.071	0.094	0.126	0.156	0.194	0.235	0.278	0.326	0.384	0.443
$\lambda_{L_1}/\text{\AA}$	175	132	98.7	79.5	63.9	52.8	44.6	38.0	32.3	28.0
E_{L_2}/keV	0.038	0.055	0.080	0.106	0.140	0.170	0.209	0.249	0.301	0.352
$\lambda_{L_2}/\text{\AA}$	325	226	154	117	88.6	72.9	59.3	49.8	41.1	35.2
$12 + \log A_Z^{\odot}$	6.17	7.53	6.37	7.51	5.36	7.14	5.50	6.18	5.08	6.31
$12 + \log A_Z^{\text{ISM}}$	6.16	7.40	6.33	7.27	5.42	7.09	5.12	6.41		6.20
$A_Z^{\text{ISM}}/A_{28}^{\text{ISM}}$	1.29	22.4	1.91	16.6	0.234	11.0	0.117	2.29		1.41

z (element)	${}_{21}\text{Sc}$	${}_{22}\text{Ti}$	${}_{23}\text{V}$	${}_{24}\text{Cr}$	${}_{25}\text{Mn}$	${}_{26}\text{Fe}$	${}_{27}\text{Co}$	${}_{28}\text{Ni}$	${}_{29}\text{Cu}$	${}_{30}\text{Zn}$
E_K/keV	4.49	4.97	5.48	6.00	6.55	7.12	7.73	8.35	8.99	9.67
$\lambda_K/\text{\AA}$	2.76	2.49	2.27	2.07	1.89	1.74	1.60	1.49	1.38	1.28
E_{L_1}/keV	0.503	0.569	0.638	0.703	0.782	0.857	0.940	1.02	1.11	1.20
$\lambda_{L_1}/\text{\AA}$	24.6	21.8	19.43	17.64	15.86	14.47	13.19	12.11	11.21	10.31
E_{L_2}/keV	0.405	0.464	0.527	0.585	0.655	0.724	0.800	0.876	0.94	1.04
$\lambda_{L_2}/\text{\AA}$	30.6	26.7	23.5	21.2	18.92	17.13	15.50	14.15	13.09	11.96
$12 + \log A_Z^{\odot}$	3.05	4.90	4.00	5.64	5.39	7.45	4.92	6.23	4.21	4.60
$12 + \log A_Z^{\text{ISM}}$		4.81		5.51	5.34	7.43	4.92	6.05		
$A_Z^{\text{ISM}}/A_{28}^{\text{ISM}}$		0.0575		0.288	0.195	24.0	0.0741	1.00		

I.2 Bound-bound line-transition wavelengths

The identification of absorption lines requires a large database of transition wavelengths. This section quotes the most important lines, which were also used in this analysis. It can never be a replacement for the numerous complete tables: All quoted wavelengths are either from the atomic database ATOMDB (see also Table A I.7) or from the table of Verner et al. (1996), except of the Na x triplet, which was only found in Mewe et al. (1985).

H-like ions

The strongest lines of H-like ions belong to the Lyman series (Table A I.2). They are also most important in photoionized plasmas, as they start at the ground state. The energies are relatively large, the spin-orbit coupling is therefore usually not resolved – in contrast to the lines of the Balmer series (Table A I.2), which comprises the transitions from the first excited state ($n = 2$) with higher states, where the energy differences are more easily noticeable.

Table A I.2: Wavelengths [in Å] of H-like ions' transitions from the ground state $1s$ ($^2S_{1/2}$)

trans. $1s \rightarrow np$	name	O VIII	Ne X	Na XI	Mg XII	Al XIII	Si XIV	S XVI	Ar XVIII	Ca XX	Fe XXVI	Ni XXVIII
$1s \rightarrow 2p$	Ly α	18.97	12.13	10.03	8.42	7.17	6.18	4.73	3.73	3.02	1.78	1.53
$1s \rightarrow 3p$	Ly β	16.01	10.24	8.46	7.11	6.05	5.22	3.99	3.15	2.55	1.50	1.29
$1s \rightarrow 4p$	Ly γ	15.18	9.71	8.02	6.74	5.74	4.95	3.78	2.99	2.42	1.42	1.23
$1s \rightarrow 5p$	Ly δ	14.82	9.48	7.83	6.58	5.60	4.83	3.70	2.92	2.36	1.39	1.20

Table A I.3: Wavelengths [in Å] of H-like ions' transitions from the first excited state ($n = 2$)

transition	O VIII	Ne X	Na XI	Mg XII	Al XIII	Si XIV	S XVI	Ar XVIII	Ca XX	Fe XXVI	Ni XXVIII
$2s$ ($^2S_{1/2}$) $\rightarrow 3p$ ($^2P_{1/2}$)	102.40	65.49	45.44	33.35	25.51	20.13	16.28	9.58	8.25		
$2s$ ($^2S_{1/2}$) $\rightarrow 3p$ ($^2P_{3/2}$)	102.36	65.45	45.40	33.31	25.46	20.08	16.23	9.54	8.20		
$2p$ ($^2P_{1/2}$) $\rightarrow 3s$ ($^2S_{1/2}$)	102.39	65.49	45.44	33.35	25.50	20.12	16.27	9.58	8.25		
$2p$ ($^2P_{3/2}$) $\rightarrow 3s$ ($^2S_{1/2}$)	102.55	65.64	45.59	33.51	25.66	20.28	16.43	9.74	8.40		
$2s$ ($^2S_{1/2}$) $\rightarrow 4p$ ($^2P_{1/2}$)	75.86	48.52	33.66	24.71	18.90	14.91	12.06	7.10	6.11		
$2s$ ($^2S_{1/2}$) $\rightarrow 4p$ ($^2P_{3/2}$)	75.84	48.50	33.65	24.70	18.89	14.90	12.05	7.09	6.10		
$2p$ ($^2P_{1/2}$) $\rightarrow 4s$ ($^2S_{1/2}$)	75.85	48.51	33.66	24.71	18.89	14.91	12.06	7.10	6.11		
$2p$ ($^2P_{1/2}$) $\rightarrow 4s$ ($^2S_{1/2}$)	75.94	48.60	33.75	24.79	18.98	15.00	12.15	7.19	6.20		

He-like ions

As described in Sect. 2.1.2, He-like triplets – resonance (r), intercombination (i) and forbidden (f) line – can be very important for the diagnostics of an optically thin plasma. Table A I.4 lists their wavelengths. As the triplets connect, however, only $n = 1$ and $n = 2$ levels, see Table A I.5 for further transitions from the ground state $1s^2$ (1S_0) to $1s np$ (1P_1) states.

Table A I.4: Wavelengths [in Å] of He-like ions' triplet transitions (from the $1s^2$ (1S_0) state)

upper level	O VII	Ne IX	Na X	Mg XI	Al XII	Si XIII	S XV	Ar XVII	Ca XIX	Fe XXV	Ni XXVII
r $1s2p$ (1P_1)	21.60	13.45	11.00	9.17	7.76	6.65	5.04	3.95	3.18	1.85	1.59
i $1s2p$ ($^3P_{1,2}$)	21.80	13.55	11.08	9.23	7.80	6.69	5.07	3.97	3.19	1.86	1.60
f $1s2s$ (3S_1)	22.10	13.70	11.19	9.31	7.87	6.74	5.10	3.99	3.21	1.87	

Table A I.5: Wavelengths [in Å] of He-like ions' transitions from the $1s^2$ (1S_0) ground state

upper level	O VII	Ne IX	Na X	Mg XI	Al XII	Si XIII	S XV	Ar XVII	Ca XIX	Fe XXV	Ni XXVII
$1s2p$ (1P_1)	21.60	13.45	11.00	9.17	7.76	6.65	5.04	3.95	3.18	1.85	1.59
$1s3p$ (1P_1)	18.63	11.54	9.43	7.85	6.63	5.68	4.30	3.37	2.71	1.57	1.35
$1s4p$ (1P_1)	17.77	11.00	8.98	7.47	6.31	5.40	4.09	3.20	2.57	1.50	1.28
$1s5p$ (1P_1)	17.40	10.77	8.79	7.31	6.18	5.29	4.00	3.13	2.51	1.46	1.25
$1s6p$ (1P_1)	17.20	10.64	8.69	7.22	6.10	5.22	3.95	3.10			
$1s7p$ (1P_1)	17.09	10.57	8.63	7.17	6.06	5.19	3.92				
$1s8p$ (1P_1)	17.01	10.51	8.59	7.14	6.03	5.16	3.90				

Li-like ions

The ground state of the alkali metal Lithium is $[1s^2] 2s (^2S_{1/2})$. The strongest transitions lead therefore (similar to the Balmer series) to $[1s^2] np (^2P)$ states. Table A I.6 lists the wavelength of these transitions and includes in case of $n = 3$ both the $^2P_{1/2}$ and the $^2P_{3/2}$ state, as the difference due to spin-orbit coupling might be resolvable.

Table A I.6: Wavelengths [in Å] of Li-like ions' transitions from the ground state $[1s^2] 2s (^2S_{1/2})$

upper level	O VI	Ne VIII	Na IX	Mg X	Al XI	Si XII	S XIV	Ar XVI	Ca XVIII	Fe XXIV	Ni XXVI
$[1s^2] 3p (^2P_{1/2})$	150.09	88.08	70.65	57.88	48.34	40.95	30.47	23.59	18.73	10.66	9.10
$[1s^2] 3p (^2P_{3/2})$	150.12	88.12	70.61	57.92	48.30	40.91	30.43	23.55	18.69	10.62	9.06
$[1s^2] 4p$	115.8	67.4	53.9	44.1	36.7	31.0	23.0	17.74	14.09	8.00	6.82
$[1s^2] 5p$	104.8	60.8	48.6	39.7	33.0	27.9	20.7	15.93	12.64	7.17	6.11
$[1s^2] 6p$									11.99	6.79	
$[1s^2] 7p$									11.62		

Level numbers in the ATOMDB

For convenient access the atomic database ATOMDB, e.g., via the `trans(Z,ion,up,low)`-function¹ in ISIS or the web-guide (<http://cxc.harvard.edu/atomdb/WebGUIDE/>), the meaning of the level numbers for H-like, He-like and Li-like ions have been compiled in Table A I.7.

Table A I.7: Quantum states assigned to the first 25 level numbers in the ATOMDB

level #	H-like	He-like	Li-like
25	$5g (^2G_{9/2})$	$1s4d (^3D_2)$	$[1s^2] 6s (^2S_{1/2})$
24	$5g (^2G_{7/2})$	$1s4d (^3D_1)$	$[1s^2] 5g (^2G_{9/2})$
23	$5f (^2F_{7/2})$	$1s4p (^1P_1)$	$[1s^2] 5g (^2G_{7/2})$
22	$5f (^2F_{5/2})$	$1s4p (^3P_2)$	$[1s^2] 5f (^2F_{7/2})$
21	$5d (^2D_{3/2})$	$1s4p (^3P_1)$	$[1s^2] 5f (^2F_{7/2})$
20	$5d (^2D_{3/2})$	$1s4p (^3P_0)$	$[1s^2] 5d (^2D_{5/2})$
19	$5p (^2P_{3/2})$	$1s4s (^1S_0)$	$[1s^2] 5d (^2D_{3/2})$
18	$5p (^2P_{1/2})$	$1s4s (^3S_1)$	$[1s^2] 5p (^2P_{3/2})$
17	$5s (^2S_{1/2})$	$1s3d (^1D_2)$	$[1s^2] 5p (^2P_{1/2})$
16	$4f (^2F_{7/2})$	$1s3d (^3D_3)$	$[1s^2] 5s (^2S_{1/2})$
15	$4f (^2F_{5/2})$	$1s3d (^3D_2)$	$[1s^2] 4f (^2F_{7/2})$
14	$4d (^2D_{5/2})$	$1s3d (^3D_1)$	$[1s^2] 4f (^2F_{5/2})$
13	$4d (^2D_{3/2})$	$1s3p (^1P_1)$	$[1s^2] 4d (^2D_{5/2})$
12	$4p (^2P_{3/2})$	$1s3p (^3P_2)$	$[1s^2] 4d (^2D_{3/2})$
11	$4p (^2P_{1/2})$	$1s3p (^3P_1)$	$[1s^2] 4p (^2P_{3/2})$
10	$4s (^2S_{1/2})$	$1s3p (^3P_0)$	$[1s^2] 4p (^2P_{1/2})$
9	$3d (^2D_{5/2})$	$1s3s (^1S_0)$	$[1s^2] 4s (^2S_{1/2})$
8	$3d (^2D_{3/2})$	$1s3s (^3S_1)$	$[1s^2] 3d (^2D_{5/2})$
7	$3p (^2P_{3/2})$	$1s2p (^1P_1)$	$[1s^2] 3d (^2D_{3/2})$
6	$3p (^2P_{1/2})$	$1s2p (^3P_2)$	$[1s^2] 3p (^2P_{3/2})$
5	$3s (^2S_{1/2})$	$1s2p (^3P_1)$	$[1s^2] 3p (^2P_{1/2})$
4	$2p (^2P_{3/2})$	$1s2p (^3P_0)$	$[1s^2] 3s (^2S_{1/2})$
3	$2p (^2P_{1/2})$	$1s2s (^1S_0)$	$[1s^2] 2p (^2P_{3/2})$
2	$2s (^2S_{1/2})$	$1s2s (^3S_1)$	$[1s^2] 2p (^2P_{1/2})$
1	$1s (^2S_{1/2})$	$1s^2 (^1S_0)$	$[1s^2] 2s (^2S_{1/2})$

¹ The function `trans` returns a boolean array telling for every line-id whether the transition matches or not. The list of matching line-ids can be obtained by `where(trans(Z,ion,up,low))`.

Further iron ions

Continuing with further less-ionized ions of all atoms is not useful due to the limited energy-range and resolution of a *Chandra/HETGS* observation. Therefore, only further iron ions will be discussed in the rest of this section. The excitation of Be-like and B-like ions can, to some extent, still be treated in a systematic way similar to the series as above for very highly ionized ions. This is, however, hardly possible for the overwhelming number of L-shell transitions of lower ionized iron in the range between $\approx 7\text{\AA}$ and $\approx 17\text{\AA}$. Therefore, the following tables only present the strongest transitions, which is even not well defined, as several weaker transitions blend in many cases and may thus effectively again produce stronger features.

Table A I.8: Further iron lines

The quoted wavelengths rely on the ATOMDB, as the table of Verner et al. (1996) is not complete and its combination of several transitions into multiplets is not so clear.

(a) Fe xxIII (Be-like ion)			(b) Fe xxII (B-like ion)		
transition from	#	λ	transition from	#	λ
$[1s^2] 2s^2 ({}^1S_0)$	1	[{\AA}]	$[1s^2 2s^2] 2p ({}^2P_{1/2})$	1	[{\AA}]
$\rightarrow [1s^2] 2s3p ({}^1P_1)$	15	10.98	$\rightarrow [1s^2 2s^2] 3s ({}^2S_{1/2})$	16	12.25
$\rightarrow [1s^2] 2s4p ({}^1P_1)$	52	8.30	$\rightarrow [1s^2 2s^2] 4s ({}^2S_{1/2})$	69	9.06
$\rightarrow [1s^2] 2s5p ({}^1P_1)$	104	7.47	$\rightarrow [1s^2 2s^2] 5s ({}^2S_{1/2})$	148	8.11
$\rightarrow [1s^2] 2s3p ({}^3P_1)$	13	11.02	$\rightarrow [1s^2 2s^2] 3d ({}^2D_{3/2})$	21	11.77
$\rightarrow [1s^2] 2s4p ({}^3P_1)$	50	8.32	$\rightarrow [1s^2 2s^2] 4d ({}^2D_{3/2})$	72	8.97
			$\rightarrow [1s^2 2s^2] 5d ({}^2D_{3/2})$	151	8.09
			$\rightarrow [1s^2] 2s2p 3p_{3/2}$	30	11.49
			$\rightarrow [1s^2] 2s2p 3p_{3/2}$	32	11.43

(c) Fe xxI (C-like ion)			
transition from	#	λ	A
$[1s^2 2s^2] 2p^2 ({}^3P_0)$	1	[{\AA}]	[$10^{12}/\text{s}$]
$\rightarrow [1s^2 2s^2] 2p 3d ({}^3D_0)$	40	12.28	18.2
$\rightarrow [1s^2] 2s 2p_{1/2} {}^2 3p_{3/2}$	58	11.97	3.09
$\rightarrow [1s^2] 2s 2p_{1/2} 2p_{3/2} 3p_{3/2}$	60	11.95	1.82
$\rightarrow [1s^2 2s^2] 2p 4d ({}^3P_1)$	248	9.48	6.12
$\rightarrow [1s^2] 2s 2p_{1/2} {}^2 4p_{3/2}$	283	9.19	2.88
$\rightarrow [1s^2 2s^2] 2p 5d_{3/2}$	460	8.57	2.85

(d) Fe xx (N-like ion)			
transition from	#	λ	A
$[1s^2 2s^2] 2p^3 ({}^4S_{3/2})$	1	[{\AA}]	[$10^{12}/\text{s}$]
$\rightarrow [1s^2 2s^2] 2p^2 3s ({}^4P_{1/2})$	16	13.96	1.19
$\rightarrow [1s^2 2s^2] 2p^2 3s ({}^4P_{3/2})$	17	13.84	1.00
$\rightarrow [1s^2 2s^2] 2p^2 3s ({}^4P_{5/2})$	19	13.77	1.02
	42	13.06	2.62
	45	12.99	2.01
	47,48	12.97...12.96	0.66 + 3.46
$\rightarrow [1s^2 2s^2] 2p^2 3d (\dots)$	50,51	12.92...12.91	0.74 + 4.91
	56,58	12.86...12.85	12.1 + 19.2
	59,60	12.83...12.82	4.90 + 17.1
	62,63	12.76...12.75	0.25 + 1.44
$\rightarrow [1s^2] 2s 2p^3 3p (\dots)$	72,73	12.58	1.44 + 4.39
	75	12.53	4.23
	285,286	10.13...10.12	0.39 + 2.12
$\rightarrow [1s^2 2s^2] 2p^2 4d (\dots)$	297,299–302	10.04...10.06	1.16 + 0.48 + 2.80 + 0.64 + 0.63
	305,306,309,313	9.99...10.01	3.01 + 5.80 + 6.56 + 0.81
$\rightarrow [1s^2] 2s 2p^3 4p (\dots)$	363,364,365	9.73...9.72	2.42 + 2.42 + 2.47
	518,526	9.20...9.19	1.04 + 1.43
$\rightarrow [1s^2 2s^2] 2p^2 5d (\dots)$	555,556,559,564	9.11...9.10	0.67 + 0.29 + 1.46 + 0.36
	590,592,594	9.07...9.06	1.16 + 2.51 + 3.21
$\rightarrow \dots$	700–702	8.82	1.07 + 1.27 + 1.37

Table A I.8b includes only the strongest transitions of Fe XXII with $A > 5 \times 10^{12}/\text{s}$. Table A I.8e lists the strongest ($A > 5 \times 10^{12}/\text{s}$) lines of Fe XIX and Table A I.8f lists all lines of Fe XVIII with $A > 9 \times 10^{11}/\text{s}$.

(e) Fe XIX (O-like ion)			
transition from [1s ² 2s ²] 2p ⁴ (3P ₂)	# 1	λ [Å]	A [10 ¹² /s]
$\rightarrow [1s^2 2s^2] 2p_{1/2} 2p_{3/2}^2 3d_{5/2}$	53	13.79	5.35
$\rightarrow [1s^2 2s^2] 2p^3 (2D) 3d ({}^3F_3)$	57	13.64	2.43
$\rightarrow [1s^2 2s^2] 2p^3 3d_{5/2}$	65,67	13.55	4.44 + 2.25
$\rightarrow [1s^2 2s^2] 2p^3 (2D) 3d ({}^3D_3)$	68	13.52	18.7
$\rightarrow [1s^2 2s^2] 2p_{1/2} 2p_{3/2}^2 3d_{3/2}$	71	13.50	12.9
$\rightarrow [1s^2 2s^2] 2p^3 (2D) 3d ({}^3S_1)$	74	13.46	14.1
$\rightarrow [1s^2 2s^2] 2p^3 (2D) 3d ({}^1F_3)$	76	13.42	5.01
$\rightarrow [1s^2] 2s 2p_{1/2} 2p_{3/2}^3 3p_{3/2}$	104	12.95	3.11
$\rightarrow [1s^2] 2s 2p_{1/2}^2 2p_{3/2}^2 3p_{3/2}$	106	12.93	3.37
$\rightarrow [1s^2 2s^2] 2p^3 ({}^4S) 4d ({}^3D_3)$	243	10.82	5.65
$\rightarrow [1s^2 2s^2] 2p^3 (2D) 4d ({}^3F_3)$	276	10.68	2.28
$\rightarrow [1s^2 2s^2] 2p^3 (2D) 4d ({}^3D_3)$	286	10.65	3.74
$\rightarrow [1s^2 2s^2] 2p^3 (2D) 4d ({}^3P_2)$	288	10.64	5.20
$\rightarrow [1s^2 2s^2] 2p^3 (2D) 4d ({}^3S_1)$	292	10.63	4.78
$\rightarrow [1s^2 2s^2] 2p^3 ({}^4S) 5d ({}^3D_3)$	432	9.86	3.59
$\rightarrow [1s^2 2s^2] 2p_{1/2} 2p_{3/2}^2 5d_{3/2}$	532,536	9.69	2.56 + 2.18

(f) Fe XVIII (F-like ion)			
transition from [1s ² 2s ²] 2p ⁵ (2P _{3/2})	# 1	λ [Å]	A [10 ¹² /s]
$\rightarrow [1s^2 2s^2] 2p^4 ({}^3P) 3s ({}^2P_{3/2})$	5	16.00	1.36
$\rightarrow [1s^2 2s^2] 2p^4 ({}^3P) 3s ({}^2P_{1/2})$	8	15.76	1.06
$\rightarrow [1s^2 2s^2] 2p^4 ({}^3P) 3d ({}^4P_{1/2})$	39	14.60	2.50
$\rightarrow [1s^2 2s^2] 2p^4 ({}^3P) 3d ({}^4P_{3/2})$	40	14.57	3.09
$\rightarrow [1s^2 2s^2] 2p^4 ({}^3P) 3d ({}^2F_{5/2})$	41	14.53	4.05
$\rightarrow [1s^2 2s^2] 2p^4 ({}^3P) 3d ({}^2D_{5/2})$	49	14.37	6.75
$\rightarrow [1s^2 2s^2] 2p^4 ({}^1D) 3d (\dots)$	52,53	14.26	12.9 + 1.29
$\rightarrow [1s^2 2s^2] 2p^4 3d (\dots)$	55,56	14.21	17.9 + 19.4
$\rightarrow [1s^2 2s^2] 2p^4 ({}^1D) 3d ({}^2D_{3/2})$	57	14.16	4.03
$\rightarrow [1s^2 2s^2] 2p^4 ({}^1D) 3d ({}^2P_{1/2})$	58	14.14	4.57
$\rightarrow [1s^2 2s^2] 2p^4 ({}^1S) 3d ({}^2D_{5/2})$	59	13.95	1.04
$\rightarrow [1s^2] 2s 2p_{1/2}^2 2p_{3/2}^3 3p_{3/2}$	69	13.41	1.09
$\rightarrow [1s^2 2s^2] 2p^5 ({}^3P) 3p ({}^2D_{5/2})$	70	13.39	1.64
$\rightarrow [1s^2 2s^2] 2p^5 ({}^3P) 3p ({}^2P_{3/2})$	72	13.36	2.31
$\rightarrow [1s^2] 2s 2p_{1/2} 2p_{3/2}^4 3p (\dots)$	73,74	13.32	3.59 + 1.17
$\rightarrow [1s^2 2s^2] 2s 2p^5 ({}^1P) 3p ({}^2S_{1/2})$	80	13.18	1.18
$\rightarrow [1s^2 2s^2] 2p_{1/2}^2 2p_{3/2}^2 4d_{5/2}$	136	11.57	1.53
$\rightarrow [1s^2 2s^2] 2p^4 4d (\dots)$	137,138	11.53	3.55 + 4.22
$\rightarrow [1s^2 2s^2] 2p^4 ({}^3P) 4d ({}^2F_{5/2})$	164	11.42	4.75
$\rightarrow [1s^2 2s^2] 2p^4 ({}^1D) 4d (\dots)$	176,178,180	11.33	4.82 + 4.48 + 3.26
$\rightarrow [1s^2 2s^2] 2p_{1/2} 2p_{3/2}^3 4d_{5/2}$	182	11.31	1.09
$\rightarrow [1s^2 2s^2] 2p^4 ({}^1D) 4d ({}^2D_{3/2})$	181	11.29	1.28
$\rightarrow [1s^2] 2s 2p_{1/2}^2 2p_{3/2}^3 4p_{3/2}$	220	10.57	1.39
$\rightarrow [1s^2 2s^2] 2s 1s^2 2p_{1/2}^2 2p_{3/2}^3 4p_{3/2}$	221	10.56	1.58
$\rightarrow [1s^2 2s^2] 2p^4 5d (\dots)$	228,231	10.54	1.22 + 2.25 + 2.60
$\rightarrow [1s^2 2s^2] 2p^4 ({}^3P) 5d ({}^2D_{5/2})$	276	10.45	2.09
$\rightarrow [1s^2 2s^2] 2p_{1/2} 2p_{3/2}^3 5d (\dots)$	323,326,328	10.36	2.36 + 1.93 + 1.25

(g) Fe xvii (Ne-like ion)

transition from [1s ² 2s ² 2p ⁶] (1S ₀)	#	λ [Å]	A [10 ¹² /s]
\rightarrow [1s ² 2s ²] 2p ⁵ (² P) 3s (³ P ₁)	3	17.05	1.00
\rightarrow [1s ² 2s ²] 2p ⁵ (² P) 3s (¹ P ₁)	5	16.78	0.90
\rightarrow [1s ² 2s ²] 2p ⁵ (² P) 3d (³ D ₁)	23	15.26	5.87
\rightarrow [1s ² 2s ²] 2p ⁵ (² P) 3d (¹ P ₁)	27	15.01	27.0
\rightarrow [1s ²] 2s 2p ⁶ 3p (¹ P ₁)	33	13.82	3.40
\rightarrow [1s ² 2s ²] 2p ⁵ (² P) 4d (³ D ₁)	59	12.27	4.21
\rightarrow [1s ² 2s ²] 2p ⁵ (² P) 4d (¹ P ₁)	71	12.12	4.83
\rightarrow [1s ² 2s ²] 2p ⁵ (² P ₂) 5d (³ D ₁)	93	11.25	2.87
\rightarrow [1s ² 2s ²] 2p ⁵ (² P) 5d (¹ P ₁)	118	11.13	2.26
\rightarrow [1s ²] 2s 2p ⁶ 4p (¹ P ₁)	131	11.03	1.75
\rightarrow [1s ² 2s ²] 2p ⁵ (² P) 6d (³ D ₁)	155	10.77	1.90
\rightarrow [1s ² 2s ²] 2p ⁵ (² P) 6d (¹ P ₁)	181	10.66	1.15
\rightarrow [1s ² 2s ²] 2p ⁵ (² P) 7d (³ D ₁)	205	10.50	1.39
\rightarrow [1s ²] 2s 2p ⁶ 5p (¹ P ₁)	245	10.12	0.99

Table A I.8: Further iron lines (end)

II Data files from the CXC

It was explained in Section 3.1 how data from the *Chandra* X-ray observatory is organized and is reduced with CIAO. Primary and secondary data files can be downloaded from <http://cda.harvard.edu:9011/chaser/>. This appendix contains a file structure listing of the most important involved files and is thought to serve as a reference during the data reduction.

All data files from the Chandra X-ray Center (CXC) are organized in the FITS (flexible image transport system) format. They are fully consistent with the OGIP standards. OGIP is “*is a division of the Laboratory for High Energy Astrophysics at Goddard Space Flight Center. They oversee the activities of the HEASARC FITS Working Group (HFWG), which makes sure that FITS formats and keywords conform to the current standards and conventions.*” (CIAO online dictionary, <http://cxc.harvard.edu/ciao/dictionary/ogip.html>)

II.1 Primary and secondary data files

While primary data products are considered (by CXC) “to be sufficient for most analyses”, all secondary (level 1) data products are needed for data reprocessing and thus essential for this work. (Primary products from standard data processing may not always be reliable.)

Table A II.1: Contents of a level 1-event file

block	#	column	unit	description
BLOCK EVENTS	1	time	s	S/C TT corresponding to mid-exposure
	2	ccd_id		CCD reporting event
	3	node_id		CCD serial readout amplifier node
	4	expno		Exposure number of CCD frame containing event
	5	chip(chipx,chipy)	pixel	Chip coords
	6	tdet(tdtx,tdty)	pixel	ACIS tiled detector coordinates
	7	det(detx,dety)	pixel	ACIS detector coordinates
	8	sky(x,y)	pixel	sky coordinates
	9	pha	adu	total pulse height of event
	10	pha_r	adu	total read-out pulse height of event
	11	corn_phा		mean of event corner pixel PHA
	12	energy	eV	nominal energy of event (eV)
	13	pi	chan	pulse invariant energy of event
	14	fltgrade		event grade, flight system
	15	grade		binned event grade
	16	status[4]		event status bits
BLOCK GTIn	1	start	s	S/C TT corresponding to mid-exposure
	2	stop	s	S/C TT corresponding to mid-exposure

Table A II.2: Contents of a aspect/PCAD file

block	#	column	unit	description
BLOCK ASPSOL	1	time	s	Time
	2	ra	deg	RA of MNC frame (x-axis)
	3	dec	deg	DEC of MNC frame (x-axis)
	4	roll	deg	ROLL of MNC frame
	5	ra_err	deg	Uncertainty in RA
	6	dec_err	deg	Uncertainty in DEC
	7	roll_err	deg	Uncertainty in ROLL
	8	dy	mm	dY of STF frame - FC frame
	9	dz	mm	dZ of STF frame - FC frame
	10	dtheta	deg	dTHETA of STF frame - FC frame
	11	dy_err	mm	Uncertainty in dY
	12	dz_err	mm	Uncertainty in dZ
	13	dtheta_err	deg	Uncertainty in dTHETA
	14	q_att[4]		S/C attitude quaternion
	15	roll_bias	deg/s	Roll bias rate
	16	pitch_bias	deg/s	Pitch bias rate
	17	yaw_bias	deg/s	Yaw bias rate
	18	roll_bias_err	deg/s	Roll bias rate error
	19	pitch_bias_err	deg/s	Pitch bias rate error
	20	yaw_bias_err	deg/s	Yaw bias rate error

Table A II.3: Contents of a parameter block file

block	#	column	unit	description
BLOCK PBK	1	ccd_id		CCD ID
	2	fep_id		Front End Processor ID
	3	vidresp		CCD video chain response selection, 0 for 1:1
	4	evt_thr[4]	adu	Event thresholds for nodes A-D (TLMIN=-4096)
	5	spl_thr[4]	adu	Split thresholds for output nodes A-D
	6	bcmplot		Slot identifier for bias map compression tab
	7	biasalg		Bias algorithm is. 1:whole frame; 2:strip
	8	biasarg0		Bias arguement 0 (TLMIN=-32768)
	9	biasarg1		Bias arguement 1 (TLMIN=-32768)
	10	biasarg2		Bias arguement 2 (TLMIN=-32768)
	11	biasarg3		Bias arguement 3 (TLMIN=-32768)
	12	biasarg4		Bias arguement 4 (TLMIN=-32768)
	13	vid_off[4]		Video offsets for CCD output nodes A-D

Table A II.4: Contents of a bias file

block	#	column	unit	description
BLOCK BIAS	1	bias[1024,1024]		

Table A II.5: Contents of a filter file

block	#	column	unit	description
BLOCK GTIn	1	start	s	S/C TT corresponding to mid-exposure
	2	stop	s	S/C TT corresponding to mid-exposure

Table A II.6: Contents of a mask file

block	#	column	unit	description
BLOCK MASKn	1	shape		region shape
	2	component		Component index
	3	chip(chipx,chipy)[2]	pixel	CHIP position
	4	samp_cyc		sampling cycle
	5	phamin	adu	minimum pulse height
	6	phamax	adu	maximum pulse height

Table A II.7: Contents of a bad pixel file

block	#	column	unit	description
BLOCK_BADPIX n	1	shape		region shape
	2	component		Component number
	3	chip(chipx,chipy)[2]	pixel	CHIP location
	4	time	s	Time pixel went bad
	5	time_stop	s	Time pixel went bad
	6	status[4]		Badpixel status code

II.2 High level data files

High level data products are the ones obtained by the data reduction. They are finally used for scientific analysis. It is possible that they have to be reprocessed to apply a new calibration.

Table A II.8: Contents of a level 1.5-event file

block	#	column	unit	description
BLOCK EVENTS	1	time	s	time tag of data record
	2	expno		
	3	rd(tg_r,tg_d)	deg	Grating angular coords
	4	chip(chipx,chipy)	pixel	Chip coords
	5	tdet(tdetx,tdety)	pixel	Tdet coords
	6	det(detx,dety)	pixel	Det coords
	7	sky(x,y)	pixel	Sky coords
	8	ccd_id		
	9	pha		
	10	pi		
	11	energy		
	12	grade		
	13	fltgrade		
	14	node_id		
	15	tg_m		Diffraction order (m)
	16	tg_lam	angstrom	wavelength (lambda)
	17	tg_llam	angstrom	Order times wavelength (m * lambda)
	18	tg_srcid		source ID, index from detect table
BLOCK REGION	19	tg_part		component index (HEG, MEG, LEG, HESF regions)
	20	tg_smap		source map; flags for up to 10 sources
	21	status[4]		event status bits
	1	source		Source Number
	2	shape		Shape of the region
	3	sky(x,y)	pixel	Sky coords
	4	r[2]	pixel	Radius Vector for SHAPE
	5	rotang	deg	Rotation angle for SHAPE
BLOCK GTIn	6	grating		Applicable grating, hetg or letg
	7	tg_part		TG_PART
	8	component		Component number

Table A II.9: Contents of a light curve file

block	#	column	unit	description
BLOCK_LIGHTCURVE	1	time_bin	channel	time tag of data record
	2	time_min	s	Minimum Value in Bin
	3	time	s	time tag of data record
	4	time_max	s	Maximum Value in Bin
	5	counts	count	Counts
	6	stat_err	count	Statistical error
	7	count_rate	count/s	Rate
	8	count_rate_err	count/s	Rate Error
	9	exposure	s	Time per interval
BLOCK_GTI n	1	start	s	time tag of data record
	2	stop	s	time tag of data record

Table A II.10: Contents of a spectra (pha2) file

block	#	column	unit	description
BLOCK SPECTRUM	1	spec_num		Spectrum Number
	2	tg_m		Diffraction order (m)
	3	tg_part		Spectral component (HEG, MEG, LEG, HESF parts)
	4	tg_srcid		Source ID, output by detect
	5	x	pixel	X sky coord of source
	6	y	pixel	Y sky coord of source
	7	channel[8192]		Vector of spectral bin numbers.
	8	counts[8192]	count	Counts array (a spectrum)
	9	stat_err[8192]	count	Statistical uncertainty (error) on counts column
	10	background_up[8192]	count	Background count vector
	11	background_down[8192]	count	Background count vector
	12	bin_lo[8192]	angstrom	Bin boundary, left edge
	13	bin_hi[8192]	angstrom	Bin boundary, right edge
BLOCK REGION	1	spec_num		Spectrum number, which points to the row in the Source or a background region?
	2	rowid		
	3	shape		Shape of region
	4	wavpos(tg_lam,tg_d)		Wavelength(angstrom), Cross Dispersion(degrees)
	5	r[2]	(angstrom, degrees)	Radius vector for SHAPE
	6	rotang	degrees	Rotation angle for SHAPE
	7	tg_part		Grating part index (HEG=1, MEG=2, LEG=3)
	8	tg_srcid		Source identification number
	9	tg_m		Diffraction order
	10	component		Component number

Table A II.11: Contents of a background (bkg2) file

block	#	column	unit	description
BLOCK SPECTRUM	1	spec_num		Spectrum Number
	2	tg_m		Diffraction order (m)
	3	tg_part		Spectral component (HEG, MEG, LEG, HESF parts)
	4	tg_srcid		Source ID, output by detect
	5	x	pixel	X sky coord of source
	6	y	pixel	Y sky coord of source
	7	channel[8192]		Vector of spectral bin numbers.
	8	bin_lo[8192]	angstrom	Bin boundary, left edge
	9	bin_hi[8192]	angstrom	Bin boundary, right edge
	10	counts[8192]		User defined column

Table A II.12: Contents of a grating redistribution matrix function (gRMF) file

block	#	column	unit	description
BLOCK MATRIX	1	energ_lo	keV	
	2	energ_hi	keV	
	3	n_grp		
	4	f_chan		
	5	n_chan		
	6	matrix[103]		
BLOCK EBOUNDS	1	channel	channel	
	2	e_min	keV	
	3	e_max	keV	

Table A II.13: Contents of a grating ancillary response function (gARF) file

block	#	column	unit	description
BLOCK SPECRESP	1	energ_lo	keV	Energy
	2	energ_hi	keV	Energy
	3	specresp	cm**2	Effective Area
	4	bin_lo	angstrom	
	5	bin_hi	angstrom	
	6	fracexpo		

III The *Chandra* observation # 3814

The analysis of the *Chandra* observation # 3814 was the main achievement of this thesis. It was discussed in great detail in chapter 4. This appendix contains completing plots and detailed tables, which were removed from the main part to keep the overview on the main procedures.

III.1 Flux-ratios of the sub-spectra

The consistency of the ‘non-dip’ sub-spectra with the whole ‘non-dip’ spectrum was investigated in Section 4.2.1 (page 57). Figs. A III.1 and A III.2 show the flux-ratios of the ‘non-dip 1’ and the ‘non-dip 3’ sub-spectra to the average ‘non-dip’ spectrum. (The same is not shown explicitly for the ‘non-dip 2’ spectrum again, which is complementary to the ‘non-dip 1’ and ‘non-dip 3’ spectra regarding the ratio to the total ‘non-dip’ spectrum. As there are almost no deviations, it is clear that the ‘non-dip 2’ spectrum would show the same behavior.)

Colors were used to visualize the consistency of the fluxratio with 1: The gray lines show bins, where the value 1 is in the middle third of the error bar ($|r - 1| \leq \Delta r/3$), red indicates positive deviations, blue negative deviations. Darker colors are used when the ratio is not consistent with 1 at all ($|r - 1| > \Delta r$). Each plot shows in its first 4 panels the individual ratios of the MEG ± 1 and HEG ± 1 spectra, while the last panel shows the average.

The same analysis was repeated for the ‘dip’ sub-spectra with respect to the whole ‘dip’ spectrum, as described in Section 4.3.1 (page 88): Figs. A III.3 – A III.5 show the analogous flux-ratios of the ‘dip 1’, ‘dip 2’ and ‘dip 3’ sub-spectra to the ‘dip’ spectrum. The trend that ‘dip 1’ is less strongly absorbed than the average ‘dip’, while ‘dip 2’ is more absorbed, can also be directly seen from the flux-corrected spectra themselves (Fig. 4.16).

III.2 Spectral analysis of the ‘non-dip’ spectrum

The detailed results for the description of lines in the ‘non-dip’ spectrum (Sect. 4.2.3) are shown on the following pages:

Table 4.10 (Sect. 4.2.3, page 73) gave the fit-parameters of all trustably identified lines. Table A III.1, which starts on page 129, however, lists the parameters of all the lines included to describe the spectrum. (It was stated that many of the (unidentified) lines might not be real, but just describe calibration uncertainties or statistical fluctuation.) The parameters are – as in Table 4.10: their position, full width at half maximum (with colored background if the confidence interval or even the width itself did not converge properly), equivalent width, improvement on the χ^2 -statistics (cf. comments to Table 4.4, page 61) and possible identifications (gray backgrounds mark emission lines): ion, electronic states of the transition (where ground states are underlined), theoretical wavelength (from CXC’s atomic database ATOMDB 1.3.1) and Einstein coefficient as a measure for the expected strength of the lines. Identifications in brackets just mean that the theoretical wavelengths are not within the range of the fitted positions (which is, however due to Doppler shifts, no reason that the identification is not correct). Trustable identifications (cf. Sect. 4.2.3) are marked by \leftarrow arrows.

The plots following this long list of lines (Fig. A III.6a-A III.6h, on pages 137-144) show the spectrum with all fitted lines in each 2 Å-wavelength-intervals. The upper panel shows the residuals $\Delta\chi$ of the continuum, i.e., before including the fitted lines in the model. Then, the combined count rates of each the MEG ± 1 and HEG ± 1 spectra are shown. This is only for clearer visualization; all spectra have been fitted independently (though simultaneously). Trusted line identifications are labeled.

III.3 Dependencies of the continuum-parameters

The next section starts at page 145.

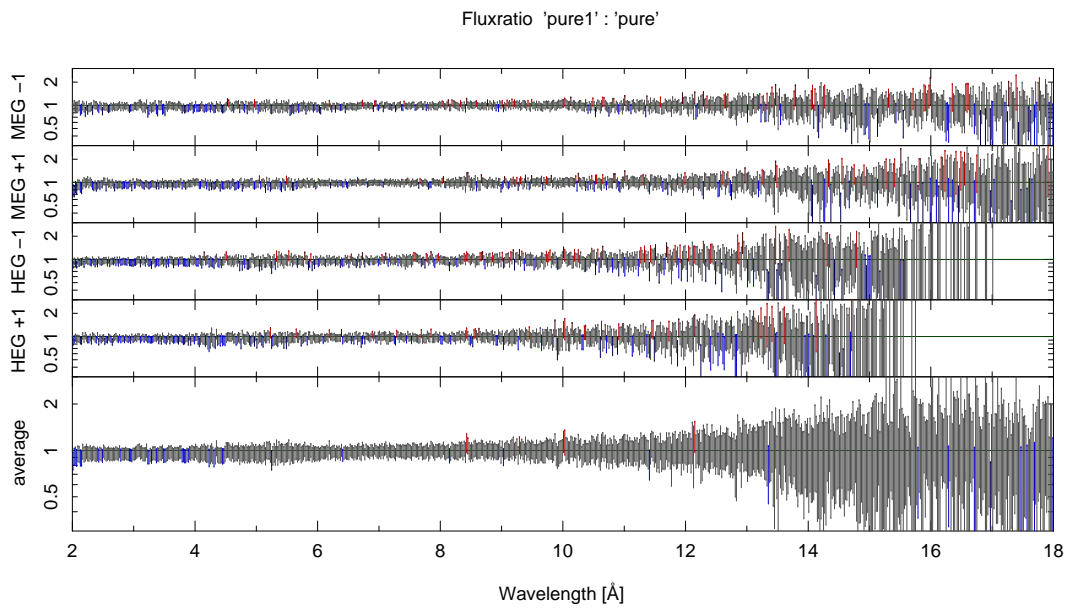


Figure A III.1: Ratio of ‘non-dip 1’ and ‘non-dip’ flux-spectrum.

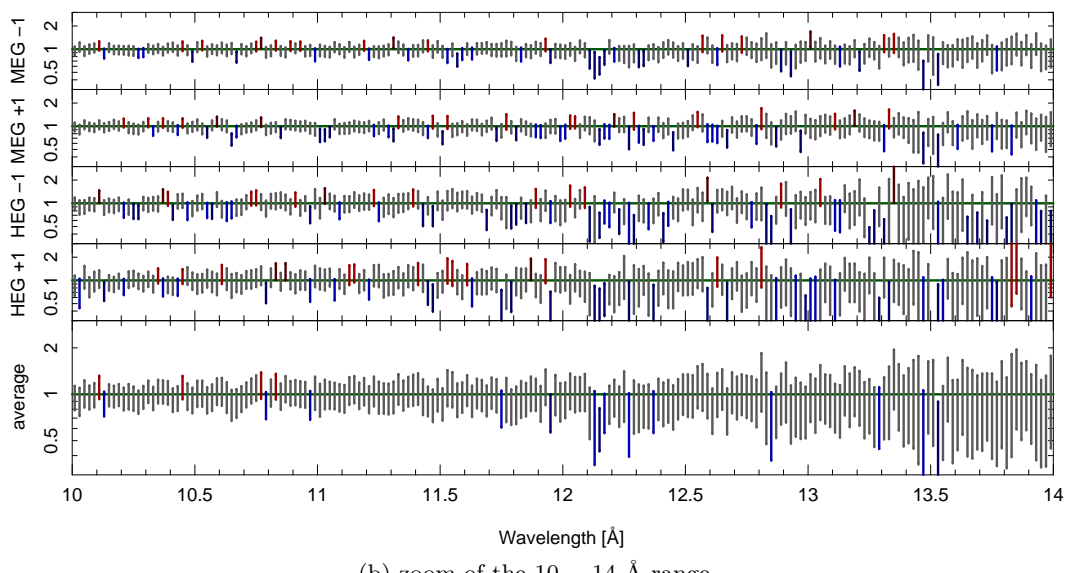
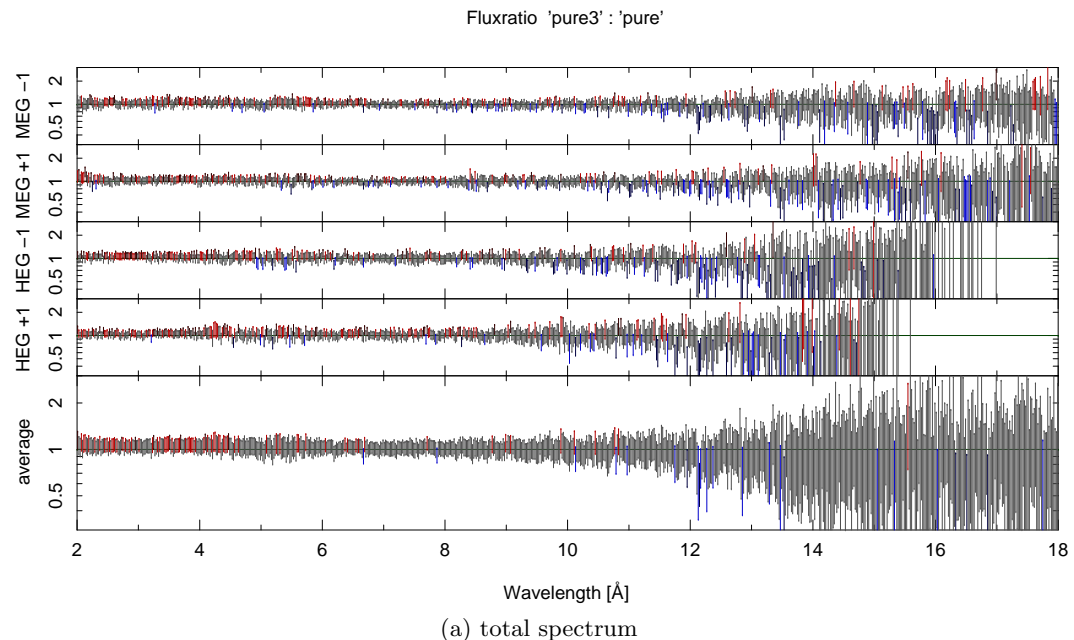


Figure A III.2: Ratio of ‘non-dip 3’ and ‘non-dip’ flux-spectrum.

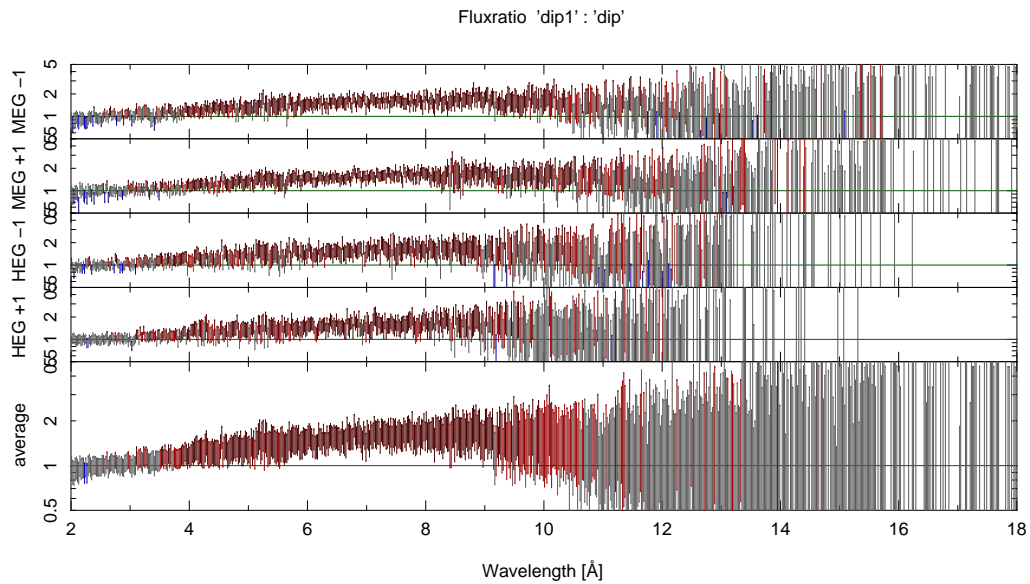


Figure A III.3: Ratio of ‘dip 1’ and ‘dip’ flux-spectrum.

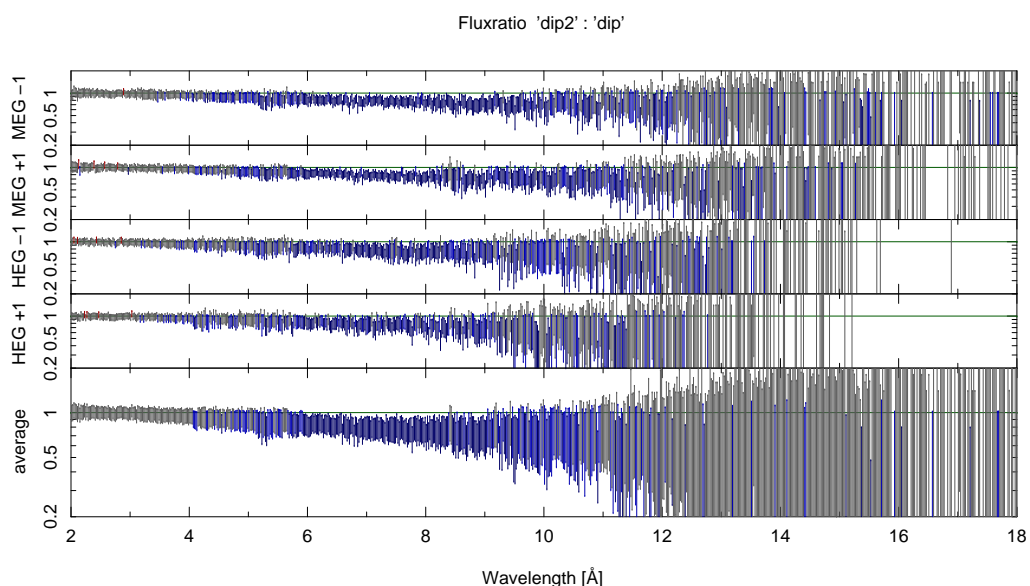


Figure A III.4: Ratio of ‘dip 2’ and ‘dip’ flux-spectrum.

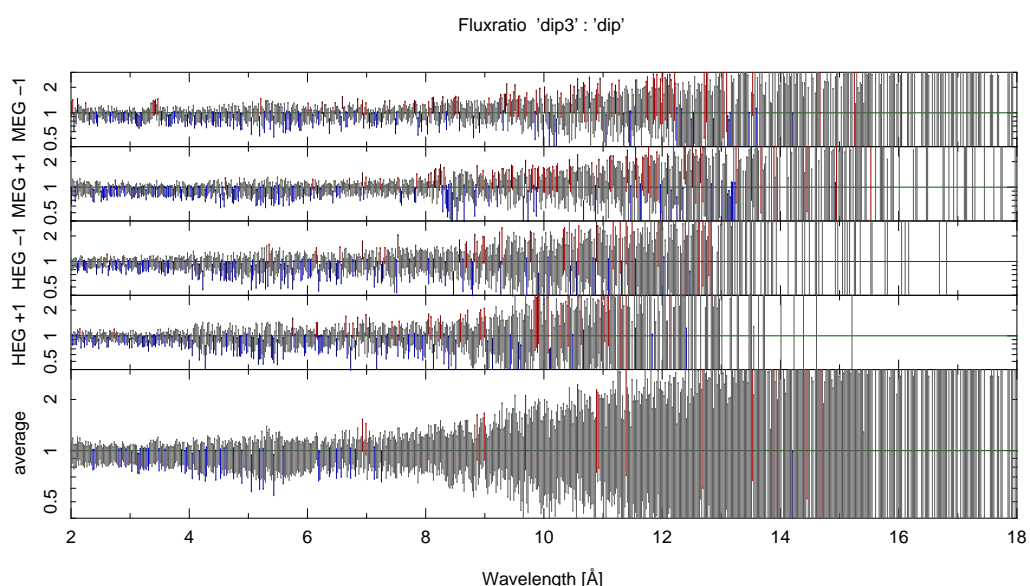


Figure A III.5: Ratio of ‘dip 3’ and ‘dip’ flux-spectrum.

Table A III.1: List of lines in the ‘non-dip’ spectrum – sorted by wavelength

λ [Å]	FWHM [mÅ]	EW [mÅ]	$\Delta\chi^2$	ion <i>i</i>	transition <i>j</i>	λ_0 [Å]	A_{ji} [Å] $\cdot 10^{12}$ s $^{-1}$	$\Delta\lambda/\lambda \cdot c$ [km/s]		
1.2146 $^{+0.0070}_{-0.0070}$	27.92 $^{+2.50}_{-15.81}$	-19.84 $^{+8.25}_{-7.53}$	0.0	(Ni XXVIII $1s$	4p	1.2268	41.2) ←	
				(Ni XXVIII $1s$	4p	1.2272	41.2)	
1.4475 $^{+0.0025}_{-0.0031}$	0.11 $^{+19.89}_{-0.11}$	-4.50 $^{+1.66}_{-3.90}$	19.3	(Fe XXV	$1s^2$	1s5p	1.4610	28.3)	
1.4670 $^{+0.0030}_{-0.0028}$	1.78 $^{+11.14}_{-1.78}$	-4.43 $^{+1.63}_{-2.07}$	19.9	(Fe XXV	$1s^2$	1s5p	1.4610	28.3)	
1.4914 $^{+0.0066}_{-0.0041}$	0.72 $^{+23.63}_{-0.72}$	-2.51 $^{+1.61}_{-2.28}$	6.5	Fe XXV	$1s^2$	1s4p	1.4950	56.3	←	
1.5180 $^{+0.0028}_{-0.0027}$	0.18 $^{+10.71}_{-0.18}$	-3.54 $^{+1.49}_{-1.49}$	14.7	(Ni XXVIII $1s$	2p	1.5304	379) ←	
				(Ni XXVIII $1s$	2p	1.5356	378)	
1.5526 $^{+0.0033}_{-0.0025}$	0.33 $^{+11.99}_{-0.33}$	-3.02 $^{+1.48}_{-1.58}$	10.9	(Fe XXV	$1s^2$	1s3p	1.5731	137)	
1.8499 $^{+0.0029}_{-0.0038}$	5.42 $^{+14.13}_{-5.42}$	-2.11 $^{+0.90}_{-1.25}$	18.6	Fe XXV	$1s^2$	1s2p	1.8504	503	←	
1.9395 $^{+0.0021}_{-0.0020}$	11.51 $^{+6.13}_{-5.28}$	5.00 $^{+1.24}_{-1.18}$	58.8	(Fe	K α	1.937) ←	385 $^{+331}_{-316}$	
1.9678 $^{+0.0086}_{-0.0043}$	0.04 $^{+25.29}_{-0.04}$	0.93 $^{+0.86}_{-0.82}$	3.8							
1.9922 $^{+0.0051}_{-0.0046}$	13.69 $^{+15.92}_{-13.69}$	2.28 $^{+1.13}_{-1.22}$	13.9							
2.0328 $^{+0.0022}_{-0.0028}$	0.00 $^{+16.47}_{-0.00}$	1.77 $^{+0.87}_{-0.83}$	13.1							
2.2900 $^{+0.0026}_{-0.0001}$	0.01 $^{+5.73}_{-0.01}$	1.81 $^{+0.80}_{-0.76}$	16.0							
2.3204 $^{+0.0200}_{-0.0090}$	10.07 $^{+65.36}_{-10.07}$	1.10 $^{+2.13}_{-0.82}$	5.4							
2.3476 $^{+0.0025}_{-0.0026}$	0.02 $^{+74.98}_{-0.02}$	1.48 $^{+0.77}_{-0.72}$	12.1							
2.4407 $^{+0.0206}_{-0.0035}$	0.12 $^{+74.88}_{-0.12}$	0.82 $^{+0.71}_{-0.66}$	4.3							
2.4618 $^{+0.0099}_{-0.0107}$	15.24 $^{+59.76}_{-15.24}$	1.47 $^{+1.53}_{-0.94}$	8.4							
2.6944 $^{+0.0065}_{-0.0200}$	13.48 $^{+61.94}_{-13.48}$	1.32 $^{+1.96}_{-0.85}$	7.9	(Ca XIX	$1s^2$	1s3p	2.7050	46.3)	
2.7000 $^{+0.0025}_{-0.0000}$	0.00 $^{+24.05}_{-0.00}$	-1.64 $^{+0.53}_{-0.50}$	23.9	(Ca XIX	$1s^2$	1s3p	2.7050	46.3) ←	
2.9776 $^{+0.0238}_{-0.0162}$	0.01 $^{+49.99}_{-0.01}$	-0.53 $^{+0.53}_{-0.55}$	2.6	Ar XVIII	$1s$	4p	2.9873	7.04	←	
				Ar XVIII	$1s$	4p	2.9878	7.03	-1017 $^{+239}_{-1625}$	
3.0201 $^{+0.0175}_{-0.0026}$	0.01 $^{+74.99}_{-0.01}$	-0.60 $^{+0.56}_{-0.54}$	3.1	Ca XX	$1s$	2p	3.0185	98.6	←	
				Ca XX	$1s$	2p	3.0239	98.5	-383 $^{+1731}_{-257}$	
3.0748 $^{+0.0002}_{-0.0048}$	0.00 $^{+8.77}_{-0.00}$	-0.85 $^{+0.56}_{-0.53}$	6.1	(Ar XVII	$1s^2$	1s5p	3.1280	6.20)	
3.1427 $^{+0.0213}_{-0.0187}$	0.16 $^{+49.84}_{-0.16}$	-0.44 $^{+0.44}_{-0.54}$	1.4	Ar XVIII	$1s$	3p	3.1502	17.3	←	
				Ar XVIII	$1s$	3p	3.1514	17.2	-822 $^{+2022}_{-1783}$	
3.1878 $^{+0.0163}_{-0.0306}$	0.00 $^{+50.42}_{-0.00}$	-0.55 $^{+0.55}_{-0.56}$	2.2	Ca XIX	$1s^2$	1s2p	3.1772	170	←	
3.1942 $^{+0.0033}_{-0.0018}$	0.00 $^{+17.52}_{-0.00}$	1.01 $^{+0.71}_{-0.68}$	6.2	(Ca XIX	$1s^2$	1s2p	3.189	0.001) ←	
				Ca XIX	$1s^2$	1s2p	3.192	4.85	484 $^{+306}_{-165}$	
3.2075 $^{+0.0025}_{-0.0050}$	0.00 $^{+27.57}_{-0.00}$	-0.93 $^{+0.51}_{-0.49}$	8.0	(Ar XVII	$1s^2$	1s4p	3.2000	12.3) ←	
3.3667 $^{+0.0158}_{-0.0067}$	0.00 $^{+0.00}_{-0.00}$	-0.60 $^{+0.59}_{-0.57}$	2.8	Ar XVII	$1s^2$	1s3p	3.3650	30.0	←	
3.7002 $^{+0.0202}_{-0.0202}$	0.00 $^{+75.00}_{-0.00}$	-0.41 $^{+0.41}_{-0.59}$	1.2	S XVI	$1s$	5p	3.6958	2.22	←	
				S XVI	$1s$	5p	3.6960	2.21	337 $^{+1637}_{-1637}$	
3.7289 $^{+0.0211}_{-0.0103}$	12.88 $^{+37.12}_{-12.88}$	-0.94 $^{+0.79}_{-1.63}$	4.0	Ar XVIII	$1s$	2p	3.7311	64.7	←	
				Ar XVIII	$1s$	2p	3.7365	64.6	-614 $^{+1694}_{-830}$	
3.7801 $^{+0.0061}_{-0.0051}$	0.04 $^{+49.96}_{-0.04}$	-0.64 $^{+0.58}_{-0.83}$	3.3	S XVI	$1s$	4p	3.7843	4.40	←	
				S XVI	$1s$	4p	3.7848	4.39	-336 $^{+486}_{-404}$	
3.9250 $^{+0.0041}_{-0.0040}$	8.53 $^{+11.89}_{-8.53}$	-1.54 $^{+0.73}_{-0.82}$	13.0							
3.9475 $^{+0.0026}_{-0.0026}$	0.03 $^{+18.90}_{-0.03}$	-1.11 $^{+0.54}_{-0.57}$	9.1	Ar XVII	$1s^2$	1s2p	3.9491	109	←	
3.9860 $^{+0.0214}_{-0.0181}$	37.50 $^{+37.50}_{-37.50}$	-1.73 $^{+1.43}_{-1.49}$	5.9	S XVI	$1s$	3p	3.9908	10.8	←	
				S XVI	$1s$	3p	3.9920	10.8	-449 $^{+1604}_{-1359}$	
4.0984 $^{+0.0088}_{-0.0093}$	20.58 $^{+31.95}_{-20.58}$	-1.88 $^{+1.18}_{-1.24}$	9.1	(S XV	$1s^2$	1s4p	4.0883	7.53) ←	
4.3019 $^{+0.0211}_{-0.0211}$	74.98 $^{+0.44}_{-64.42}$	-3.88 $^{+2.47}_{-1.82}$	12.4	S XV	$1s^2$	1s3p	4.2990	18.3	←	
4.3876 $^{+0.0049}_{-0.0048}$	0.14 $^{+16.57}_{-0.14}$	-1.09 $^{+0.68}_{-0.84}$	6.3	S XV	$1s^2$ 2p	(autoion.)	4.3910		-235 $^{+337}_{-330}$	
4.4150 $^{+0.0075}_{-0.0075}$	0.00 $^{+75.00}_{-0.00}$	-0.66 $^{+0.66}_{-0.71}$	2.7	S XV	$1s^2$ 2p	(autoion.)	4.4149		8 $^{+511}_{-511}$	
4.7285 $^{+0.0015}_{-0.0017}$	7.78 $^{+9.06}_{-5.76}$	-4.13 $^{+0.92}_{-1.18}$	93.6	S XVI	$1s$	2p	4.7274	40.4	←	
				(S XVI	$1s$	2p	4.7328	40.3)	-272 $^{+93}_{-109}$
4.9518 $^{+0.0032}_{-0.0018}$	0.01 $^{+13.26}_{-0.01}$	-1.42 $^{+0.69}_{-0.73}$	11.2	(Si XIV	$1s$	4p	4.9468	2.58) ←	
				(Si XIV	$1s$	4p	4.9472	2.57)	305 $^{+196}_{-112}$
5.0397 $^{+0.0020}_{-0.0020}$	9.26 $^{+7.70}_{-5.73}$	-3.80 $^{+0.91}_{-1.05}$	62.7	S XV	$1s^2$	1s2p	5.0387	66.7	←	
				S XV	$1s^2$	1s2p	5.063	0.000	←	
5.0656 $^{+0.0244}_{-0.0156}$	5.27 $^{+44.73}_{-5.27}$	0.77 $^{+0.93}_{-0.77}$	2.2	S XV	$1s^2$	1s2p	5.066	0.59	143 $^{+1447}_{-921}$	
				S XV	$1s^2$	1s2p	5.066	0.59	-55 $^{+1446}_{-921}$	
5.1004 $^{+0.0196}_{-0.0204}$	0.22 $^{+49.78}_{-0.22}$	0.34 $^{+0.84}_{-0.34}$	0.6	S XV	$1s^2$	1s2s	5.101	0.000	←	
				S XV	$1s^2$	1s2s	5.101	0.000	-64 $^{+1151}_{-1199}$	
5.2193 $^{+0.0077}_{-0.0048}$	22.15 $^{+20.59}_{-11.94}$	-4.03 $^{+1.41}_{-2.18}$	33.5	Si XIV	$1s$	3p	5.2168	6.32	←	
				Si XIV	$1s$	3p	5.2180	6.31	79 $^{+444}_{-274}$	
5.3750 $^{+0.0050}_{-0.0050}$	0.00 $^{+37.24}_{-0.00}$	-1.42 $^{+0.84}_{-0.76}$	6.9							
5.4033 $^{+0.0043}_{-0.0008}$	0.01 $^{+25.54}_{-0.01}$	-1.42 $^{+0.77}_{-1.05}$	8.7	Si XIII	$1s^2$	1s4p	5.4045	4.30	←	
				Si XIII	$1s^2$ 2s	(autoion.)	5.5424		-68 $^{+237}_{-45}$	
5.5306 $^{+0.0044}_{-0.0007}$	0.01 $^{+13.42}_{-0.01}$	-1.44 $^{+0.80}_{-0.78}$	8.5	(Si XIII	$1s^2$ 2s	(autoion.)	5.5425)	-641 $^{+237}_{-38}$

Table A III.1: List of lines in the ‘non-dip’ spectrum – sorted by wavelength (continued)

λ [Å]	FWHM [mÅ]	EW [mÅ]	$\Delta\chi^2$	ion <i>i</i>	transition <i>j</i>	λ_0 [Å]	A_{ji} [Å] $\cdot 10^{12}$ s $^{-1}$	$\Delta\lambda/\lambda \cdot c$ [km/s]	
5.5750 $^{+0.0050}_{-0.0025}$	0.00 $^{+41.16}_{-0.00}$	-1.41 $^{+0.68}_{-0.74}$	10.7	(Si XIII	$1s^2 2p$	(autoion.)	5.5618)	713 $^{+268}_{-137}$
				(Si XIII	$1s^2 2p$	(autoion.)	5.5627)	665 $^{+268}_{-137}$
5.6809 $^{+0.0037}_{-0.0036}$	22.02 $^{+14.30}_{-10.29}$	-4.64 $^{+1.29}_{-1.47}$	58.5	Si XIII	$1s^2$	$1s3p$	5.6805	10.4 ←	23 $^{+195}_{-190}$
5.8572 $^{+0.0003}_{-0.0047}$	0.00 $^{+26.23}_{-0.00}$	-1.11 $^{+0.63}_{-0.63}$	8.0	(Ni XXV	$1s^2 2s^2$	$1s^2 2s7p$	5.8598	0.19)	-133 $^{+13}_{-243}$
				(Ni XXV	$1s^2 2s^2$	$1s^2 2s7p$	5.8584	1.25)	-60 $^{+13}_{-243}$
6.0602 $^{+0.0121}_{-0.0093}$	14.48 $^{+5.52}_{-14.48}$	-1.28 $^{+0.87}_{-1.05}$	7.0	Al XIII	$1s$	$3p$	6.0526	4.70 ←	376 $^{+598}_{-459}$
				Al XIII	$1s$	$3p$	6.0537	4.69	321 $^{+598}_{-459}$
6.1810 $^{+0.0005}_{-0.0009}$	13.80 $^{+2.31}_{-1.75}$	-10.31 $^{+0.78}_{-0.85}$	888.9	Si XIV	$1s$	$2p$	6.1804	23.7 ←	29 $^{+25}_{-42}$
				(Si XIV	$1s$	$2p$	6.1858	23.6)	-233 $^{+25}_{-42}$
6.3150 $^{+0.0150}_{-0.0050}$	0.00 $^{+50.00}_{-0.00}$	-0.37 $^{+0.37}_{-0.65}$	1.3	Al XII	$1s^2$	$1s4p$	6.3140	3.14 ←	48 $^{+711}_{-238}$
6.6346 $^{+0.0045}_{-0.0024}$	0.88 $^{+10.91}_{-0.88}$	-1.81 $^{+1.10}_{-2.12}$	0.0	Al XII	$1s^2$	$1s3p$	6.6350	7.63 ←	-18 $^{+201}_{-109}$
6.6468 $^{+0.0009}_{-0.0010}$	9.50 $^{+2.50}_{-2.18}$	-6.62 $^{+1.01}_{-1.07}$	215.5	(Si XIII	$1s^2$	$1s2p$	6.6479	37.7) ←	-51 $^{+42}_{-44}$
				Ni XXIV	$1s^2 2s^2 2p$	$1s^2 2s2p5p$	6.7029	0.17	9 $^{+161}_{-181}$
6.7031 $^{+0.0036}_{-0.0040}$	18.94 $^{+16.40}_{-12.14}$	-3.67 $^{+1.57}_{-1.30}$	45.4	(Si XIII	$1s^2$	$1s2p$	6.6850	0.000)	810 $^{+161}_{-181}$
				(Si XIII	$1s^2$	$1s2p$	6.6882	0.16)	666 $^{+161}_{-181}$
6.7223 $^{+0.0033}_{-0.0034}$	14.39 $^{+10.73}_{-6.92}$	-2.96 $^{+0.95}_{-1.07}$	37.2	Ni XXIV	$1s^2 2s^2 2p$	$1s^2 2s^2 6d$	6.7190	2.11	148 $^{+146}_{-151}$
6.7445 $^{+0.0023}_{-0.0019}$	7.50 $^{+6.33}_{-7.50}$	2.77 $^{+0.94}_{-0.85}$	36.1	(Si XIII	$1s^2$	$1s2s$	6.740:	0.000) ←	189 $^{+102}_{-86}$
6.7613 $^{+0.0041}_{-0.0047}$	6.57 $^{+15.96}_{-6.57}$	1.35 $^{+0.89}_{-0.72}$	9.9	Ni XXIV	$1s^2 2s2p^2$	$1s^2 2s2p6d$	6.759:	2.86	95 $^{+182}_{-210}$
				Ni XXIV	$1s^2 2s2p^2$	$1s^2 2s2p6d$	6.759:	1.58	64 $^{+182}_{-210}$
				Ni XXV	$1s^2 2p^2$	$1s^2 2p5d$	6.7796	3.87	19 $^{+108}_{-95}$
6.7800 $^{+0.0024}_{-0.0021}$	0.03 $^{+14.37}_{-0.03}$	-1.66 $^{+0.39}_{-0.66}$	28.7	(Fe XXV	$1s2s$	$1s5p$	6.7880	1.98)	-353 $^{+107}_{-95}$
				(Fe XXV	$1s2s$	$1s5p$	6.7880	1.95)	-353 $^{+107}_{-95}$
				(Fe XXV	$1s2s$	$1s5p$	6.7880	1.94)	-353 $^{+107}_{-95}$
7.1050 $^{+0.0025}_{-0.0000}$	0.01 $^{+5.89}_{-0.01}$	-2.31 $^{+0.43}_{-0.72}$	49.6	Mg XII	$1s$	$3p$	7.1058	3.41 ←	-33 $^{+105}_{-1}$
				Mg XII	$1s$	$3p$	7.1069	3.41	-81 $^{+105}_{-1}$
7.1687 $^{+0.0027}_{-0.0020}$	9.91 $^{+7.80}_{-9.90}$	-3.04 $^{+0.79}_{-0.99}$	46.2	Al XIII	$1s$	$2p$	7.1710	17.6 ←	-98 $^{+113}_{-83}$
				(Al XIII	$1s$	$2p$	7.1764	17.6)	-323 $^{+113}_{-83}$
7.2777 $^{+0.0116}_{-0.0077}$	20.00 $^{+32.33}_{-13.07}$	2.06 $^{+1.48}_{-1.29}$	11.6	Ni XXIV	$1s^2 2s2p^2$	$1s^2 2s2p5d$	7.278:	6.10	-46 $^{+479}_{-315}$
7.3168 $^{+0.0200}_{-0.0147}$	6.36 $^{+43.64}_{-6.36}$	1.17 $^{+1.94}_{-0.82}$	6.0	Mg XI	$1s^2$	$1s5p$	7.310:	1.13	274 $^{+820}_{-603}$
7.3525 $^{+0.0050}_{-0.0075}$	0.00 $^{+75.00}_{-0.00}$	1.02 $^{+0.84}_{-0.67}$	6.2	Ni XXV	$1s^2 2p^2$	$1s^2 2p4d$	7.345:	9.01	289 $^{+204}_{-306}$
				(Ni XXV	$1s^2 2p^2$	$1s^2 2p4d$	7.359:	8.55)	-269 $^{+204}_{-305}$
7.4774 $^{+0.0001}_{-0.0049}$	0.00 $^{+11.26}_{-0.00}$	-1.80 $^{+0.56}_{-0.52}$	24.9	Mg XI	$1s^2$	$1s4p$	7.4730	2.24 ←	175 $^{+5}_{-196}$
				(Fe XXIII	$1s^2 2s^2$	$1s^2 2s5p$	7.4780	2.51)	-25 $^{+5}_{-195}$
7.6245 $^{+0.0043}_{-0.0104}$	14.77 $^{+35.42}_{-11.65}$	2.69 $^{+1.82}_{-1.03}$	22.9	Ni XXIII	$1s^2 2s2p^3$	$1s^2 2s2p2p5$	7.625:	0.85	-43 $^{+168}_{-408}$
				Ni XXIII	$1s^2 2s2p^3$	$1s^2 2s2p2p5$	7.628:	1.61	-148 $^{+168}_{-408}$
				(Ni XXI	$2s^2 2p^4$	$2s2p^2 2p5p$	7.629:	0.97)	-210 $^{+168}_{-408}$
7.7532 $^{+0.0056}_{-0.0090}$	0.41 $^{+34.00}_{-0.41}$	-1.09 $^{+0.75}_{-1.49}$	5.6	Al XII	$1s^2$	$1s2p$	7.7573	27.5 ←	-158 $^{+217}_{-347}$
7.7676 $^{+0.0049}_{-0.0026}$	0.00 $^{+18.45}_{-0.00}$	-1.15 $^{+0.78}_{-0.70}$	5.9	(Al XII	$1s^2$	$1s2p$	7.7573	27.5) ←	398 $^{+190}_{-101}$
7.7908 $^{+0.0067}_{-0.0033}$	0.00 $^{+39.61}_{-0.00}$	1.46 $^{+0.97}_{-0.94}$	6.7	(Al XII	$1s^2$	$1s2p$	7.807:	0.082) ←	-620 $^{+257}_{-127}$
				(Al XII	$1s^2$	$1s2p$	7.803:	0.000)	-501 $^{+257}_{-127}$
7.8150 $^{+0.0092}_{-0.0211}$	7.03 $^{+42.97}_{-7.03}$	1.26 $^{+1.74}_{-1.04}$	4.1	Al XII	$1s^2$	$1s2p$	7.807:	0.082 ←	310 $^{+352}_{-809}$
				Al XII	$1s^2$	$1s2p$	7.803:	0.000	430 $^{+352}_{-810}$
7.8482 $^{+0.0022}_{-0.0025}$	14.35 $^{+8.95}_{-6.36}$	-4.78 $^{+1.30}_{-1.55}$	62.4	Mg XI	$1s^2$	$1s3p$	7.8503	5.43 ←	-81 $^{+85}_{-95}$
7.8751 $^{+0.0200}_{-0.0200}$	0.02 $^{+49.98}_{-0.02}$	0.47 $^{+1.03}_{-0.47}$	1.2	Al XII	$1s^2$	$1s2s$	7.872:	0.000 ←	112 $^{+762}_{-762}$
				(Fe XXII	$1s^2 2s^2 2p$	$1s^2 2s2p5p$	7.8806	1.82)	888 $^{+274}_{-544}$
				(Fe XXII	$1s^2 2s^2 2p$	$1s^2 2s2p5p$	7.8838	1.49)	765 $^{+274}_{-544}$
				(Ni XXIV	$1s^2 2s2p^2$	$1s^2 2s2p4d$	7.8844	7.31)	745 $^{+274}_{-544}$
7.9040 $^{+0.0072}_{-0.0143}$	13.39 $^{+38.70}_{-13.39}$	-1.30 $^{+0.88}_{-1.27}$	6.7	(Ni XXIV	$1s^2 2s2p^2$	$1s^2 2s2p4d$	7.8851	5.30)	717 $^{+274}_{-544}$
				(Ni XXIV	$1s^2 2s2p^2$	$1s^2 2s2p4d$	7.8872	2.73)	638 $^{+274}_{-544}$
				(Fe XXII	$1s^2 2s^2 2p$	$1s^2 2s2p5p$	7.8883	1.20)	597 $^{+274}_{-544}$
				(Ni XXII	$2s^2 2p^3$	$2s2p^2 2p5d$	7.8892	2.70)	560 $^{+274}_{-544}$
				(Ni XXII	$2s^2 2p^3$	$2s2p2p5d$	7.9065	4.31)	701 $^{+190}_{-95}$
				(Ni XXII	$2s^2 2p^3$	$2s2p2p5d$	7.9076	3.38)	660 $^{+190}_{-95}$
7.9250 $^{+0.0050}_{-0.0025}$	0.00 $^{+26.40}_{-0.00}$	-0.82 $^{+0.71}_{-0.57}$	3.7	(Ni XXII	$2s^2 2p^3$	$2s2p2p5d$	7.9097	1.56)	580 $^{+190}_{-95}$
				(Ni XXII	$2s^2 2p^3$	$2s2p2p5d$	7.9137	1.27)	429 $^{+189}_{-95}$
				(Ni XXII	$2s^2 2p^3$	$2s2p2p5d$	7.9144	2.24)	401 $^{+189}_{-95}$
				(Ni XXII	$2s^2 2p^3$	$2s2p2p5d$	7.9146	1.22)	393 $^{+189}_{-95}$
7.9607 $^{+0.0052}_{-0.0040}$	6.29 $^{+15.26}_{-6.29}$	1.65 $^{+1.26}_{-0.80}$	12.9	(Ni XXII	$2s2p^4$	$2s2p2p5d$	7.952:	4.34)	295 $^{+195}_{-152}$
				(Ni XXIII	$1s^2 2s^2 2p^2$	$1s^2 2s2p4p$	7.960:	3.66	22 $^{+195}_{-152}$
7.9745 $^{+0.0005}_{-0.0020}$	0.00 $^{+12.13}_{-0.00}$	2.04 $^{+0.90}_{-0.84}$	20.3	(Ni XXIV	$1s^2 2s2p^2$	$1s^2 2s2p4d$	7.972:	4.32	74 $^{+18}_{-76}$

Table A III.1: List of lines in the ‘non-dip’ spectrum – sorted by wavelength (continued)

λ [Å]	FWHM [mÅ]	EW [mÅ]	$\Delta\chi^2$	ion <i>i</i>	transition <i>j</i>	λ_0 [Å] $\times 10^{12}$ s ⁻¹	A_{ji}	$\Delta\lambda/\lambda \cdot c$ [km/s]	
7.9900 ^{+0.0024} _{-0.0032}	0.15 ^{+16.77} _{-0.15}	-1.77 ^{+0.68} _{-0.92}	21.2	(Fe XXIV	<u>1s²2s</u>	1s ² 4p	7.9857	3.24) ←	160 ⁺⁸⁹ ₋₁₂₂
				(Fe XXIV	<u>1s²2s</u>	1s ² 4p	7.9960	3.30)	-226 ⁺⁸⁹ ₋₁₂₁
8.0291 ^{+0.0077} _{-0.0044}	0.14 ^{+37.27} _{-0.14}	0.91 ^{+0.80} _{-0.72}	4.4	Ni XXII	2s2p ⁴	2s2p ² 2p5d	8.032:	1.61	-116 ⁺²⁸⁷ ₋₁₆₃
				Ni XXII	2s ² 2p ³	2p2p ³ 4d	8.034:	1.43	-189 ⁺²⁸⁷ ₋₁₆₃
				Ni XXII	2s ² 2p ³	2s ² 2p ² 5d	8.034'	3.89	-210 ⁺²⁸⁷ ₋₁₆₃
8.0485 ^{+0.0056} _{-0.0044}	2.93 ^{+26.44} _{-2.93}	1.58 ^{+0.71} _{-0.89}	10.2	(Ni XXIV	<u>1s²2s2p</u> ²	1s ² 2s2p4d	8.043'	4.10)	178 ⁺²⁰⁷ ₋₁₆₃
				Ni XXIV	<u>1s²2s2p</u> ²	1s ² 2s2p4d	8.048:	3.83	1 ⁺²⁰⁷ ₋₁₆₃
				Ni XXII	2s2p ⁴	2s2p ³ 5d	8.049:	4.98	-33 ⁺²⁰⁷ ₋₁₆₃
				Ni XXIII	1s ² 2s ² p ²	1s ² 2s2p2p4	8.0490	3.52	-40 ⁺²⁰⁷ ₋₁₆₃
				Ni XXIV	<u>1s²2s2p</u> ²	1s ² 2s2p4d	8.053:	9.77	-177 ⁺²⁰⁷ ₋₁₆₃
8.1000 ^{+0.0200} _{-0.0200}	0.00 ^{+75.42} _{-0.00}	0.61 ^{+0.84} _{-0.61}	2.2	Fe XXII	<u>1s²2s2p</u> ²	1s ² 2s2p5d	8.106:	3.83	-232 ⁺⁷⁴⁰ ₋₇₄₀
				Fe XXII	<u>1s²2s2p</u> ²	1s ² 2s2p5d	8.107:	2.19	-284 ⁺⁷⁴⁰ ₋₇₄₀
8.1325 ^{+0.0399} _{-0.0399}	0.00 ^{+50.00} _{-0.00}	0.44 ^{+0.78} _{-0.44}	1.0	Ni XXI	2s2p ⁵	2s2p ⁴ 5d	8.115:	3.28	621 ⁺¹⁴⁷⁵ ₋₁₄₇₅
				Ni XXI	2s2p ⁵	2s2p ⁴ 5d	8.117:	1.65	555 ⁺¹⁴⁷⁵ ₋₁₄₇₅
8.1625 ^{+0.0050} _{-0.0025}	0.00 ^{+14.67} _{-0.00}	0.95 ^{+0.78} _{-0.81}	3.9	Ni XXII	2s2p ⁴	2s2p ³ 5d	8.166:	3.16	-159 ⁺¹⁸² ₋₉₃
				Ni XXI	2p ⁶	2p2p ⁴ 5d	8.168:	5.24)	-205 ⁺¹⁸² ₋₉₃
				Fe XXII	<u>1s²2s²2p</u>	1s ² 2s ² 5d	8.168:	2.88)	-215 ⁺¹⁸² ₋₉₃
8.2201 ^{+0.0050} _{-0.0026}	0.00 ^{+22.48} _{-0.00}	1.13 ^{+0.87} _{-0.84}	5.1	Ni XXIII	<u>1s²2s2p</u> ³	1s ² 2s2p ² 4d	8.220:	1.21	-3 ⁺¹⁸¹ ₋₉₃
				Ni XXII	2s2p ⁴	2p2p ³ 4p	8.226:	1.95)	-217 ⁺¹⁸⁰ ₋₉₃
				Ni XXIII	<u>1s²2s2p</u> ³	1s ² 2s2p ² 4d	8.227:	1.50)	-259 ⁺¹⁸⁰ ₋₉₃
				Ni XXII	2s ² 2p ³	2s2p2p ² 4p	8.228:	1.09)	-294 ⁺¹⁸⁰ ₋₉₃
8.2726 ^{+0.0074} _{-0.0026}	0.01 ^{+16.66} _{-0.01}	1.10 ^{+0.83} _{-0.85}	4.7	Ni XXIII	<u>1s²2s2p</u> ³	1s ² 2s2p2p4	8.276:	11.4	-139 ⁺²⁶⁸ ₋₉₄
				Fe XXII	<u>1s²2s2p</u> ²	1s ² 2s2p5d	8.274:	4.53	-51 ⁺²⁶⁸ ₋₉₄
				Ni XXII	2s2p ⁴	2s2p ² 5d	8.272:	3.65	-12 ⁺²⁶⁸ ₋₉₄
8.3062 ^{+0.0038} _{-0.0014}	0.02 ^{+19.98} _{-0.02}	-1.72 ^{+0.66} _{-0.60}	17.6	(Fe XXIII	<u>1s²2s</u> ²	1s ² 2s4p	8.3038	4.66) ←	88 ⁺¹³⁵ ₋₄₉
				(Ni XXIII	<u>1s²2s²2p</u> ²	1s ² 2s ² 2p4d	8.384:	5.08	-140 ⁺¹⁶⁰ ₋₃₅₈
8.3808 ^{+0.0045} _{-0.0100}	0.08 ^{+50.32} _{-0.08}	1.53 ^{+0.87} _{-0.87}	9.1	(Ni XXIII	<u>1s²2s²2p</u> ²	1s ² 2s ² 2p4d	8.389:	14.0)	-313 ⁺¹⁶⁰ ₋₃₅₇
				Ni XXI	2s ² 2p ⁴	2s2p2p ³ 4p	8.3958	0.11	154 ⁺¹⁷⁷ ₋₁₈₇
8.4001 ^{+0.0049} _{-0.0053}	0.10 ^{+32.23} _{-0.10}	-0.86 ^{+0.61} _{-0.95}	5.0	(Ni XXIII	<u>1s²2s²2p</u> ²	1s ² 2s ² 2p4d	8.4051	2.65)	-179 ⁺¹⁷⁶ ₋₁₈₇
				(Ni XXIII	<u>1s²2s²2p</u> ²	1s ² 2s ² 2p4d	8.3896	14.0)	375 ⁺¹⁷⁷ ₋₁₈₈
				(Mg XII	<u>1s</u>	2p	8.4192	12.8) ←	39 ⁺²⁶ ₋₂₉
8.4203 ^{+0.0007} _{-0.0008}	15.23 ^{+2.60} _{-1.66}	-11.98 ^{+0.90} _{-1.12}	780.0	(Mg XII	<u>1s</u>	2p	8.4246	12.8)	-154 ⁺²⁶ ₋₂₉
				Fe XXI	<u>1s²2s²2p</u> ²	1s ² 2s ² 2p5d	8.5740	2.85 ←	28 ⁺²¹⁴ ₋₁₈₀
				Fe XXI	<u>1s²2s²2p</u> ²	1s ² 2s ² 2p5d	8.5740	2.43	28 ⁺²¹⁴ ₋₁₈₀
8.5748 ^{+0.0061} _{-0.0051}	10.91 ^{+18.46} _{-10.91}	-1.75 ^{+0.90} _{-1.14}	11.0	Fe XXI	<u>1s²2s²2p</u> ²	1s ² 2s ² 2p5d	8.5740	1.55	28 ⁺²¹⁴ ₋₁₈₀
				Fe XXI	<u>1s²2s2p</u>	1s ² 2s4d	8.617:	7.04)	98 ⁺¹⁷⁴ ₋₈₇
				Fe XXI	<u>1s²2s2p</u> ³	1s ² 2s2p ² 5d	8.589:	1.67	5 ⁺¹³⁸ ₋₁₄₅
8.6200 ^{+0.0050} _{-0.0025}	0.00 ^{+16.42} _{-0.00}	1.32 ^{+1.20} _{-0.68}	8.6	Fe XXI	<u>1s²2s2p</u> ³	1s ² 2s2p ² 5d	8.591:	1.31	-66 ⁺¹³⁸ ₋₁₄₅
				Ni XXIII	2s ² 2s2p ³	1s ² 2s2p2p4	8.617:	3.42	84 ⁺¹⁷⁴ ₋₈₇
				Ni XXIII	2s ² 2s2p ³	1s ² 2s2p2p4	8.620:	4.89	-14 ⁺¹⁷⁴ ₋₈₇
				Ni XXIII	2s ² 2s2p ³	1s ² 2s2p2p4	8.623:	4.29	-122 ⁺¹⁷⁴ ₋₈₇
8.7141 ^{+0.0128} _{-0.0192}	21.69 ^{+28.31} _{-21.69}	-1.77 ^{+1.49} _{-0.98}	5.1	(Fe XXIII	<u>1s²2s2p</u> ²	1s ² 2s2p4d	8.7331	2.2e+05)	-654 ⁺⁴³⁹ ₋₆₅₈
				Ni XXVII	2s2p	1s3d	8.7069	1.7e+05	245 ⁺⁴⁴⁰ ₋₆₆₀
				(Ni XXVII	2s2p	1s3d	8.7331	1.1e+05)	-654 ⁺⁴³⁹ ₋₆₅₈
8.7403 ^{+0.0046} _{-0.0029}	0.00 ^{+17.16} _{-0.00}	-1.11 ^{+0.76} _{-0.63}	6.0	Ni XXVII	1s2s	1s3p	8.7135	1.5e+04	21 ⁺⁴⁴⁰ ₋₆₆₀
				Ni XXVII	2s ² 2p ³	2s ² 2p2p4d	8.7204	8.82	-429 ⁺⁴⁴⁰ ₋₆₅₉
				Ni XXVII	2s ² 2p ³	2s ² 2p2p4d	8.7227	7.80	-296 ⁺⁴⁴⁰ ₋₆₅₉
				(Fe XXII	<u>1s²2s2p</u> ²	1s ² 2s4d	8.7254	3.54) ←	513 ⁺¹⁶⁰ ₋₉₈
				(Fe XXII	<u>1s²2s2p</u> ²	1s ² 2s2p4p	8.7360	1.31)	149 ⁺¹⁶⁰ ₋₉₈
				Ni XXII	2s2p ⁴	2s2p34d	8.778:	4.38	254 ⁺³⁹³ ₋₂₈₈
				Ni XXII	2s2p ⁴	2s2p34d	8.782:	1.42	144 ⁺³⁹³ ₋₂₈₈
8.7862 ^{+0.0115} _{-0.0084}	0.09 ^{+74.91} _{-0.09}	0.87 ^{+0.88} _{-0.81}	3.0	Ni XX	2s2p ⁶	2s2p ² 2p ³ 5d	8.782:	5.42	121 ⁺³⁹² ₋₂₈₈
				Ni XXII	2s ² 2p ³	2s ² 2p ² 4d	8.783:	1.08	86 ⁺³⁹² ₋₂₈₈
				Fe XXI	<u>1s²2s2p</u> ³	1s ² 2s2p ² 5d	8.784:	1.58	49 ⁺³⁹² ₋₂₈₈
				Ni XX	2s2p ⁶	2s2p ² 2p ³ 5d	8.789:	2.22	-122 ⁺³⁹² ₋₂₈₈
				Ni XXII	2s2p ⁴	2s2p2p ² 4d	8.790:	1.00	-141 ⁺³⁹² ₋₂₈₈
				Ni XXII	2s2p ⁴	2s2p2p ² 4d	8.886:	9.27	204 ⁺¹³⁵ ₋₂₅₁
				Ni XXII	2s2p ⁴	2s2p2p ² 4d	8.890:	5.52	57 ⁺¹³⁵ ₋₂₅₁
8.8924 ^{+0.0040} _{-0.0074}	2.97 ^{+14.38} _{-2.97}	1.48 ^{+0.99} _{-0.85}	8.2	Ni XXII	2p ⁵	2p2p ³ 4d	8.891:	6.91	42 ⁺¹³⁵ ₋₂₅₁

Table A III.1: List of lines in the ‘non-dip’ spectrum – sorted by wavelength (continued)

λ [Å]	FWHM [mÅ]	EW [mÅ]	$\Delta\chi^2$	ion <i>i</i>	transition <i>j</i>	λ_0 [Å] $\times 10^{12}$	A_{ji} [Å] $\times 10^{12}$	$\Delta\lambda/\lambda \cdot c$ [km/s]	
8.9125 ^{+0.0150} _{-0.0100}	0.00 ^{+75.00} _{-0.00}	0.96 ^{+0.79} _{-0.95}	2.8	Ni XXI	$2s2p^5$	$2s2p^44d$	8.905 [!]	8.11	235 ⁺⁵⁰⁶ ₋₃₃₆
				Ni XXII	$2s^22p^3$	$2s^22p^24d$	8.906 [!]	9.54	200 ⁺⁵⁰⁶ ₋₃₃₆
				Ni XXII	$2s2p^4$	$2s2p^34d$	8.908 [!]	6.78	132 ⁺⁵⁰⁵ ₋₃₃₆
				Ni XXI	$2s^22p^4$	$2s^22p^34d$	8.920 [!]	7.75	-277 ⁺⁵⁰⁵ ₋₃₃₅
8.9275 ^{+0.0025} _{-0.0075}	0.00 ^{+52.16} _{-0.00}	1.40 ^{+0.89} _{-0.87}	7.3	Ni XXI	$2s^22p^4$	$2s^22p^2p^24d$	8.921 [!]	3.18	189 ⁺⁸⁵ ₋₂₅₁
				Fe XXIII	$1s^22p^2$	$1s^22p4d$	8.929 [!]	6.22	-67 ⁺⁸⁵ ₋₂₅₁
8.9775 ^{+0.0002} _{-0.0030}	0.05 ^{+21.73} _{-0.05}	-2.73 ^{+0.67} _{-0.22}	41.6	Fe XXII	$1s^22s^22p$	$1s^22s^24d$	8.9748	5.30 ←	89 ⁺⁵ ₋₁₀₀
9.0478 ^{+0.0075} _{-0.0079}	9.45 ^{+18.09} _{-9.45}	1.29 ^{+1.17} _{-0.90}	5.4	Ni XXII	$2s2p^4$	$2s2p^22p4d$	9.040 [!]	8.33	229 ⁺²⁵⁰ ₋₂₆₁
				Ni XXI	$2s^22p^4$	$2s^22p^2p^24d$	9.041 [!]	8.23	200 ⁺²⁵⁰ ₋₂₆₁
				Ni XXI	$2s^22p^4$	$2s^22p^34d$	9.044 [!]	7.60	99 ⁺²⁵⁰ ₋₂₆₁
				Ni XXI	$2s^22p^4$	$2s^22p^2p^24d$	9.046 [!]	6.43	31 ⁺²⁵⁰ ₋₂₆₁
				Ni XXI	$2s^22p^4$	$2s^22p^34d$	9.053 [!]	12.8	-179 ⁺²⁵⁰ ₋₂₆₁
9.1672 ^{+0.0011} _{-0.0016}	17.02 ^{+4.41} _{-3.44}	-8.97 ^{+1.14} _{-1.18}	293.7	(Mg XI	$1s^2$	$1s2p$	9.1687	19.5) ←	-52 ⁺³⁷ ₋₅₃
9.1918 ^{+0.0032} _{-0.0048}	13.21 ^{+8.85} _{-6.83}	-3.35 ^{+1.28} _{-1.02}	35.3	Fe XXI	$1s^22s^22p^2$	$1s^22s2p^24p$	9.1944	2.88 ←	-85 ⁺¹⁰⁵ ₋₁₅₆
				(Fe XX	$2s^22p^3$	$2s2p2p^24p$	9.1979	1.04)	-200 ⁺¹⁰⁵ ₋₁₅₆
				(Fe XX	$2s^22p^3$	$2s^22p^25d$	9.1979	0.49)	-197 ⁺¹⁰⁵ ₋₁₅₆
9.2350 ^{+0.0000} _{-0.0050}	0.00 ^{+12.46} _{-0.00}	2.02 ^{+1.00} _{-0.95}	13.2	(Mg XI	$1s^2$	$1s2p$	9.228 [!]	0.000) ←	222 ⁺⁰ ₋₁₆₂
				Mg XI	$1s^2$	$1s2p$	9.231 [!]	0.034	123 ⁺⁰ ₋₁₆₂
9.2600 ^{+0.0028} _{-0.0031}	0.09 ^{+14.38} _{-0.09}	1.85 ^{+0.88} _{-0.94}	10.8	Ni XX	$2s2p^6$	$2s2p2p^44d$	9.261 [!]	7.19	-57 ⁺⁸⁹ ₋₁₀₁
				(Fe XXII	$1s^22s2p^2$	$1s^22s2p4d$	9.263 [!]	5.69)	-95 ⁺⁸⁹ ₋₁₀₁
				(Ni XX	$2s2p^6$	$2s2p^2p^34d$	9.264 [!]	4.87)	-143 ⁺⁸⁹ ₋₁₀₁
				(Ni XXV	$1s^22s2p$	$1s^22p3p$	9.268 [!]	8.79)	-261 ⁺⁸⁹ ₋₁₀₁
				Ni XXI	$2s^22p^4$	$2s^22p^2p4s$	9.2763	0.86	68 ⁺¹²⁴ ₋₁₅₇
9.2784 ^{+0.0038} _{-0.0049}	5.57 ^{+21.39} _{-5.57}	-1.94 ^{+0.83} _{-1.28}	15.0	Fe XX	$2s2p^4$	$2s2p2p^25d$	9.2788	2.21	-11 ⁺¹²⁴ ₋₁₅₇
				Fe XX	$2s2p^4$	$2s2p2p^25d$	9.2792	2.08	-24 ⁺¹²⁴ ₋₁₅₇
				Fe XX	$2s2p^4$	$2s2p^35d$	9.2812	2.42	-90 ⁺¹²⁴ ₋₁₅₇
9.3100 ^{+0.0050} _{-0.0000}	0.00 ^{+16.24} _{-0.00}	2.45 ^{+1.05} _{-0.99}	17.9	Mg XI	$1s^2$	$1s2s$	9.314 [!]	0.000	-140 ⁺¹⁶¹ ₋₀
9.3311 ^{+0.0073} _{-0.0087}	13.00 ^{+34.72} _{-13.00}	1.94 ^{+1.46} _{-1.12}	9.0	Ni XXV	$1s^22s2p$	$1s^22p3p$	9.323 [!]	1.36	238 ⁺²³⁵ ₋₂₈₀
				Fe XX	$2s2p^4$	$2p2p^34p$	9.331 [!]	1.33	4 ⁺²³⁵ ₋₂₈₀
				Fe XX	$2s2p^4$	$2p2p^34p$	9.324 [!]	0.88	207 ⁺²³⁵ ₋₂₈₀
				Fe XX	$2s^22p^3$	$2s2p^34p$	9.321 [!]	0.87)	297 ⁺²³⁵ ₋₂₈₀
				Fe XXI	$1s^22s2p^3$	$1s^22s2p^24d$	9.323 [!]	0.83	252 ⁺²³⁵ ₋₂₈₀
9.3676 ^{+0.0062} _{-0.0062}	22.07 ^{+21.35} _{-12.07}	-3.18 ^{+1.26} _{-1.50}	21.0						
9.3956 ^{+0.0083} _{-0.0038}	2.39 ^{+30.98} _{-2.39}	-1.69 ^{+0.87} _{-1.50}	11.0	(Ni XXV	$1s^22s^2$	$1s^22s3p$	9.3900	6.30)	178 ⁺²⁶⁷ ₋₁₂₁
9.4048 ^{+0.0004} _{-0.0073}	0.03 ^{+19.97} _{-0.03}	1.46 ^{+0.97} _{-0.93}	6.9	Ni XXV	$1s^22s2p$	$1s^22p3p$	9.399 [!]	9.21	178 ⁺¹⁴ ₋₂₃₂
				Fe XX	$2s2p^4$	$2s2p^2p5d$	9.404 [!]	3.65	19 ⁺¹⁴ ₋₂₃₂
				Fe XXI	$1s^22s2p^3$	$1s^22p2p^24p$	9.402 [!]	2.09	72 ⁺¹⁴ ₋₂₃₂
9.4745 ^{+0.0023} _{-0.0012}	11.02 ^{+4.74} _{-8.19}	-6.05 ^{+1.12} _{-1.11}	131.3	(Ne X	$1s$	$5p$	9.4807	0.34) ←	-195 ⁺⁷³ ₋₃₈
				(Ne X	$1s$	$5p$	9.4809	0.34)	-202 ⁺⁷³ ₋₃₈
				(Fe XXI	$1s^22s^22p^2$	$1s^22s2p2p4d$	9.4797	6.12)	-164 ⁺⁷³ ₋₃₈
9.5116 ^{+0.0043} _{-0.0046}	12.29 ^{+17.79} _{-12.29}	3.14 ^{+1.46} _{-1.25}	19.9	(Fe XXI	$1s^22s^2p^3$	$1s^22s2p2p4$	9.512 [!]	4.02	-19 ⁺¹³⁶ ₋₁₄₆
				Fe XXI	$1s^22s^2p^3$	$1s^22s2p2p4$	9.514 [!]	2.45	-13 ⁺¹³⁶ ₋₁₄₆
				Fe XXI	$1s^22s^2p^3$	$1s^22s2p2p4$	9.514 [!]	2.33	-93 ⁺¹³⁶ ₋₁₄₆
				(Fe XXVI	$2s$	$3p$	9.536 [!]	10.1)	53 ⁺¹⁵⁶ ₋₁₆
9.7080 ^{+0.0028} _{-0.0020}	23.47 ^{+4.99} _{-5.70}	-8.57 ^{+1.38} _{-1.29}	153.7	Ne X	$1s$	$4p$	9.7080	0.67 ←	-1 ⁺⁸⁵ ₋₆₂
				Ne X	$1s$	$4p$	9.7085	0.67	-15 ⁺⁸⁵ ₋₆₂
9.8161 ^{+0.0043} _{-0.0043}	9.07 ^{+15.05} _{-9.07}	2.77 ^{+1.26} _{-1.25}	15.6	Fe XXI	$1s^22s2p^3$	$1s^22s2p24d$	9.818 [!]	4.90	-82 ⁺¹³¹ ₋₁₃₂
				Fe XXI	$1s^22s2p^3$	$1s^22s2p^24d$	9.819 [!]	2.45	-96 ⁺¹³¹ ₋₁₃₂
				Fe XX	$2s2p^4$	$2p2p^24p$	9.812 [!]	0.87	108 ⁺¹³² ₋₁₃₂
9.8739 ^{+0.0200} _{-0.0200}	0.10 ^{+49.90} _{-0.10}	0.93 ^{+1.08} _{-0.93}	2.3	Fe XXI	$1s^22s2p^3$	$1s^22s2p2p4$	9.871 [!]	3.19	70 ⁺⁶⁰⁷ ₋₆₀₇
				Ni XXV	$1s^22p^2$	$1s^22p3d$	9.873 [!]	16.5	27 ⁺⁶⁰⁷ ₋₆₀₇
9.9066 ^{+0.0040} _{-0.0037}	2.75 ^{+21.58} _{-2.75}	2.48 ^{+1.23} _{-1.16}	12.7	(Ni XXV	$1s^22p^2$	$1s^22p3d$	9.924 [!]	9.00)	-526 ⁺¹²² ₋₁₁₁
				(Ni XXV	$1s^22p^2$	$1s^22p3d$	9.938 [!]	8.84)	-948 ⁺¹²² ₋₁₁₁
9.9361 ^{+0.0063} _{-0.0168}	22.66 ^{+27.34} _{-15.63}	2.36 ^{+1.78} _{-1.43}	7.4	(Ni XXV	$1s^22p^2$	$1s^22p3d$	9.907 [!]	1.86)	862 ⁺¹⁹² ₋₅₀₉
				(Ni XXIII	$1s^22s^22p^2$	$1s^22s2p23p$	9.906 [!]	0.69)	906 ⁺¹⁹² ₋₅₀₉
				(Fe XXI	$1s^22s2p^3$	$1s^22s2p2p4$	9.911 [!]	0.57)	737 ⁺¹⁹² ₋₅₀₉
				(Fe XXI	$1s^22s2p^3$	$1s^22s2p2p4$	9.908 [!]	0.54)	835 ⁺¹⁹² ₋₅₀₉
9.9724 ^{+0.0400} _{-0.0000}	21.56 ^{+18.44} _{-21.56}	-0.19 ^{+0.19} _{-1.48}	0.0	(Ni XXV	$1s^22p^2$	$1s^22p3d$	9.9240	9.00)	1461 ⁺¹²⁰⁸ ₋₀
				(Ni XXV	$1s^22p^2$	$1s^22p3d$	9.9380	8.84)	1036 ⁺¹²⁰⁷ ₋₀

Table A III.1: List of lines in the ‘non-dip’ spectrum – sorted by wavelength (continued)

λ [Å]	FWHM [mÅ]	EW [mÅ]	$\Delta\chi^2$	ion <i>i</i>	transition <i>j</i>	λ_0 [Å] $\times 10^{12}$	A_{ji} [Å] $\times 10^{12}$	$\Delta\lambda/\lambda \cdot c$ [km/s]	
9.9924 $^{+0.0041}_{-0.0030}$	7.10 $^{+10.08}_{-7.10}$	-2.76 $^{+1.05}_{-1.00}$	20.4	(Fe XX	$2s^2 2p^3$	$2s^2 2p_2 p4d$	9.9977	6.56) ←
				(Fe XX	$2s^2 2p^3$	$2s^2 2p^2 4d$	10.0004	5.80)
				Fe XX	$2s^2 2p^3$	$2s^2 2p_2 p4d$	9.9935	0.81	-33 $^{+124}_{-89}$
				(Fe XX	$2s^2 2p^3$	$2s^2 2p^2 4d$	10.0054	3.01) -391 $^{+123}_{-89}$
10.0335 $^{+0.0030}_{-0.0029}$	21.88 $^{+6.75}_{-5.11}$	-6.85 $^{+1.33}_{-1.43}$	86.7						
10.1249 $^{+0.0054}_{-0.0200}$	4.37 $^{+33.85}_{-4.37}$	-1.77 $^{+0.99}_{-2.05}$	8.9	Fe XX	$2s^2 2p^3$	$2s^2 2p^2 4d$	10.1203	2.12	← 137 $^{+160}_{-592}$
10.2377 $^{+0.0023}_{-0.0004}$	0.26 $^{+2.86}_{-0.26}$	-4.80 $^{+0.68}_{-0.48}$	108.5	(Fe XX	$2s^2 2p^3$	$2s^2 2p^2 4d$	10.1322	0.39) -216 $^{+160}_{-592}$
				Ne X	$1s$	$3p$	10.2385	1.65	← -24 $^{+68}_{-11}$
				Ne X	$1s$	$3p$	10.2396	1.64	-56 $^{+68}_{-11}$
10.2799 $^{+0.0025}_{-0.0105}$	0.23 $^{+40.24}_{-0.23}$	2.86 $^{+1.20}_{-1.16}$	19.7	(Ni XXIV	$1s^2 2s^2 2p$	$1s^2 2s^2 3d$	10.2771	21.9	
				Fe XX	$2p^5$	$2p_2 p^3 4d$	10.2698	5.14	295 $^{+74}_{-307}$
				(Fe XX	$2p^5$	$2s_2 p_2 p^2 5f$	10.2644	1.83) 453 $^{+74}_{-307}$
				(Fe XX	$2p^5$	$2s_2 p_2 p^2 5f$	10.2644	1.44) 453 $^{+74}_{-307}$
10.3025 $^{+0.0034}_{-0.0025}$	0.08 $^{+11.95}_{-0.08}$	2.55 $^{+1.47}_{-1.02}$	18.0	(Ni XXIII	$1s^2 2s_2 p^3$	$1s^2 2p_2 p^2 3p$	10.2991	3.26)
				Ni XXIII	$1s^2 2s_2 2p^2$	$1s^2 2s_2 p^2 3p$	10.3011	1.01	102 $^{+98}_{-73}$
10.3201 $^{+0.0024}_{-0.0001}$	0.01 $^{+5.83}_{-0.01}$	2.83 $^{+1.22}_{-1.17}$	18.0	(Ni XXIII	$1s^2 2s_2 p^3$	$1s^2 2p^3 3p$	10.3081	8.10) 33 $^{+98}_{-73}$
				(Fe XVIII	$2s^2 2p^5$	$2s^2 2p^4 5d$	10.3101	2.14) 276 $^{+71}_{-4}$
10.3375 $^{+0.0050}_{-0.0025}$	0.00 $^{+12.39}_{-0.00}$	1.94 $^{+1.05}_{-1.22}$	8.1	Ni XXIV	$1s^2 2s_2 p^2$	$1s^2 2s_2 p_3 d$	10.3371	5.45	
				Fe XX	$2p^5$	$2p^4 4s$	10.3381	0.81	-23 $^{+145}_{-72}$
10.4825 $^{+0.0049}_{-0.0006}$	0.01 $^{+15.33}_{-0.07}$	3.49 $^{+0.87}_{-0.95}$	28.6	Ni XXIII	$1s^2 2s_2 s^2 p^2$	$1s^2 2s_2 p^2 3p$	10.4841	5.77	
				Ni XXII	$2s_2 p^4$	$2p_2 p^2 3p$	10.4831	3.43	-64 $^{+140}_{-19}$
10.6207 $^{+0.0010}_{-0.0013}$	5.19 $^{+3.91}_{-5.18}$	-6.65 $^{+0.87}_{-1.03}$	164.0	(Fe XXIV	$1s^2 2s$	$1s^2 3p$	10.6190	7.19) ← 47 $^{+30}_{-37}$
				(Fe XXIV	$1s^2 2s$	$1s^2 3p$	10.6190	7.19) ← 47 $^{+30}_{-37}$
10.6389 $^{+0.0025}_{-0.0027}$	5.01 $^{+11.16}_{-5.01}$	-3.83 $^{+1.05}_{-1.47}$	42.7						
				(Fe XXIV	$1s^2 2s$	$1s^2 3p$	10.6190	7.19) ← 47 $^{+30}_{-37}$
10.6613 $^{+0.0037}_{-0.0035}$	19.99 $^{+10.15}_{-8.78}$	-5.63 $^{+1.51}_{-1.60}$	51.4	Fe XXIV	$1s^2 2s$	$1s^2 3p$	10.6630	7.41	← -47 $^{+105}_{-99}$
				(Fe XVII	$2s^2 2p^6$	$2s^2 2p^5 6d$	10.6570	1.15) 122 $^{+105}_{-99}$
10.7071 $^{+0.0064}_{-0.0051}$	21.87 $^{+13.61}_{-15.62}$	4.76 $^{+1.95}_{-1.79}$	20.7	(Ni XXIII	$1s^2 2s_2 s^2 p^2$	$1s^2 2s_2 p_3 d$	10.7071	17.6	-22 $^{+179}_{-144}$
				Ni XXIII	$1s^2 2s_2 s^2 p^2$	$1s^2 2s_2 p_3 d$	10.7091	14.3	-54 $^{+179}_{-144}$
				Ni XXIV	$1s^2 2s_2 s^2 p^2$	$1s^2 2s_2 p_3 d$	10.7011	8.86	144 $^{+179}_{-144}$
				(Ni XXIII	$1s^2 2s_2 s^2 p^3$	$1s^2 2s_2 p_3 d$	10.7131	5.64	-171 $^{+179}_{-144}$
				(Ni XXIII	$1s^2 2s_2 s^2 p^3$	$1s^2 2s_2 p_3 d$	10.7001	5.18) 188 $^{+179}_{-144}$
10.7223 $^{+0.0027}_{-0.0023}$	0.35 $^{+6.94}_{-0.35}$	3.52 $^{+1.41}_{-1.34}$	21.3	Ni XXIII	$1s^2 2s_2 s^2 p^2$	$1s^2 2s_2 p_3 d$	10.7211	24.5	24 $^{+76}_{-63}$
				Ni XXII	$2s^2 2p^3$	$2s_2 p^3 3p$	10.7201	4.58	41 $^{+76}_{-63}$
				Ni XXII	$2s_2 p^4$	$2p_2 p^3 3p$	10.7201	2.76	57 $^{+76}_{-63}$
10.7407 $^{+0.0143}_{-0.0032}$	0.17 $^{+29.25}_{-0.17}$	2.15 $^{+1.25}_{-1.21}$	8.8	Ni XXIII	$1s^2 2s_2 p^3$	$1s^2 2s_2 p_3 d$	10.7431	34.9	-87 $^{+398}_{-89}$
				Ni XXIII	$1s^2 2s_2 p^3$	$1s^2 2s_2 p_3 d$	10.7521	29.9	-326 $^{+398}_{-89}$
				(Ni XXIII	$1s^2 2s_2 s^2 p^2$	$1s^2 2s_2 p_3 d$	10.7581	10.6	-483 $^{+397}_{-89}$
				(Ni XXIII	$1s^2 2s_2 s^2 p^3$	$1s^2 2s_2 p_3 d$	10.7361	8.86	117 $^{+398}_{-89}$
10.7600 $^{+0.0050}_{-0.0025}$	0.00 $^{+12.06}_{-0.00}$	-0.87 $^{+0.57}_{-1.80}$	4.2	(Ne IX	$1s^2$	$1s 5p$	10.7650	0.52) ← -138 $^{+138}_{-71}$
10.8175 $^{+0.0075}_{-0.0025}$	0.00 $^{+11.04}_{-0.00}$	-1.59 $^{+0.90}_{-1.09}$	7.5	Ni XXIII	$1s^2 2s_2 p^3$	$1s^2 2s_2 p_3 d$	10.8197	18.3	-60 $^{+207}_{-70}$
				Ni XXIII	$1s^2 2s_2 p^3$	$1s^2 2s_2 p_3 d$	10.8215	11.0	-110 $^{+207}_{-70}$
				Fe XIX	$2s^2 2p^4$	$2s_2 p^3 4d$	10.8156	9.49	53 $^{+207}_{-70}$
				Fe XIX	$2s^2 2p^4$	$2s_2 p_2 p^2 4d$	10.8160	6.12	42 $^{+207}_{-70}$
				Fe XIX	$2s^2 2p^4$	$2s_2 p^3 4d$	10.8160	5.65	42 $^{+207}_{-70}$
10.8859 $^{+0.0037}_{-0.0072}$	5.09 $^{+15.34}_{-5.09}$	3.34 $^{+1.37}_{-1.31}$	18.0	(Ni XXIII	$1s^2 2p^4$	$1s^2 2p_3 d$	10.8881	18.5	-76 $^{+102}_{-199}$
				(Ni XXIII	$1s^2 2s_2 p^3$	$1s^2 2s_2 p_3 d$	10.8931	9.34	-201 $^{+102}_{-199}$
				Ni XXIV	$1s^2 2s_2 s^2 p^2$	$1s^2 2s_2 p_3 s$	10.8801	6.30	138 $^{+102}_{-199}$
10.9150 $^{+0.0025}_{-0.0027}$	0.05 $^{+19.52}_{-0.05}$	3.66 $^{+1.58}_{-1.10}$	24.7	(Ni XXIII	$1s^2 2p^4$	$1s^2 2p_2 p^2 3d$	10.9201	11.7	-143 $^{+68}_{-74}$
				(Fe XIX	$2p^6$	$2p_2 p^4 4d$	10.9231	8.25	-222 $^{+68}_{-74}$
10.9450 $^{+0.0000}_{-0.0050}$	0.00 $^{+27.55}_{-0.00}$	3.82 $^{+1.42}_{-1.32}$	23.8	Ni XXIII	$1s^2 2p^4$	$1s^2 2p_2 p^2 3d$	10.9401	28.8	130 $^{+0}_{-137}$
				Ni XXIII	$1s^2 2s_2 s^2 p^2$	$1s^2 2s_2 p_3 d$	10.9431	8.04	49 $^{+0}_{-137}$
10.9871 $^{+0.0019}_{-0.0021}$	13.68 $^{+5.10}_{-4.50}$	-7.05 $^{+1.30}_{-1.33}$	104.5	(Fe XXIII	$1s^2 2s_2$	$1s^2 2s_3 p$	10.9810	7.56) ← 167 $^{+51}_{-58}$
				(Fe XXII	$1s^2 2s_2 2p$	$1s^2 2s_2 p_3 p$	10.9935	1.35) -174 $^{+51}_{-58}$
11.0071 $^{+0.0032}_{-0.0031}$	17.86 $^{+8.15}_{-6.54}$	-5.69 $^{+1.40}_{-1.49}$	56.1	(Ne IX	$1s^2$	$1s 4p$	11.0010	1.03) ← 165 $^{+86}_{-85}$
11.0225 $^{+0.0033}_{-0.0025}$	0.03 $^{+11.44}_{-0.03}$	-2.24 $^{+0.83}_{-1.05}$	16.6	(Fe XXIII	$1s^2 2s_2$	$1s^2 2s_3 p$	11.0190	4.68) ← 96 $^{+90}_{-68}$
				(Fe XVII	$2s^2 2p^6$	$2s_2 p^6 4p$	11.0260	1.75) -95 $^{+90}_{-68}$
11.0886 $^{+0.0070}_{-0.0085}$	40.42 $^{+0.00}_{-14.98}$	8.28 $^{+2.18}_{-2.17}$	42.1	(Ni XXIII	$1s^2 2p^4$	$1s^2 2p_2 p^2 3d$	11.0891	13.3	-13 $^{+189}_{-229}$
				(Ni XXIII	$1s^2 2p^4$	$1s^2 2p_2 p^2 3d$	11.0951	12.9	-175 $^{+189}_{-228}$
				(Ni XXIII	$1s^2 2s_2 p^3$	$1s^2 2s_2 p_2 p_3 d$	11.0891	12.3	-20 $^{+189}_{-229}$
				(Ni XXI	$2s_2 p^5$	$2s_2 p_2 p^3 3d$	11.0951	10.8	-177 $^{+189}_{-228}$

Table A III.1: List of lines in the ‘non-dip’ spectrum – sorted by wavelength (continued)

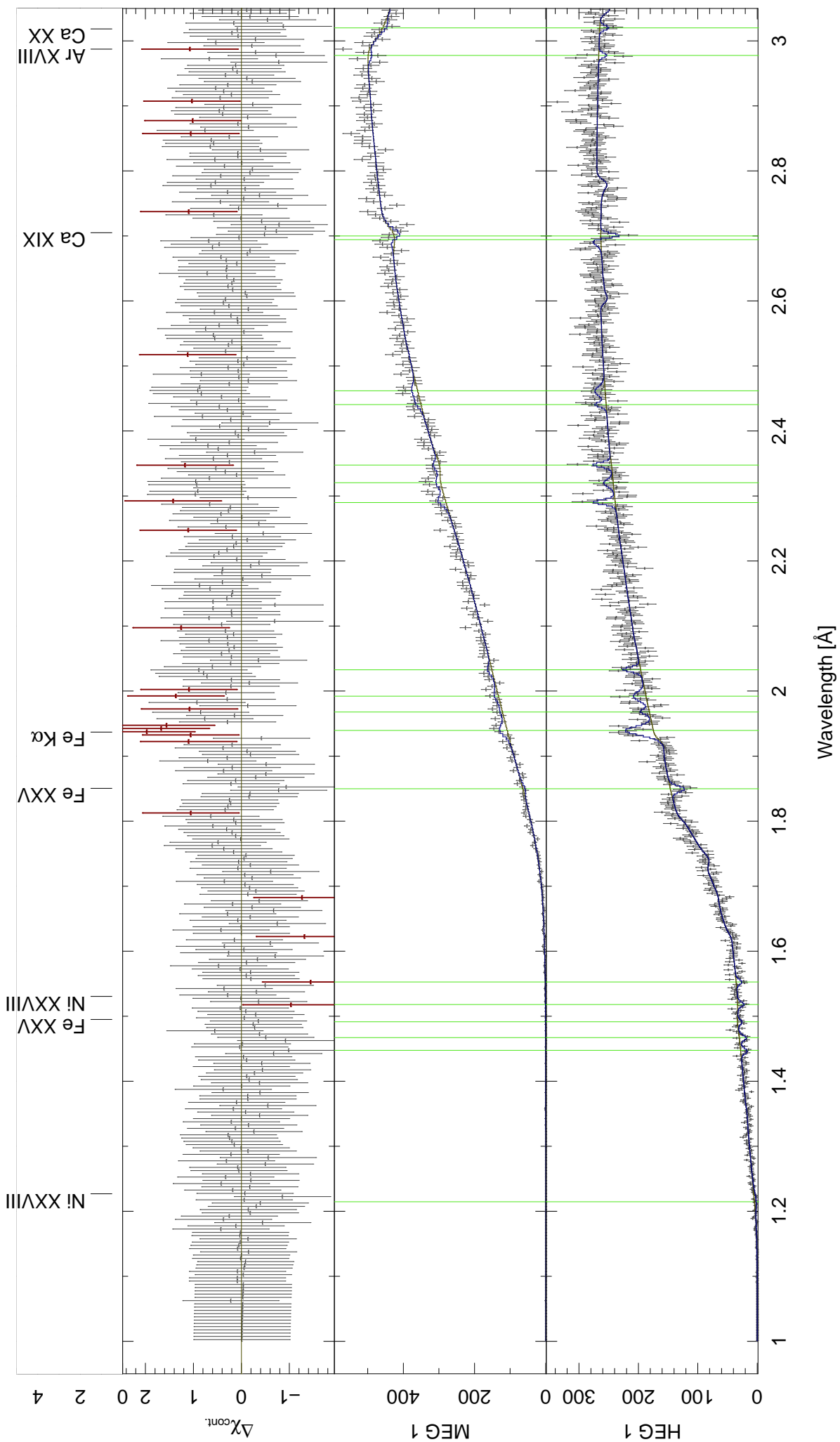
λ [Å]	FWHM [mÅ]	EW [mÅ]	$\Delta\chi^2$	ion <i>i</i>	transition <i>j</i>	λ_0 [Å] $\times 10^{12}$	A_{ji} [Å] $\times 10^{12}$	$\Delta\lambda/\lambda \cdot c$ [km/s]
11.1212 ^{+0.0188} _{-0.0212}	6.25 ^{+43.75} _{-6.25}	1.20 ^{+2.66} _{-1.20}	3.1	Ni XXIII	$1s^2 2p^4$	$1s^2 2p^3 3d$	11.117	37.9
				Ni XXIII	$1s^2 2p^4$	$1s^2 2p_2 p^3 3d$	11.115	16.5
				Ni XXIII	$1s^2 2p^4$	$1s^2 2p_2 p^2 3d$	11.125	16.5
				Ni XXI	$2s 2p^5$	$2s 2p_2 p^3 3d$	11.128	9.20
11.1516 ^{+0.0084} _{-0.0079}	24.59 ^{+25.41} _{-24.59}	4.26 ^{+2.24} _{-2.55}	15.8	Ni XXII	$2s^2 2p^3$	$2s^2 2p^2 3d$	11.146	5.26
				Ni XXIII	$1s^2 2s 2p^3$	$1s^2 2s_2 p_2 p_3$	11.149	4.51
				Ni XXIII	$1s^2 2s 2p^3$	$1s^2 2s_2 p_2 p_3$	11.147	4.46
11.1790 ^{+0.0053} _{-0.0057}	22.21 ^{+18.06} _{-10.95}	5.78 ^{+2.22} _{-2.27}	27.2	Ni XXII	$2s^2 2p^3$	$2s^2 2p_2 p_3 d$	11.181	23.0
				Fe XXIV	$1s^2 2p$	$1s^2 3d$	11.176	21.5
11.2140 ^{+0.0053} _{-0.0057}	21.20 ^{+18.30} _{-21.20}	5.55 ^{+2.31} _{-2.50}	26.4	Ni XXII	$2s^2 2p^3$	$2s^2 2p_2 p_3 d$	11.211	16.3
				Ni XXII	$2s^2 2p^3$	$2s^2 2p_2 p_3 d$	11.218	12.8
				Ni XXII	$2s 2p^4$	$2s 2p_2 p^3 d$	11.210	11.0
11.3153 ^{+0.0025} _{-0.0005}	0.08 ^{+9.91} _{-0.08}	-3.10 ^{+1.04} _{-1.02}	23.2	(Fe XVIII	$2s^2 2p^5$	$2s^2 2p_4 4d$	11.3260	4.82) ←
				(Fe XVIII	$2s^2 2p^5$	$2s^2 2p_4 4d$	11.3260	4.48)
				(Fe XVIII	$2s^2 2p^5$	$2s^2 2p_4 4d$	11.3260	3.26)
11.3710 ^{+0.0065} _{-0.0025}	0.32 ^{+43.78} _{-0.32}	3.25 ^{+1.65} _{-1.41}	14.8	Ni XXI	$2s 2p^5$	$2s 2p_2 p^2 3d$	11.375	15.5
				Ni XXI	$2s^2 2p^4$	$2s^2 2p_2 p^2 3d$	11.369	10.9
				(Fe XXIII	$1s^2 2s 2p$	$1s^2 2s_3 d$	11.366	9.35)
				Ni XXII	$2s 2p^4$	$2s 2p_2 p^2 3d$	11.372	8.88
11.4264 ^{+0.0036} _{-0.0029}	7.40 ^{+7.17} _{-7.40}	-3.96 ^{+1.15} _{-1.40}	29.9	Fe XXII	$1s^2 2s^2 2p$	$1s^2 2s_2 p_3 p$	11.4270	5.85 ←
11.4789 ^{+0.0059} _{-0.0025}	4.73 ^{+8.91} _{-4.73}	-3.16 ^{+1.47} _{-1.24}	15.4	(Fe XXII	$1s^2 2s^2 2p$	$1s^2 2s_2 p_3 p$	11.4900	6.40) ←
				(Fe XXII	$1s^2 2s^2 2p$	$1s^2 2s_2 p_3 p$	11.4900	1.68)
11.5312 ^{+0.0013} _{-0.0037}	0.00 ^{+10.14} _{-0.00}	-3.48 ^{+1.02} _{-1.01}	34.7	(Fe XVIII	$2s^2 2p^5$	$2s^2 2p_2 p^2 4d$	11.5270	3.55) ←
				(Fe XVIII	$2s^2 2p^5$	$2s^2 2p_4 4d$	11.5270	4.22)
11.5426 ^{+0.0024} _{-0.0001}	0.01 ^{+7.31} _{-0.01}	-3.47 ^{+1.05} _{-1.03}	28.4	Ne IX	$1s^2$	$1s 3p$	11.5440	2.48 ←
11.5942 ^{+0.0049} _{-0.0051}	21.03 ^{+19.40} _{-14.99}	6.56 ^{+2.62} _{-2.42}	28.9	(Ni XXII	$2s 2p^4$	$2s 2p_2 p^2 3d$	11.599	7.34)
				Ni XXII	$2s 2p^4$	$2s 2p_3 d$	11.598	7.32
				Fe XXIII	$1s^2 2p^2$	$1s^2 2p_3 d$	11.590	4.29
				Fe XXI	$1s^2 2s 2p^3$	$1s^2 2p_2 p_3 p$	11.596	3.75
				Fe XXI	$1s^2 2s 2p^3$	$1s^2 2p_2 p_3 p$	11.594	3.33
11.6256 ^{+0.0082} _{-0.0082}	30.39 ^{+10.04} _{-11.24}	6.30 ^{+2.98} _{-2.43}	20.9	(Fe XXIII	$1s^2 2p^2$	$1s^2 2p_3 d$	11.616	12.3)
				(Ni XXII	$2s 2p^4$	$2s 2p_2 p^2 3d$	11.615	9.54)
				Ni XXII	$2s 2p^4$	$2s 2p_3 d$	11.619	8.82
11.6609 ^{+0.0052} _{-0.0051}	28.21 ^{+12.21} _{-10.80}	8.85 ^{+2.83} _{-2.58}	39.7	(Ni XXII	$2s 2p^4$	$2s 2p_3 d$	11.662	10.8
				(Ni XXII	$2s 2p^4$	$2s 2p_2 p^2 3d$	11.652	2.52)
11.6952 ^{+0.0078} _{-0.0090}	40.42 ^{+0.00} _{-9.78}	8.77 ^{+2.75} _{-2.36}	34.1	(Fe XXIII	$1s^2 2p^2$	$1s^2 2p_3 d$	11.684	6.69)
				Ni XXI	$2s 2p^5$	$2s 2p_2 p^3 3d$	11.689	2.99
11.7698 ^{+0.0012} _{-0.0014}	8.77 ^{+3.89} _{-4.92}	-10.01 ^{+0.98} _{-1.94}	248.9	Fe XXII	$1s^2 2s^2 2p$	$1s^2 2s^2 3d$	11.7700	16.3 ←
				(Fe XX	$2s^2 2p^3$	$2s 2p_2 p_3 p$	11.7620	1.66)
11.8435 ^{+0.0040} _{-0.0035}	0.00 ^{+18.05} _{-0.00}	2.71 ^{+1.65} _{-1.60}	7.3	Ni XX	$2s^2 2p^5$	$2s^2 2p_2 p^3 3d$	11.846	24.1
				Fe XXII	$1s^2 2s 2p^2$	$1s^2 2s_2 p_3 d$	11.844	11.2
11.8887 ^{+0.0057} _{-0.0053}	29.52 ^{+10.90} _{-10.27}	8.81 ^{+2.78} _{-2.62}	37.3	(Fe XXII	$1s^2 2s 2p^2$	$1s^2 2s_2 p_3 d$	11.881	12.5)
				Fe XXI	$1s^2 2s 2p^2$	$1s^2 2s_2 p_2 p_3 j$	11.894	3.73
11.9700 ^{+0.0050} _{-0.0000}	0.00 ^{+9.96} _{-0.00}	-3.06 ^{+1.24} _{-1.21}	16.1	(Fe XXI	$1s^2 2s 2p^2$	$1s^2 2s_2 p_2 p_3 p$	11.9750	3.09) ←
12.0440 ^{+0.0012} _{-0.0040}	0.03 ^{+9.49} _{-0.03}	3.71 ^{+1.74} _{-1.70}	13.0	(Ca XX	$2p$	$4d$	12.048	2.70)
				(Ca XX	$2s$	$4p$	12.051	1.52)
12.0695 ^{+0.0060} _{-0.0059}	18.34 ^{+13.45} _{-9.07}	5.23 ^{+2.31} _{-2.12}	17.0	Fe XXII	$1s^2 2s 2p^2$	$1s^2 2s_2 p_3 d$	12.075	9.55
				Fe XXI	$1s^2 2s 2p^3$	$1s^2 2s_2 p_2 p_3 d$	12.076	3.49)
				Fe XX	$2s 2p^4$	$2p_2 p^3 3p$	12.071	2.58
12.1141 ^{+0.0014} _{-0.0024}	1.72 ^{+9.08} _{-1.72}	-4.09 ^{+1.08} _{-1.07}	45.2	(Fe XVII	$2s^2 2p^6$	$2s^2 2p_5 4d$	12.1240	4.83) ←
12.1287 ^{+0.0012} _{-0.0009}	19.38 ^{+3.03} _{-2.59}	-18.90 ^{+1.59} _{-1.85}	736.5	(Ne X	$1s$	$2p$	12.1321	6.16) ←
				(Ne X	$1s$	$2p$	12.1375	6.16)
12.1540 ^{+0.0045} _{-0.0048}	12.60 ^{+11.63} _{-12.60}	5.40 ^{+2.16} _{-2.12}	21.4	Ni XX	$2s^2 2p^5$	$2s^2 2p_4 3d$	12.156	3.37
				Fe XX	$2s 2p^4$	$2p_2 p_3 3p$	12.150	1.98
12.1845 ^{+0.0034} _{-0.0037}	2.15 ^{+11.41} _{-2.15}	3.15 ^{+1.72} _{-1.78}	9.9	(Fe XXI	$1s^2 2s 2p^3$	$1s^2 2s_2 p_2 p_3 d$	12.191	6.59)
				(Fe XXI	$1s^2 2s 2p^3$	$1s^2 2s_2 p_2 p_3 d$	12.193	3.99)
12.2144 ^{+0.0058} _{-0.0061}	15.87 ^{+16.52} _{-10.32}	5.07 ^{+2.41} _{-2.25}	16.2	(Fe XXI	$1s^2 2s 2p^3$	$1s^2 2s_2 p_2 p_3 d$	12.204	8.54)
				Fe XXII	$1s^2 2s 2p^2$	$1s^2 2s_2 p_3 d$	12.210	8.24
				Fe XXI	$1s^2 2s 2p^3$	$1s^2 2s_2 p_2 p_3 d$	12.209	6.40
12.2523 ^{+0.0027} _{-0.0023}	0.07 ^{+13.90} _{-0.07}	-4.27 ^{+1.25} _{-1.21}	26.3	Fe XXII	$1s^2 2s 2p^2$	$1s^2 2s_2 3s$	12.2519	0.91 ←
12.2650 ^{+0.0025} _{-0.0011}	0.32 ^{+7.58} _{-0.32}	-5.38 ^{+1.04} _{-1.23}	61.8	Fe XVII	$2s^2 2p^6$	$2s^2 2p_5 4d$	12.2660	4.21 ←
				Fe XVII	$2s^2 2p^6$	$2s^2 2p_5 4d$	12.2660	-24 ⁺⁶⁰ ₋₂₆
12.2821 ^{+0.0012} _{-0.0008}	12.49 ^{+2.02} _{-4.46}	-14.47 ^{+1.39} _{-0.98}	467.7	(Fe XXI	$1s^2 2s 2p^2$	$1s^2 2s_2 2p_3 d$	12.2840	18.2) ←
								-46 ⁺³⁰ ₋₂₀

Table A III.1: List of lines in the ‘non-dip’ spectrum – sorted by wavelength (continued)

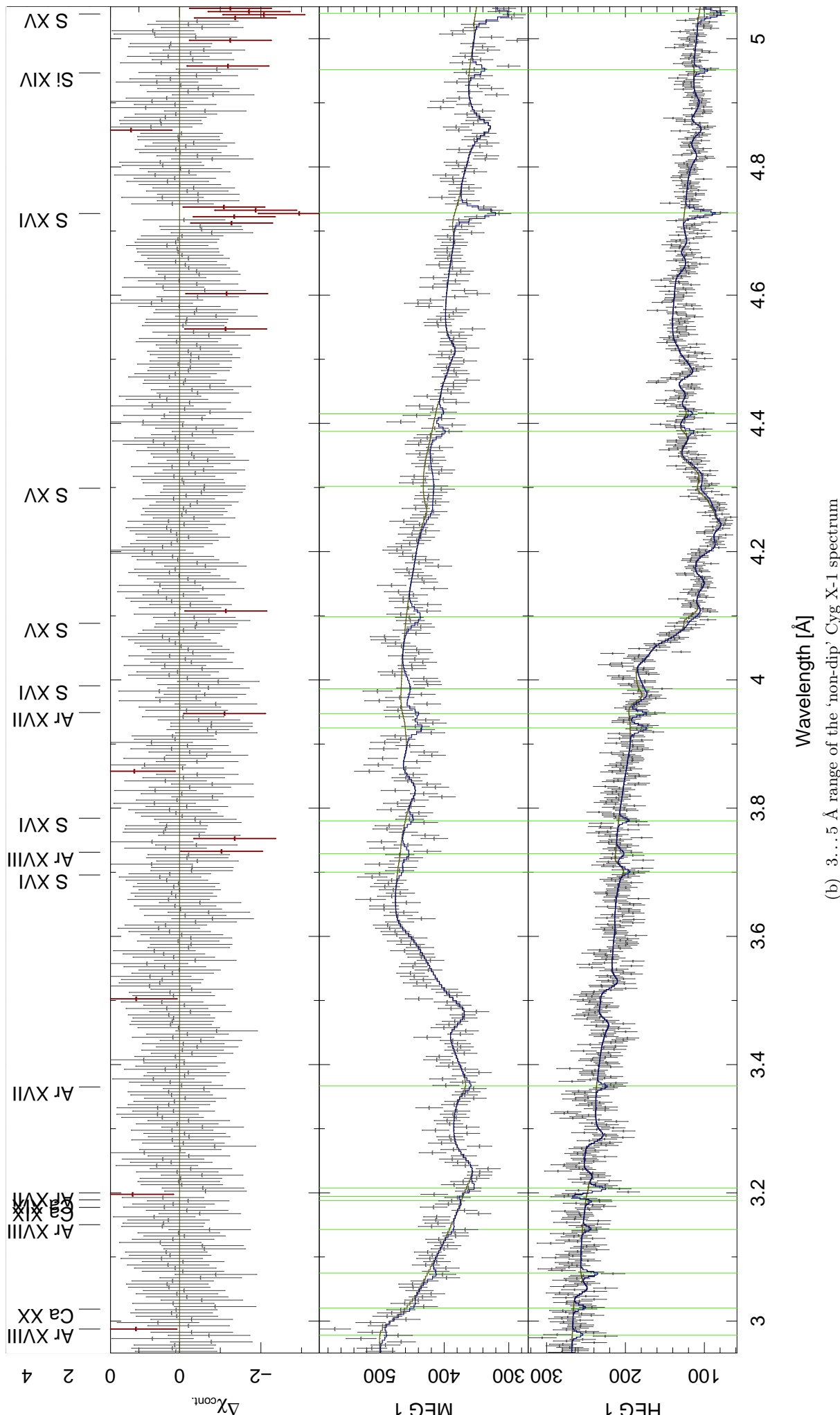
λ [Å]	FWHM [mÅ]	EW [mÅ]	$\Delta\chi^2$	ion <i>i</i>	transition <i>j</i>	λ_0 [Å] $\parallel 10^{12}\text{s}^{-1}$	A_{ji} [Å] $\parallel 10^{12}\text{s}^{-1}$	$\Delta\lambda/\lambda \cdot c$ [km/s]	
12.3150 $^{+0.0050}_{-0.0000}$	0.00 $^{+10.08}_{-0.00}$	-2.24 $^{+1.41}_{-1.38}$	7.2	(Fe XXI	$1s^2 2s2p^3$	$1s^2 2p2p^2 3p$	12.3182	3.37	-78 $^{+122}_{-0}$
				(Fe XX	$2s^2 2p^3$	$2s2p2p^2 3p$	12.3244	2.34)	-229 $^{+122}_{-0}$
12.4757 $^{+0.0081}_{-0.0091}$	25.87 $^{+14.56}_{-10.57}$	6.15 $^{+2.90}_{-2.68}$	16.0	(Fe XXI	$1s^2 2s2p^3$	$1s^2 2s2p^2 3d$	12.465t	26.9)	242 $^{+194}_{-219}$
				(Fe XXI	$1s^2 2p^4$	$1s^2 2p^3 3d$	12.463t	14.6)	302 $^{+194}_{-219}$
				Fe XXI	$1s^2 2s2p^3$	$1s^2 2s2p^2 3d$	12.472t	9.00	74 $^{+194}_{-218}$
				Fe XXI	$1s^2 2s2p^3$	$1s^2 2p2p^2 3p$	12.467t	5.82	196 $^{+194}_{-219}$
12.5661 $^{+0.0044}_{-0.0046}$	3.97 $^{+19.79}_{-3.97}$	-3.56 $^{+1.46}_{-2.27}$	15.9	(Fe XX	$2s^2 2p^3$	$2s2p2p^2 3p$	12.5760	4.39)	-237 $^{+104}_{-111}$
				(Fe XX	$2s^2 2p^3$	$2s2p^3 3p$	12.5760	4.44)	-237 $^{+104}_{-111}$
12.5810 $^{+0.0033}_{-0.0042}$	11.62 $^{+12.40}_{-11.62}$	-5.68 $^{+2.07}_{-2.15}$	31.6	(Fe XX	$2s^2 2p^3$	$2s2p2p^2 3p$	12.5760	4.39) ←	120 $^{+79}_{-99}$
				(Fe XX	$2s^2 2p^3$	$2s2p^3 3p$	12.5760	4.44)	120 $^{+79}_{-99}$
12.6233 $^{+0.0045}_{-0.0033}$	0.04 $^{+17.14}_{-0.04}$	3.44 $^{+1.98}_{-1.94}$	8.3	(Ca XVIII	$1s^2 2s$	$1s^2 5p$	12.636t	0.54)	-301 $^{+106}_{-78}$
				(Ca XVIII	$1s^2 2s$	$1s^2 5p$	12.636t	0.54)	-301 $^{+106}_{-78}$
12.6834 $^{+0.0124}_{-0.0133}$	43.24 $^{+0.04}_{-43.24}$	7.78 $^{+3.35}_{-3.32}$	14.9	Fe XXI	$1s^2 2p^4$	$1s^2 2p2p^2 3d$	12.673t	3.97	245 $^{+294}_{-314}$
				Fe XXI	$1s^2 2p^4$	$1s^2 2p2p^2 3d$	12.689t	2.00	-147 $^{+294}_{-314}$
				Fe XX	$2s2p^4$	$2s2p^3 3d$	12.688t	1.34	-121 $^{+294}_{-314}$
12.8099 $^{+0.0001}_{-0.0050}$	0.02 $^{+14.55}_{-0.02}$	-5.44 $^{+1.28}_{-2.67}$	58.1	(Ni XX	$2s^2 2p^5$	$2s^2 2p^4 3s$	12.8122	1.10)	-55 $^{+2}_{-116}$
				Fe XX	$2s2p^4$	$2s2p^2 2p3d$	12.8084	0.83	35 $^{+2}_{-116}$
12.8281 $^{+0.0012}_{-0.0016}$	18.73 $^{+4.33}_{-3.22}$	-17.49 $^{+2.14}_{-2.24}$	393.4	(Fe XX	$2s^2 2p^3$	$2s^2 2p2p3d$	12.8240	17.1) ←	95 $^{+29}_{-37}$
				Fe XX	$2s^2 2p^3$	$2s^2 2p2p3d$	12.8270	4.90	25 $^{+29}_{-37}$
12.8500 $^{+0.0016}_{-0.0021}$	0.36 $^{+13.32}_{-0.35}$	-7.08 $^{+1.38}_{-1.24}$	79.7	(Fe XX	$2s^2 2p^3$	$2s^2 2p2p3d$	12.8460	19.2) ←	92 $^{+38}_{-48}$
				(Fe XX	$2s^2 2p^3$	$2s^2 2p2p3d$	12.8640	12.1)	-327 $^{+38}_{-48}$
12.9023 $^{+0.0050}_{-0.0033}$	17.65 $^{+17.25}_{-9.52}$	-8.60 $^{+2.17}_{-3.70}$	55.7	Fe XX	$2s2p^4$	$2s2p2p^2 3d$	12.9010	11.4	31 $^{+117}_{-77}$
				Fe XX	$2s2p^4$	$2s2p2p^2 3d$	12.9030	7.58	-15 $^{+117}_{-77}$
12.9200 $^{+0.0025}_{-0.0000}$	0.01 $^{+21.12}_{-0.01}$	-4.74 $^{+1.42}_{-1.43}$	30.6	(Fe XX	$2s^2 2p^3$	$2s^2 2p2p3d$	12.9120	4.92) ←	186 $^{+59}_{-1}$
				Fe XX	$2s^2 2p^3$	$2s^2 2p2p3d$	12.9211	0.74	-25 $^{+59}_{-1}$
12.9538 $^{+0.0025}_{-0.0026}$	14.50 $^{+8.23}_{-5.82}$	-9.91 $^{+2.29}_{-2.52}$	80.3	(Fe XIX	$2s^2 2p^4$	$2s2p2p^3 3p$	12.9450	3.11) ←	204 $^{+58}_{-61}$
				(Fe XX	$2s^2 2p^3$	$2s^2 2p2p3d$	12.9650	3.46)	-259 $^{+58}_{-61}$
				(Fe XX	$2s^2 2p^3$	$2s^2 2p2p3d$	12.9654	0.66)	-268 $^{+58}_{-61}$
13.0287 $^{+0.0034}_{-0.0043}$	14.32 $^{+11.36}_{-14.32}$	-6.46 $^{+2.41}_{-2.05}$	27.9	(Fe XX	$2p^5$	$2p^4 3d$	13.0238	14.1)	113 $^{+78}_{-98}$
				(Fe XX	$2s2p^4$	$2s2p2p^2 3d$	13.0328	6.60)	-94 $^{+78}_{-98}$
				Fe XX	$2s2p^4$	$2s2p^3 3d$	13.0281	3.49	14 $^{+78}_{-98}$
13.0522 $^{+0.0051}_{-0.0031}$	11.16 $^{+13.73}_{-11.16}$	-5.76 $^{+1.90}_{-2.52}$	25.0	(Fe XX	$2s^2 2p^3$	$2s^2 2p^2 3d$	13.0610	2.62) ←	-203 $^{+116}_{-71}$
13.0725 $^{+0.0299}_{-0.0299}$	0.00 $^{+50.42}_{-0.00}$	1.77 $^{+2.22}_{-1.77}$	2.2	(Fe XX	$2s2p^4$	$2s2p2p^2 3d$	12.921t	0.74)	3529 $^{+693}_{-693}$
				(Fe XX	$2s^2 2p^3$	$2s^2 2p2p3d$	12.921t	0.74)	3513 $^{+693}_{-693}$
13.1152 $^{+0.0211}_{-0.0211}$	34.47 $^{+15.95}_{-34.47}$	4.51 $^{+3.75}_{-3.94}$	8.6	(Fe XX	$2s2p^4$	$2s2p2p^2 3d$	13.084t	24.9)	711 $^{+484}_{-484}$
				(Fe XX	$2s^2 2p^3$	$2s^2 2p^2 3d$	13.087t	15.1)	642 $^{+484}_{-484}$
				(Fe XX	$2s^2 2p^3$	$2s^2 2p^2 3d$	13.088t	13.9)	615 $^{+484}_{-484}$
				Fe XX	$2s2p^4$	$2s2p^3 3d$	13.095t	12.4	454 $^{+484}_{-484}$
				(Fe XX	$2s^2 2p^3$	$2s^2 2p^2 3d$	13.093t	8.09)	505 $^{+484}_{-484}$
				Fe XX	$2s^2 2p^3$	$2s^2 2p^2 3d$	13.100t	6.76	349 $^{+484}_{-484}$
				Fe XX	$2p^5$	$2p2p^3 3d$	13.114t	5.35	26 $^{+483}_{-483}$
				Fe XX	$2s2p^4$	$2s2p^3 3d$	13.124t	4.38	-209 $^{+483}_{-483}$
				Fe XX	$2p^5$	$2p2p^3 3d$	13.129t	3.08	-333 $^{+483}_{-483}$
				(Fe XX	$2s^2 2p^3$	$2s^2 2p2p3d$	13.137t	2.80)	-497 $^{+482}_{-482}$
13.1383 $^{+0.0044}_{-0.0033}$	0.02 $^{+17.29}_{-0.02}$	-3.19 $^{+1.95}_{-2.03}$	-1.1	Fe XX	$2s^2 2p^3$	$2s^2 2p2p3d$	13.1370	2.80	29 $^{+101}_{-75}$
				Fe XVIII	$2s2p^6$	$2p^2 2p^4 3p$	13.1427	1.95	-101 $^{+101}_{-74}$
				(Fe XX	$2s2p^4$	$2s2p2p^2 3d$	13.1458	1.82)	-172 $^{+101}_{-74}$
13.1500 $^{+0.0000}_{-0.0050}$	0.00 $^{+11.56}_{-0.00}$	7.94 $^{+2.32}_{-2.27}$	28.1	(Fe XVIII	$2s2p^6$	$2p^2 2p^4 3p$	13.142t	1.95)	167 $^{+0}_{-114}$
				Fe XX	$2s2p^4$	$2s2p2p^2 3d$	13.145t	1.82	96 $^{+0}_{-114}$
13.1550 $^{+0.0001}_{-0.0050}$	0.00 $^{+12.15}_{-0.00}$	-5.43 $^{+1.91}_{-2.13}$	31.6	Fe XX	$2s2p^4$	$2s2p^3 3d$	13.1521	6.12	65 $^{+1}_{-113}$
				Fe XX	$2s2p^4$	$2s2p2p^2 3d$	13.1547	3.95	6 $^{+1}_{-113}$
				Fe XX	$2s^2 2p^3$	$2s^2 2p2p3d$	13.1530	3.82	45 $^{+1}_{-113}$
				Fe XX	$2s^2 2p^3$	$2s^2 2p2p3d$	13.1530	2.12	45 $^{+1}_{-113}$
13.4202 $^{+0.0043}_{-0.0118}$	9.72 $^{+16.28}_{-9.72}$	-4.08 $^{+1.57}_{-2.96}$	25.2	Fe XIX	$2s^2 2p^4$	$2s^2 2p^3 3d$	13.4230	5.01 ←	-61 $^{+97}_{-263}$
13.4403 $^{+0.0020}_{-0.0021}$	19.29 $^{+4.08}_{-4.44}$	-18.54 $^{+2.47}_{-2.28}$	301.1	(Ne IX	$1s^2$	$1s2p$	13.4473	8.87) ←	-155 $^{+45}_{-46}$
13.4647 $^{+0.0030}_{-0.0035}$	20.44 $^{+8.49}_{-9.09}$	-11.81 $^{+3.60}_{-2.00}$	68.4	Fe XIX	$2s^2 2p^4$	$2s^2 2p^3 3d$	13.4620	14.1 ←	61 $^{+66}_{-79}$
13.5026 $^{+0.0019}_{-0.0016}$	17.55 $^{+4.32}_{-4.83}$	-17.72 $^{+2.57}_{-2.18}$	241.5	(Fe XIX	$2s^2 2p^4$	$2s^2 2p2p^2 3d$	13.4970	12.9) ←	125 $^{+41}_{-36}$
13.5251 $^{+0.0014}_{-0.0030}$	10.44 $^{+7.45}_{-6.78}$	-10.90 $^{+2.47}_{-1.82}$	88.5	(Fe XIX	$2s^2 2p^4$	$2s^2 2p^3 3d$	13.5180	18.7) ←	156 $^{+31}_{-67}$
				(Fe XIX	$2s^2 2p^4$	$2s^2 2p2p^2 3d$	13.5146	1.21)	232 $^{+31}_{-67}$
13.6279 $^{+0.0055}_{-0.0062}$	5.84 $^{+22.03}_{-5.84}$	-5.06 $^{+2.45}_{-3.41}$	14.5						
13.6501 $^{+0.0061}_{-0.0055}$	20.29 $^{+19.29}_{-10.10}$	-8.11 $^{+3.14}_{-3.48}$	22.3	Fe XIX	$2s^2 2p^4$	$2s^2 2p^3 3d$	13.6450	2.43 ←	112 $^{+135}_{-122}$
13.6657 $^{+0.0069}_{-0.0057}$	0.23 $^{+47.54}_{-0.23}$	-3.38 $^{+2.04}_{-2.72}$	7.3						

Table A III.1: List of lines in the ‘non-dip’ spectrum – sorted by wavelength (continued)

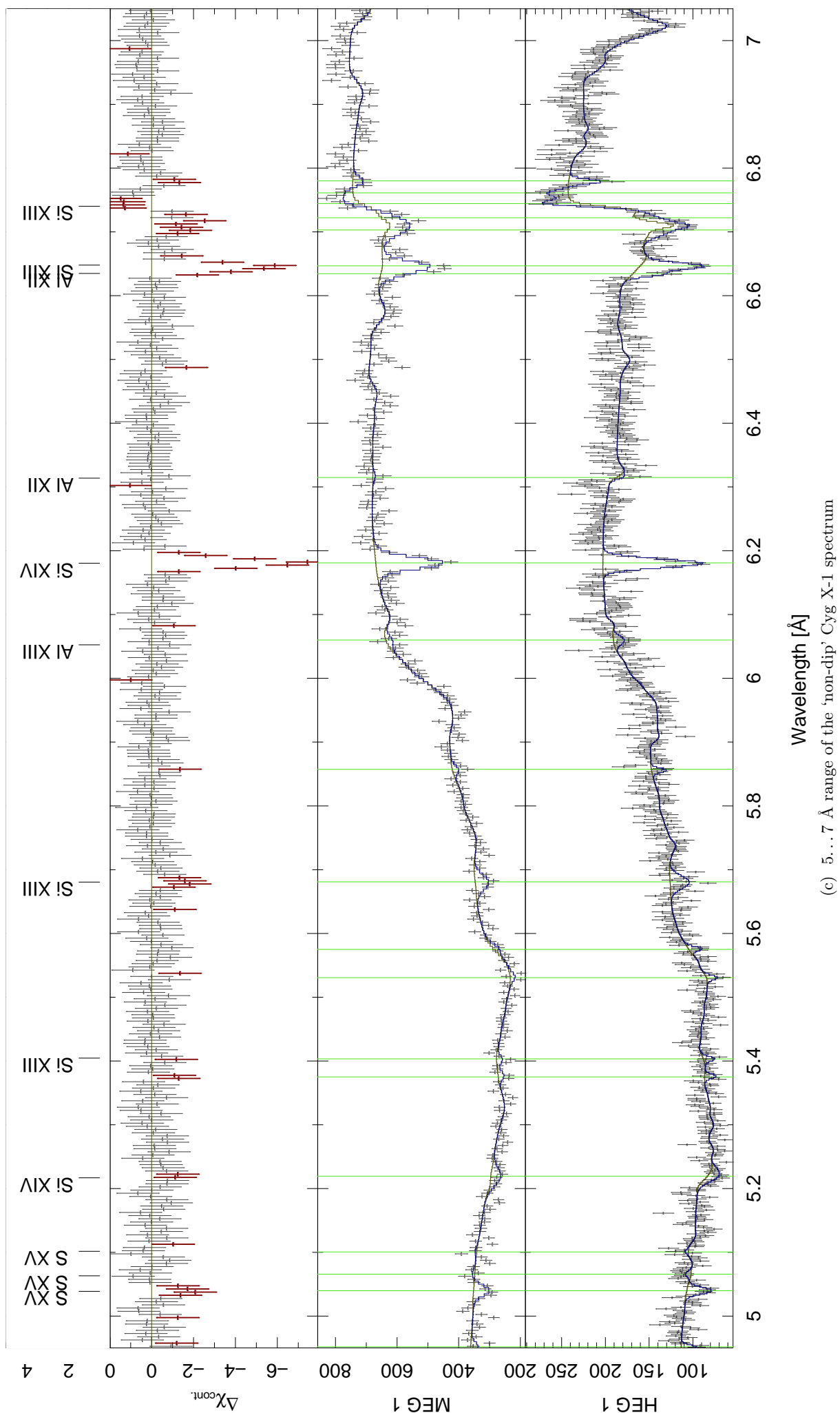
λ [Å]	FWHM [mÅ]	EW [mÅ]	$\Delta\chi^2$	ion <i>i</i>	transition <i>j</i>	λ_0 [Å] $[10^{12}\text{s}^{-1}]$	A_{ji}	$\Delta\lambda/\lambda \cdot c$ [km/s]	
13.7551 ^{+0.0099} _{-0.0049}	0.02 ^{+47.63} _{-0.02}	-4.74 ^{+2.67} _{-2.62}	8.4	(Fe XX	$2s^2 2p^3$	$2s^2 2p^2 3s$	13.7670	1.02) ←	-259 ⁺²¹⁵ ₋₁₀₈
13.7914 ^{+0.0116} _{-0.0058}	26.00 ^{+24.00} _{-19.82}	-9.25 ^{+4.05} _{-4.96}	17.8	Fe XIX	$2s^2 2p^4$	$2s^2 2p^2 2p^3 d$	13.7950	5.35 ←	-78 ⁺²⁵² ₋₁₂₆
13.8318 ^{+0.0088} _{-0.0085}	28.25 ^{+17.58} _{-20.33}	-9.17 ^{+5.40} _{-3.95}	15.6	Fe XIX	$2s^2 2p^4$	$2s^2 2p^2 2p^3 d$	13.8390	1.75 ←	-155 ⁺¹⁹⁰ ₋₁₈₅
				(Fe XX	$2s^2 2p^3$	$2s^2 2p^2 3s$	13.8430	1.00)	-242 ⁺¹⁹⁰ ₋₁₈₅
				Fe XVII	$2s^2 2p^6$	$2s 2p^6 3p$	13.8250	3.40	148 ⁺¹⁹⁰ ₋₁₈₅
14.2010 ^{+0.0029} _{-0.0034}	26.41 ^{+8.47} _{-7.78}	-21.96 ^{+4.77} _{-4.27}	142.4	(Fe XVIII	$2s^2 2p^5$	$2s^2 2p^2 p^3 3d$	14.2080	17.9) ←	-148 ⁺⁶² ₋₇₁
				(Fe XVIII	$2s^2 2p^5$	$2s^2 2p^4 3d$	14.2080	19.4)	-148 ⁺⁶² ₋₇₁
				Fe XVIII	$2s 2p^6$	$2s 2p^2 2p^3 3d$	14.2007	13.5	6 ⁺⁶² ₋₇₁
14.2525 ^{+0.0043} _{-0.0031}	10.00 ^{+13.77} _{-10.00}	-11.44 ^{+2.84} _{-4.96}	41.6	Fe XVIII	$2s^2 2p^5$	$2s^2 2p^4 3d$	14.2560	12.9 ←	-74 ⁺⁹¹ ₋₆₅
				Fe XVIII	$2s^2 2p^5$	$2s^2 2p^2 p^3 d$	14.2560	1.29	-74 ⁺⁹¹ ₋₆₅
14.3700 ^{+0.0100} _{-0.0050}	0.00 ^{+26.25} _{-0.00}	-4.49 ^{+2.94} _{-3.95}	6.3	Fe XVIII	$2s^2 2p^5$	$2s^2 2p^4 3d$	14.3730	6.75 ←	-62 ⁺²⁰⁹ ₋₁₀₄
14.5301 ^{+0.0099} _{-0.0001}	0.00 ^{+75.00} _{-0.00}	-5.97 ^{+3.07} _{-3.02}	10.1	Fe XVIII	$2s^2 2p^5$	$2s^2 2p^4 3d$	14.5340	4.05 ←	-81 ⁺²⁰⁴ ₋₂
14.6240 ^{+0.0048} _{-0.0035}	5.02 ^{+18.37} _{-5.02}	-8.80 ^{+2.78} _{-3.38}	27.1	(Fe XVIII	$2s^2 2p^5$	$2s^2 2p^4 3d$	14.6160	0.95)	164 ⁺⁹⁸ ₋₇₂
				(Fe XIX	$2s^2 2p^4$	$2s^2 2p^3 3s$	14.6359	0.11)	-244 ⁺⁹⁸ ₋₇₂
14.7150 ^{+0.0035} _{-0.0043}	0.85 ^{+19.30} _{-0.85}	10.14 ^{+4.76} _{-4.15}	15.2	(Fe XVIII	$2s 2p^6$	$2s 2p^2 2p^3 d$	14.7260	11.8)	-224 ⁺⁷¹ ₋₈₈
				(Fe XIX	$2s 2p^5$	$2s 2p^2 p^3 s$	14.7200	1.30)	-114 ⁺⁷¹ ₋₈₈
				Fe XX	$2s 2p^4$	$2s^2 2p 2p^3 p$	14.7110	0.015	73 ⁺⁷¹ ₋₈₈
15.0033 ^{+0.0058} _{-0.0026}	13.76 ^{+9.96} _{-13.75}	-13.12 ^{+3.16} _{-4.82}	42.4	(Fe XVII	$2s^2 2p^6$	$2s^2 2p^5 3d$	15.0140	27.0) ←	-214 ⁺¹¹⁶ ₋₅₁
15.1721 ^{+0.0082} _{-0.0072}	0.03 ^{+40.38} _{-0.03}	-4.71 ^{+3.24} _{-5.68}	5.7	O VIII	$1s$	$4p$	15.1760	0.27 ←	-77 ⁺¹⁶¹ ₋₁₄₂
				O VIII	$1s$	$4p$	15.1765	0.27	-86 ⁺¹⁶¹ ₋₁₄₂
15.2551 ^{+0.0259} _{-0.0259}	0.00 ^{+26.76} _{-0.00}	-3.28 ^{+3.28} _{-2.97}	2.5	Fe XVII	$2s^2 2p^6$	$2s^2 2p^5 3d$	15.2610	5.87 ←	-117 ⁺⁵⁰⁹ ₋₅₀₉
15.6200 ^{+0.0200} _{-0.0051}	0.31 ^{+74.69} _{-0.31}	-7.54 ^{+3.31} _{-3.86}	12.9	Fe XVIII	$2s^2 2p^5$	$2s^2 2p^4 3s$	15.6250	0.87	-96 ⁺³⁸⁴ ₋₉₈
16.0002 ^{+0.0051} _{-0.0043}	25.00 ^{+14.56} _{-12.27}	-20.38 ^{+5.40} _{-6.26}	63.1	(O VIII	$1s$	$3p$	16.0055	0.67) ←	-99 ⁺⁹⁶ ₋₈₀
				(O VIII	$1s$	$3p$	16.0067	0.67)	-120 ⁺⁹⁶ ₋₈₀
				Fe XVIII	$2s^2 2p^5$	$2s^2 2p^4 3s$	16.0040	1.36	-70 ⁺⁹⁶ ₋₈₀
16.2411 ^{+0.0100} _{-0.0050}	15.00 ^{+15.00} _{-15.00}	-7.95 ^{+5.09} _{-7.71}	7.3	(Ca XX	$2p$	$3d$	16.2294	8.48)	217 ⁺¹⁸⁵ ₋₉₂
				(Ca XX	$2s$	$3p$	16.2343	3.53)	127 ⁺¹⁸⁵ ₋₉₂
16.3893 ^{+0.0002} _{-0.0198}	75.00 ^{+0.00} _{-19.45}	-24.67 ^{+8.07} _{-10.59}	21.2	Ca XX	$2p$	$3d$	16.3716	10.2	324 ⁺³ ₋₃₆₃
				Ca XX	$2p$	$3d$	16.3872	1.70	39 ⁺³ ₋₃₆₂
16.7700 ^{+0.0100} _{-0.0049}	0.00 ^{+23.84} _{-0.00}	-7.34 ^{+5.71} _{-4.33}	4.8	Fe XVII	$2s^2 2p^6$	$2s^2 2p^5 3s$	16.7800	0.90 ←	-179 ⁺¹⁷⁹ ₋₈₈
17.7495 ^{+0.0200} _{-0.0200}	16.42 ^{+58.58} _{-16.42}	-5.83 ^{+5.83} _{-11.86}	1.5	Ar XVI	$1s^2 2s$	$1s^2 4p$	17.7320	0.65 ←	297 ⁺³³⁸ ₋₃₃₈
				Ar XVI	$1s^2 2s$	$1s^2 4p$	17.7420	0.65	127 ⁺³³⁸ ₋₃₃₈
18.6277 ^{+0.0162} _{-0.0177}	50.00 ^{+0.00} _{-14.23}	-33.47 ^{+14.91} _{-11.47}	16.0	O VII	$1s^2$	$1s 3p$	18.6270	0.93 ←	12 ⁺²⁶¹ ₋₂₈₅
18.7387 ^{+0.0074} _{-0.0100}	0.05 ^{+74.95} _{-0.05}	-14.83 ^{+7.61} _{-7.43}	10.3	Ca XVIII	$1s^2 2s$	$1s^2 3p$	18.7320	2.36 ←	107 ⁺¹¹⁸ ₋₁₆₀
18.9394 ^{+0.0306} _{-0.0094}	55.92 ^{+90.91} _{-22.72}	-55.11 ^{+18.40} _{-116.40}	38.1	O VIII	$1s$	$2p$	18.9671	2.52 ←	-438 ⁺⁴⁸³ ₋₁₄₉
				(O VIII	$1s$	$2p$	18.9725	2.52)	-523 ⁺⁴⁸³ ₋₁₄₉

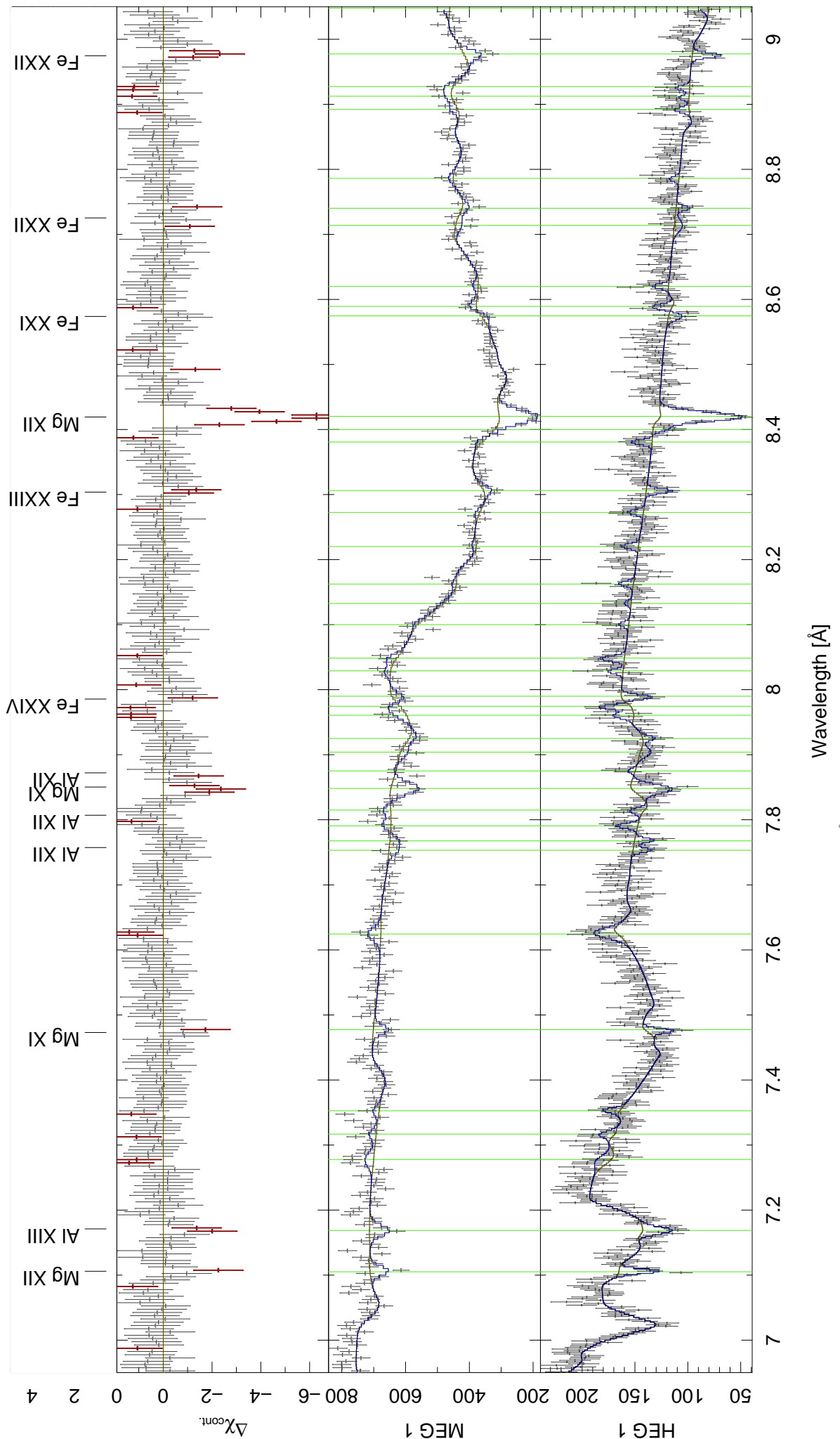


(a) 1...3 \AA range of the 'non-dip' Cyg X-1 spectrum

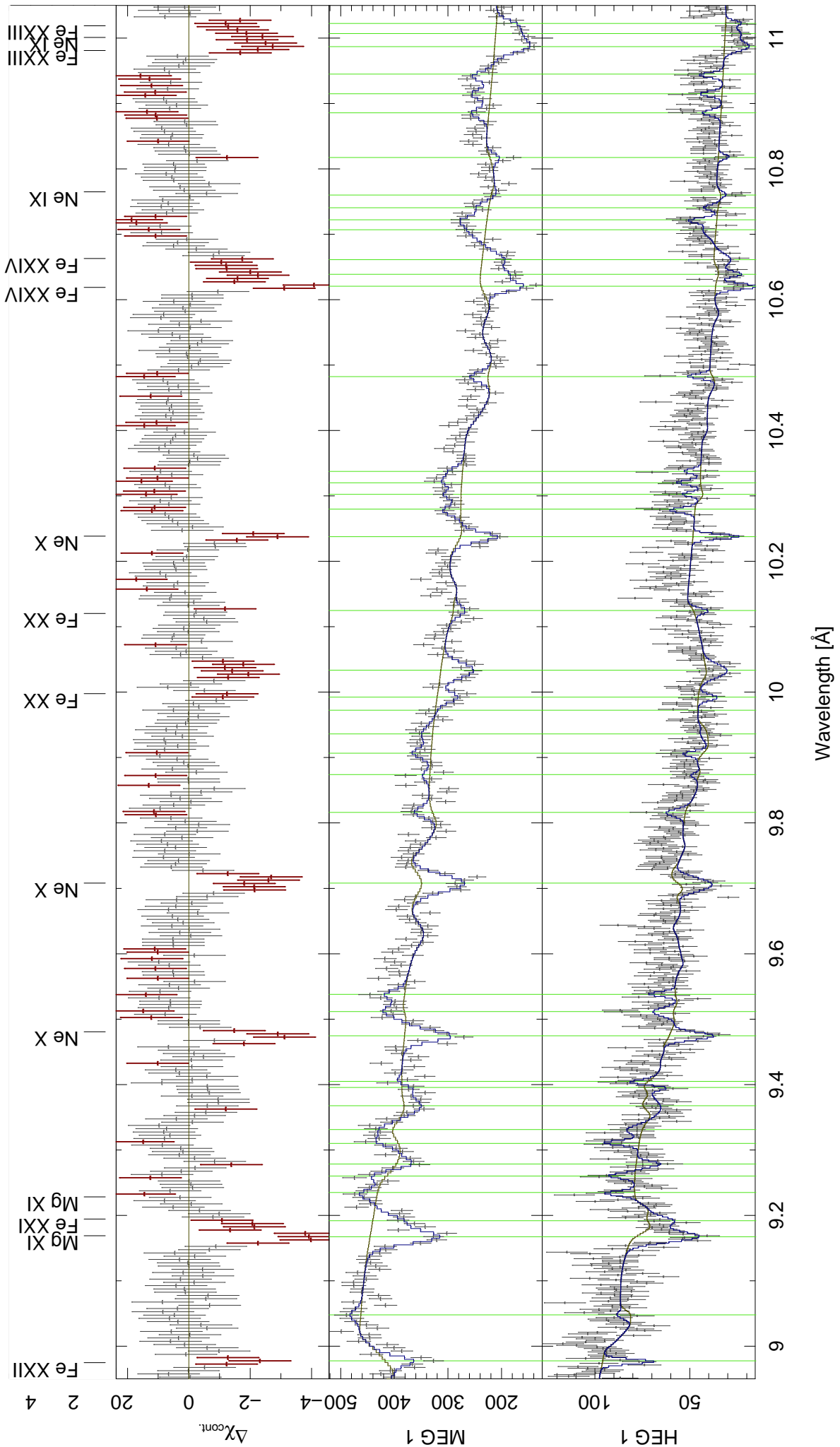


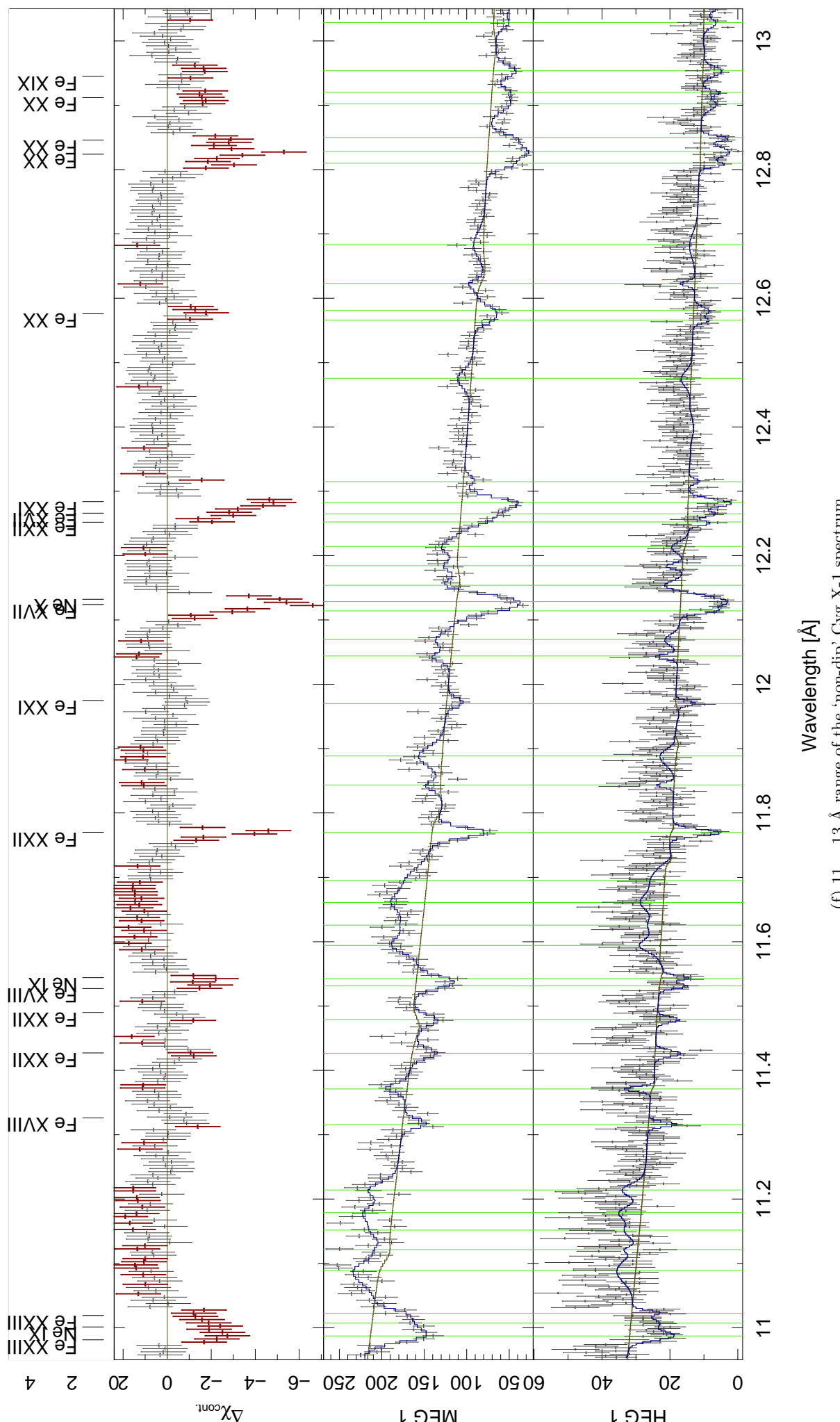
(b) 3...5 Å range of the ‘non-dip’ Cyg X-1 spectrum



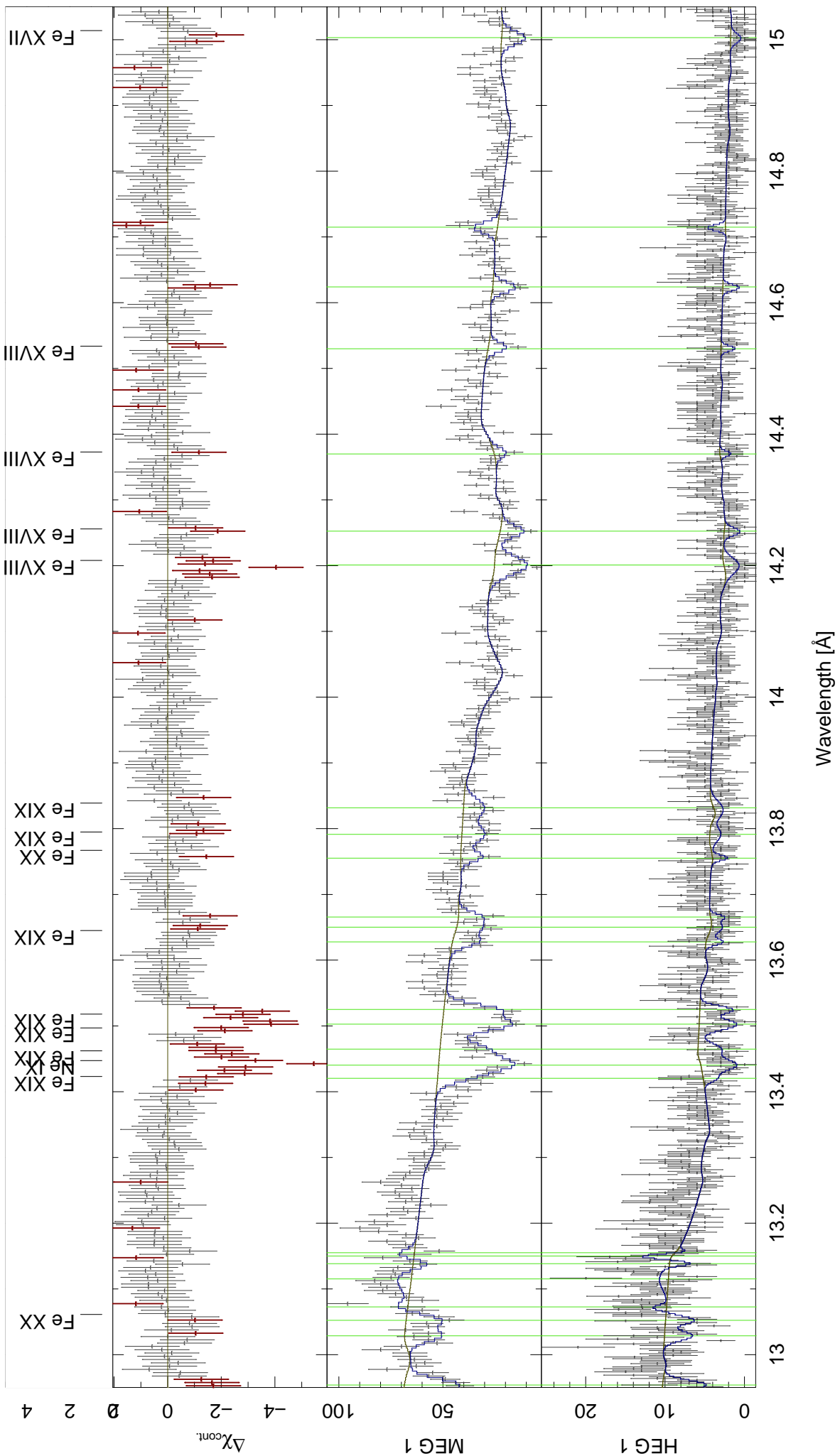


(d) $7 \dots 9 \text{ \AA}$ range of the ‘non-dip’ Cyg X-1 spectrum





(f) 11...13 Å range of the ‘non-dip’ Cyg X-1 spectrum



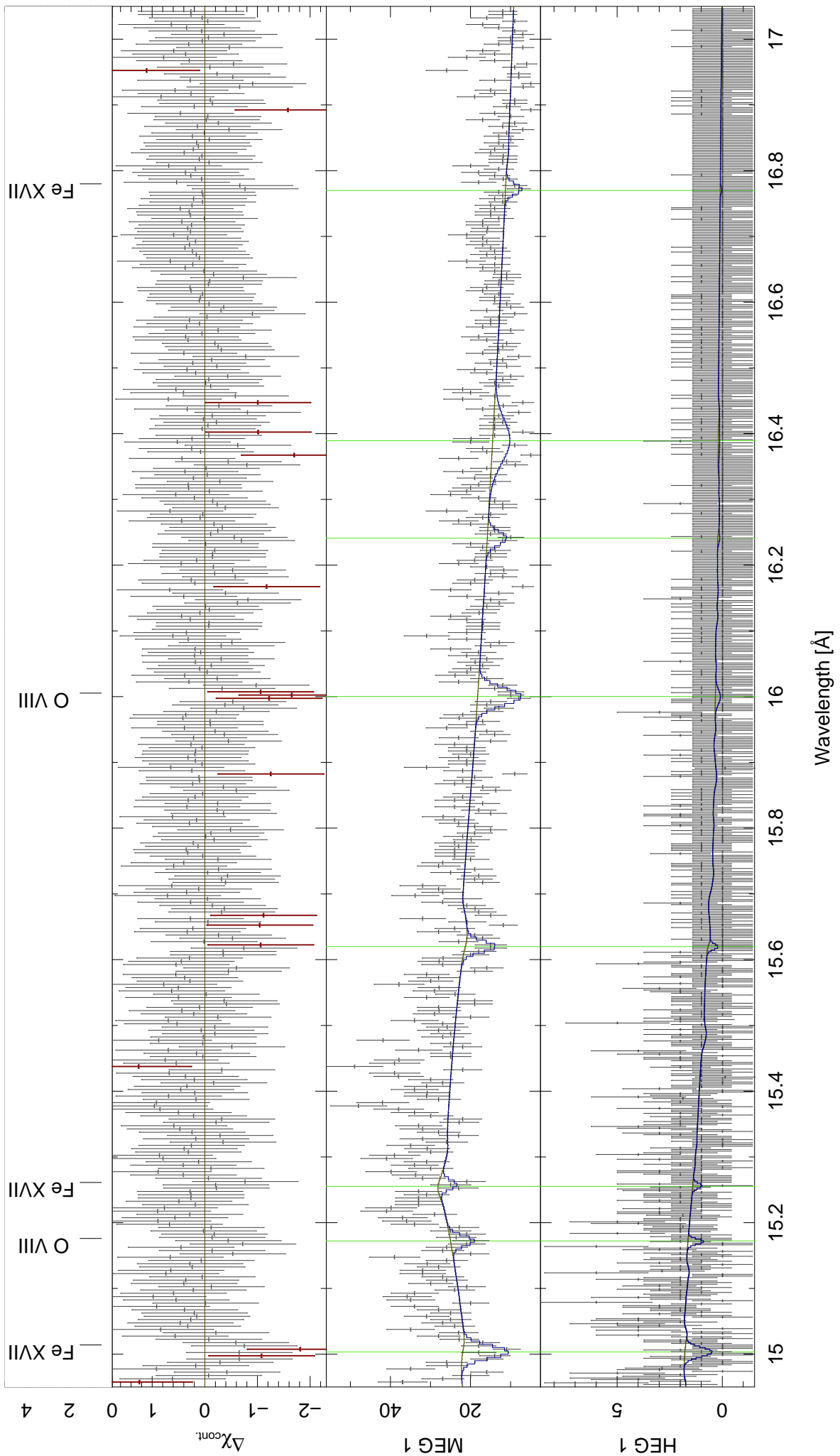


Figure A III.6: The fitted ‘non-dip’ Cyg X-1 spectrum, including all lines.

III.3 Dependencies of the continuum-parameters

In Section 4.3.2 (page 88), the dependence of the best fit parameters on **A**) a (fixed) given value of Γ was investigated, as well as the dependence on **B**) the wavelength range used for fitting, in order to justify the introduction of a new model for the continuum, namely a two component (partial covered) photoabsorbed power law with pile-up reduction (model 4.6) for the ‘dip’ spectrum.

The ‘non-dip’ spectrum: A) Γ -dependence

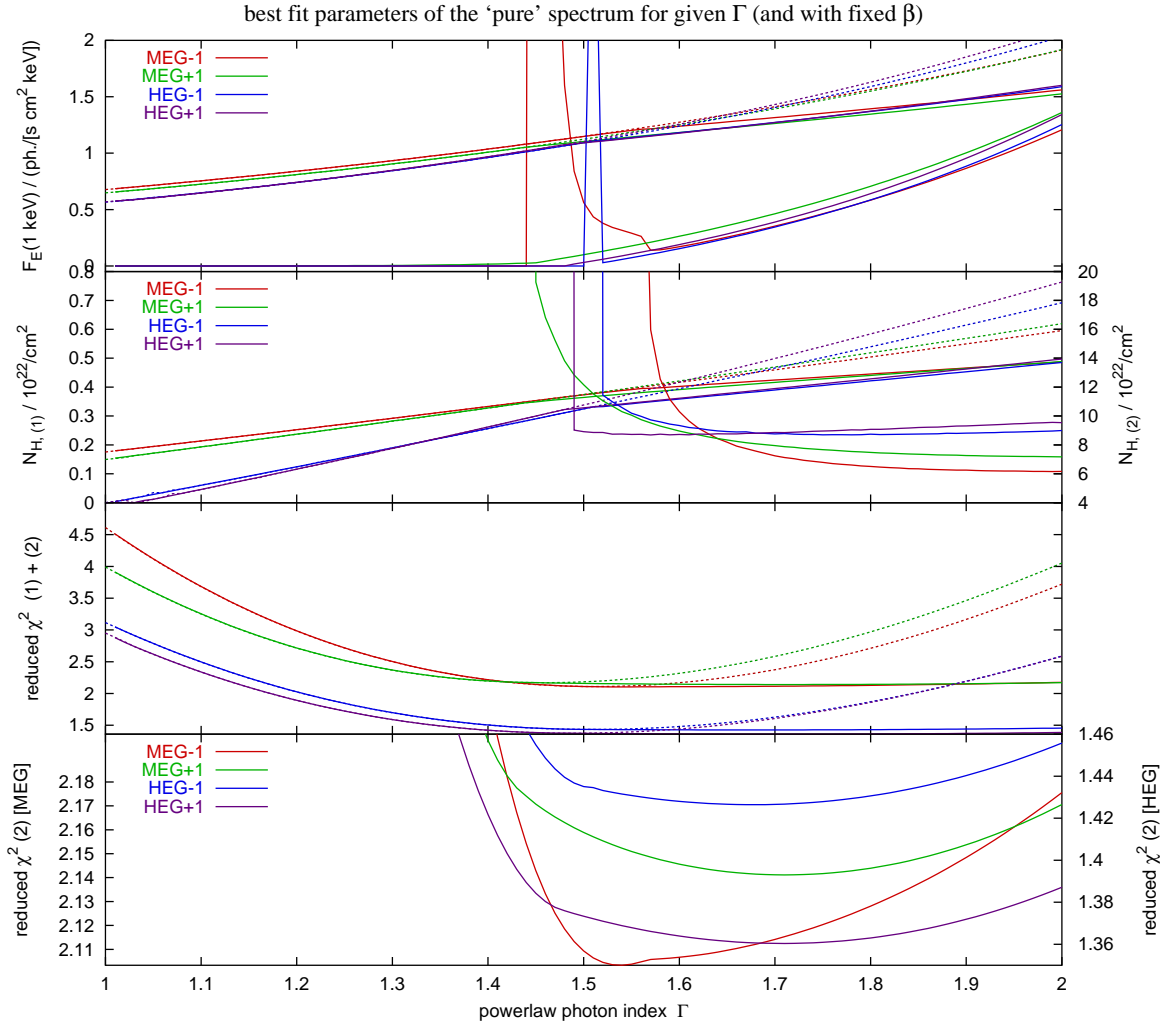


Figure A III.7: The ‘non-dip’ spectrum: Γ -dependence for both models’ fit parameteres (rebinned to ≥ 30 counts/bin; [1 Å, 20 Å] range noticed).

The ‘non-dip’ spectrum: B) λ_2 -dependence (with pile-up scales thawed)

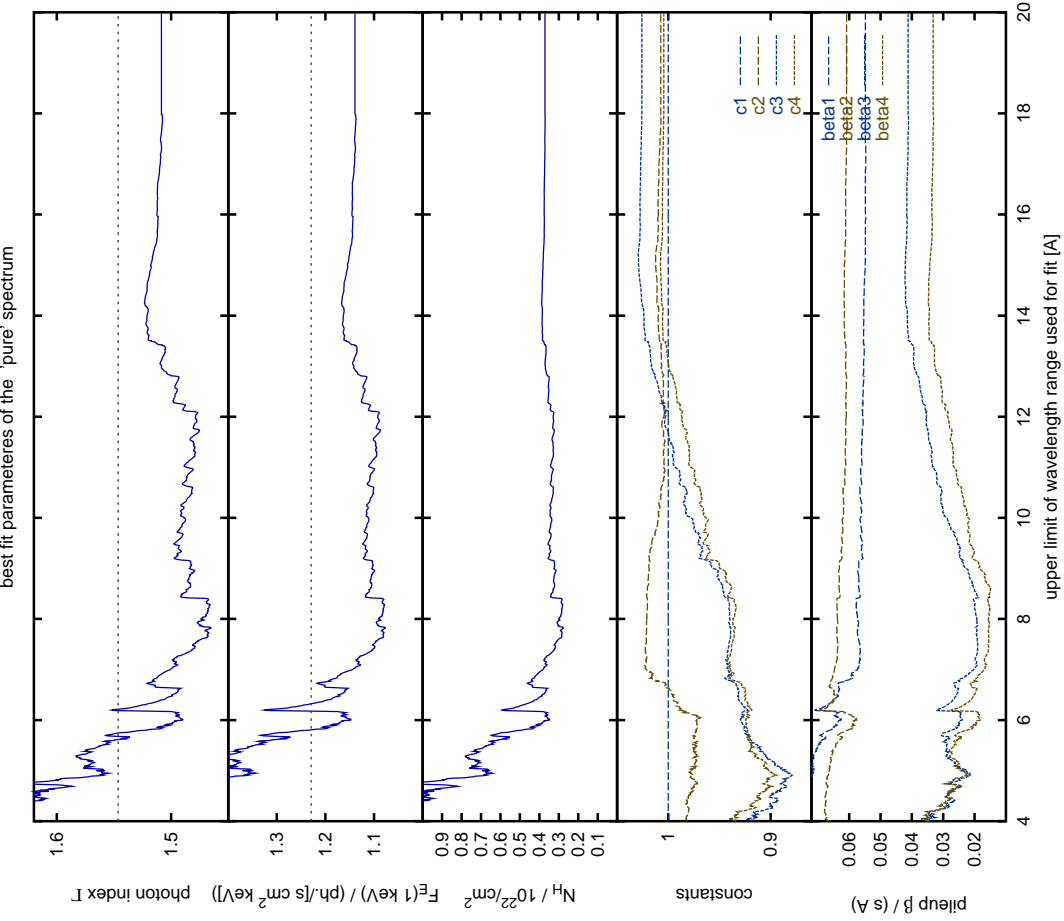


Figure A III.8: λ_2 -dependence of the 1-comp. model's fit parameters.
For these investigations, the wavelength range $[\lambda_1 = 1 \text{ \AA}, \lambda_2]$ that was considered for the fitting was varied.

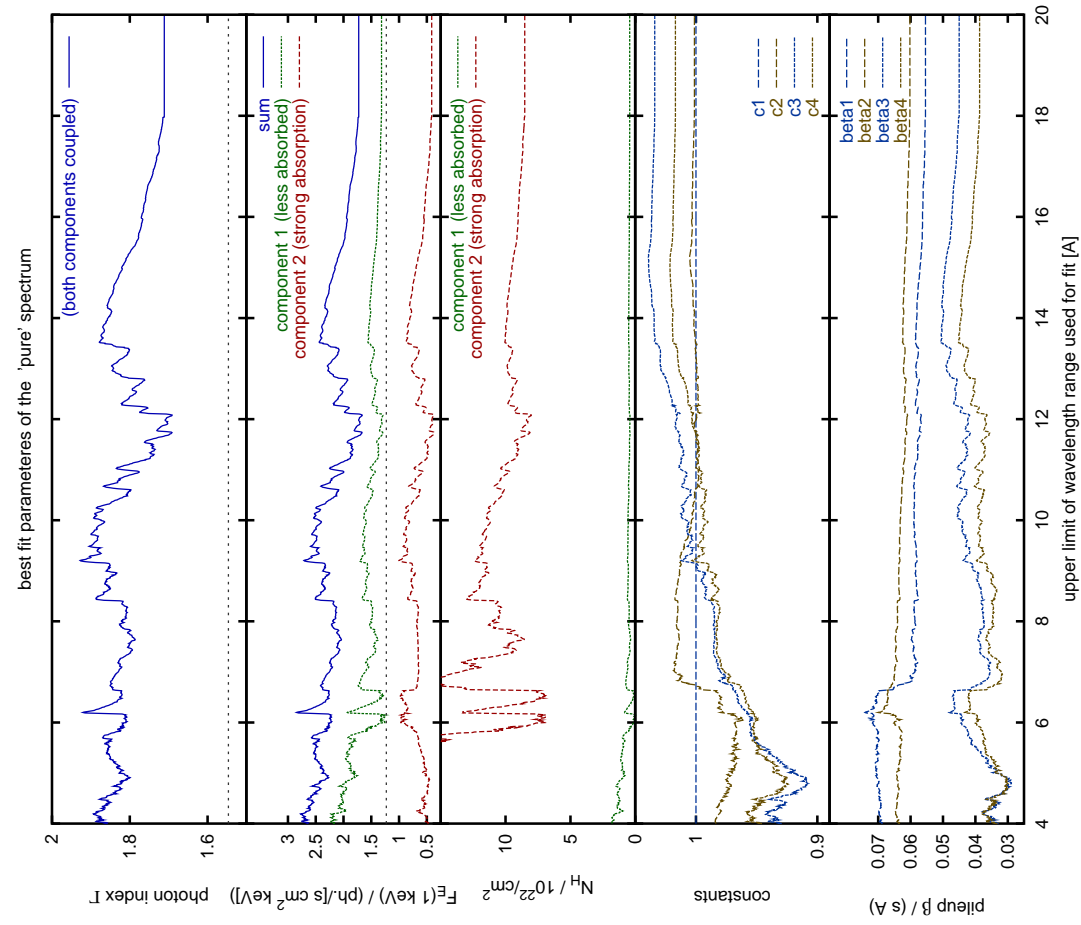


Figure A III.9: λ_2 -dependence of the 2-comp. model's fit parameters.
For these investigations, the wavelength range $[\lambda_1 = 1 \text{ \AA}, \lambda_2]$ that was considered for the fitting was varied.

The ‘dip’ spectrum: A) Γ -dependence

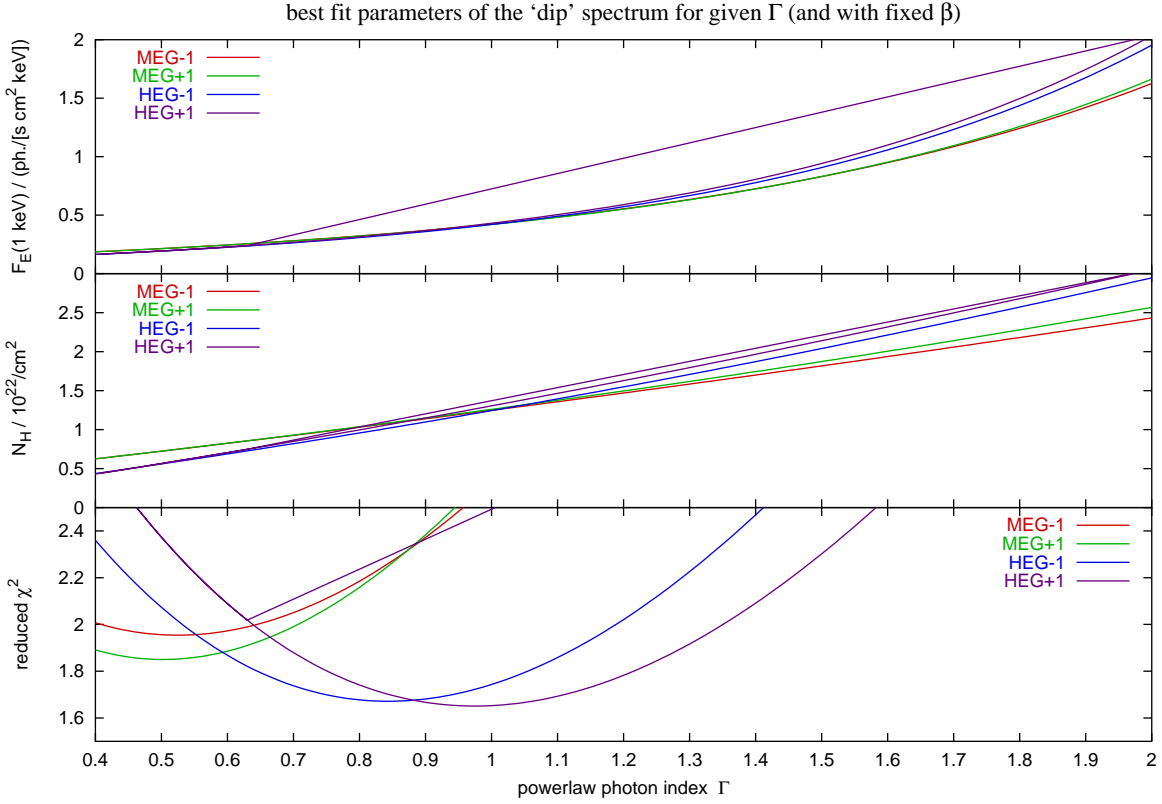


Figure A III.10: The ‘dip’ spectrum: Γ -dependence of the 1-comp. model’s fit parameters (rebinned to ≥ 30 counts/bin; [1 Å, 20 Å] range noticed).

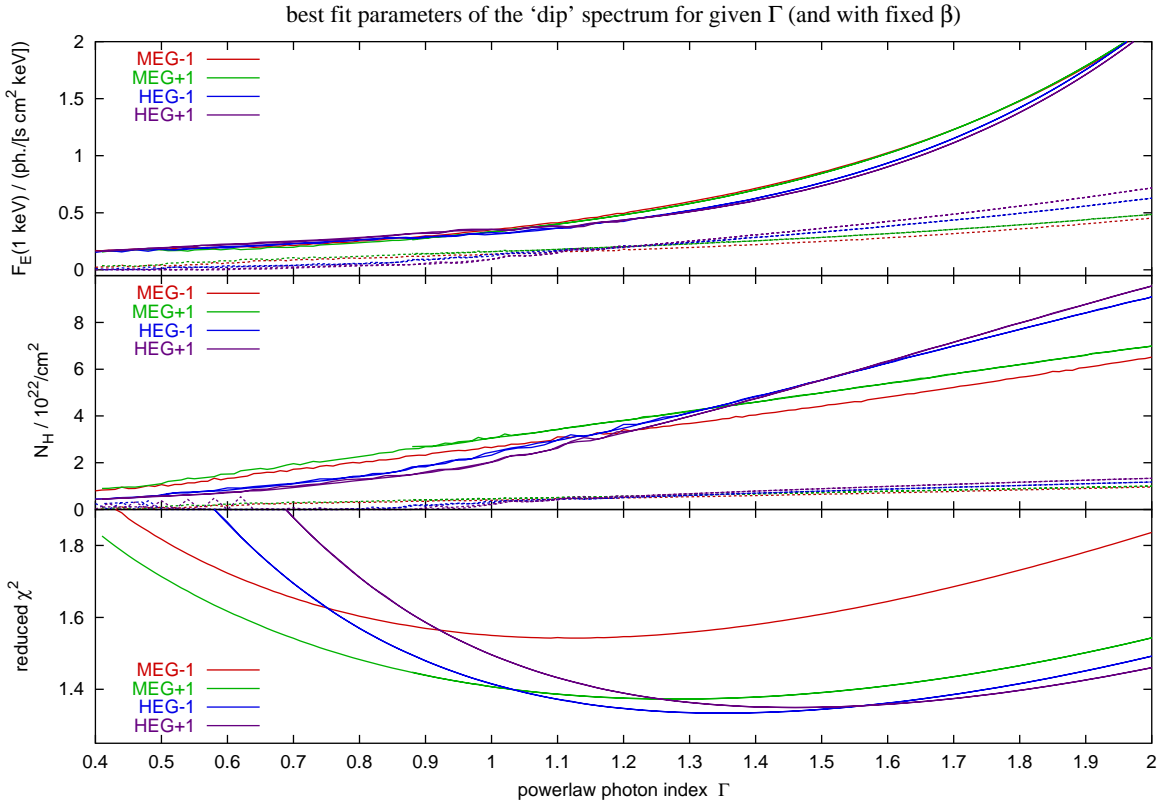


Figure A III.11: The ‘dip’ spectrum: Γ -dependence of the 2-comp. model’s fit parameters (rebinned to ≥ 30 counts/bin; [1 Å, 20 Å] range noticed).

The ‘dip’ spectrum: B) λ_2 -dependence (with pile-up scales thawed)

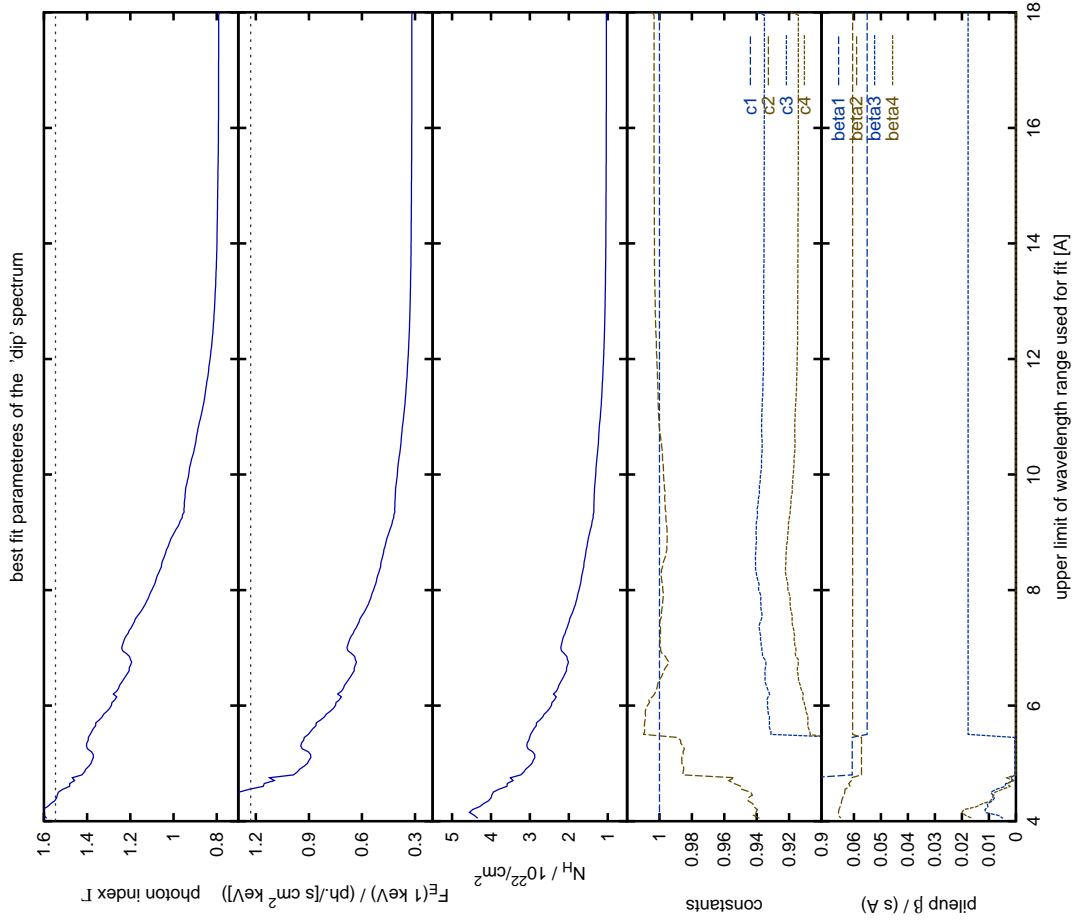


Figure A III.12: λ_2 -dependence of the 1-comp. model's fit parameters.
For these investigations, the wavelength range [$\lambda_1 = 1 \text{\AA}$, λ_2] that was considered for the fitting was varied.

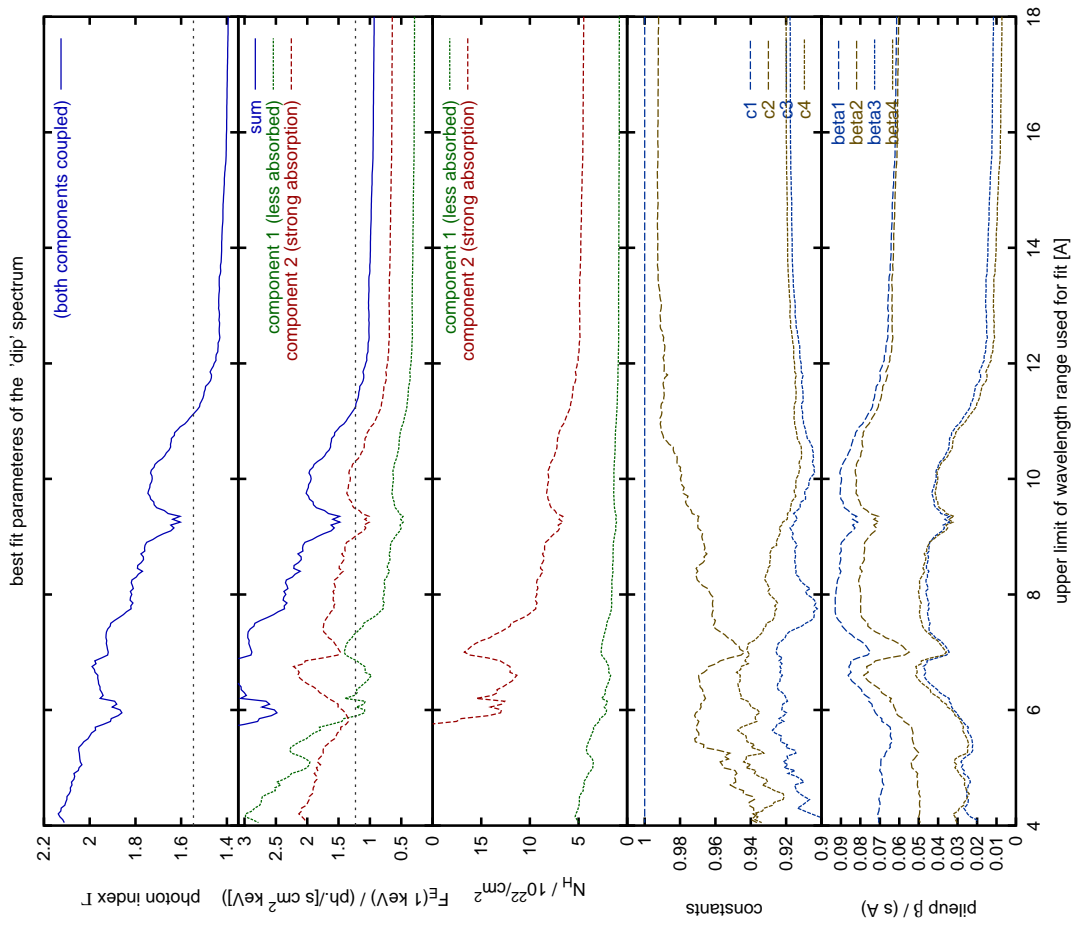


Figure A III.13: λ_2 -dependence of the 2-comp. model's fit parameters.
For these investigations, the wavelength range [$\lambda_1 = 1 \text{\AA}$, λ_2] that was considered for the fitting was varied.

The ‘dip 1’ spectrum: A) Γ -dependence

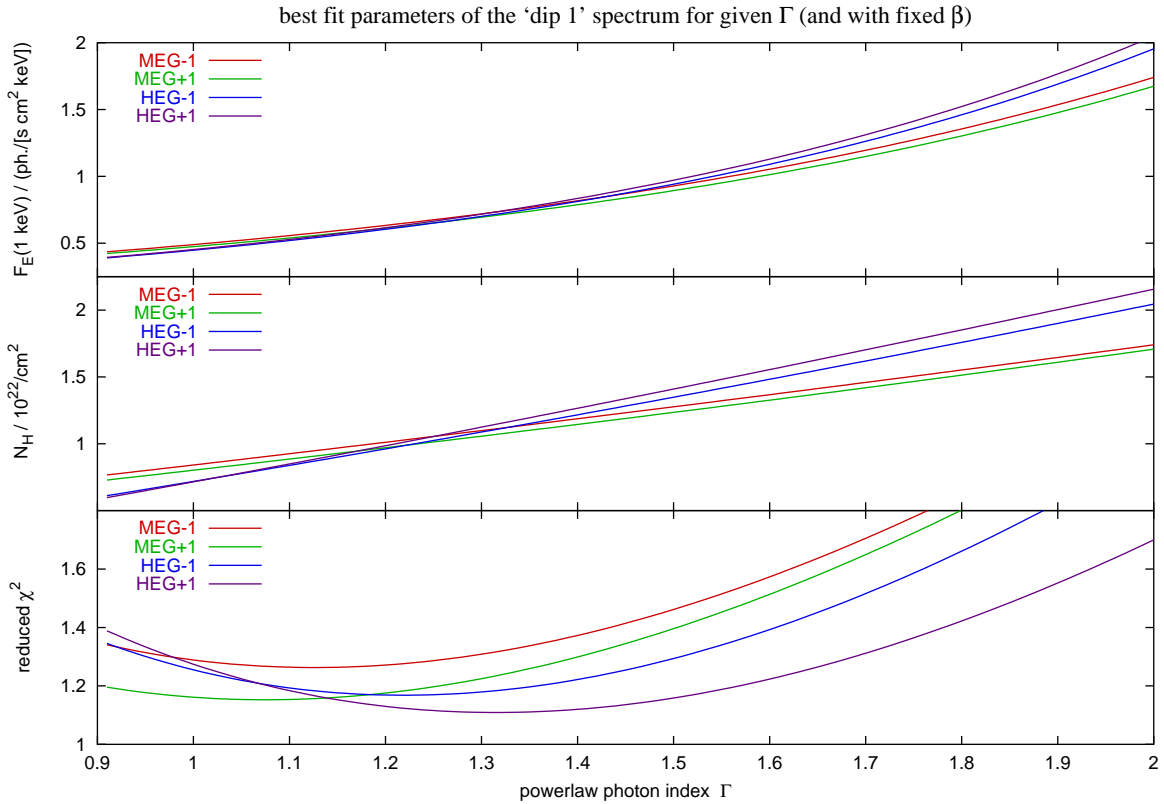


Figure A III.14: The ‘dip 1’ spectrum: Γ -dependence of the 1-comp. model’s fit parameters (rebinned to ≥ 30 counts/bin; [1 Å, 20 Å] range noticed).

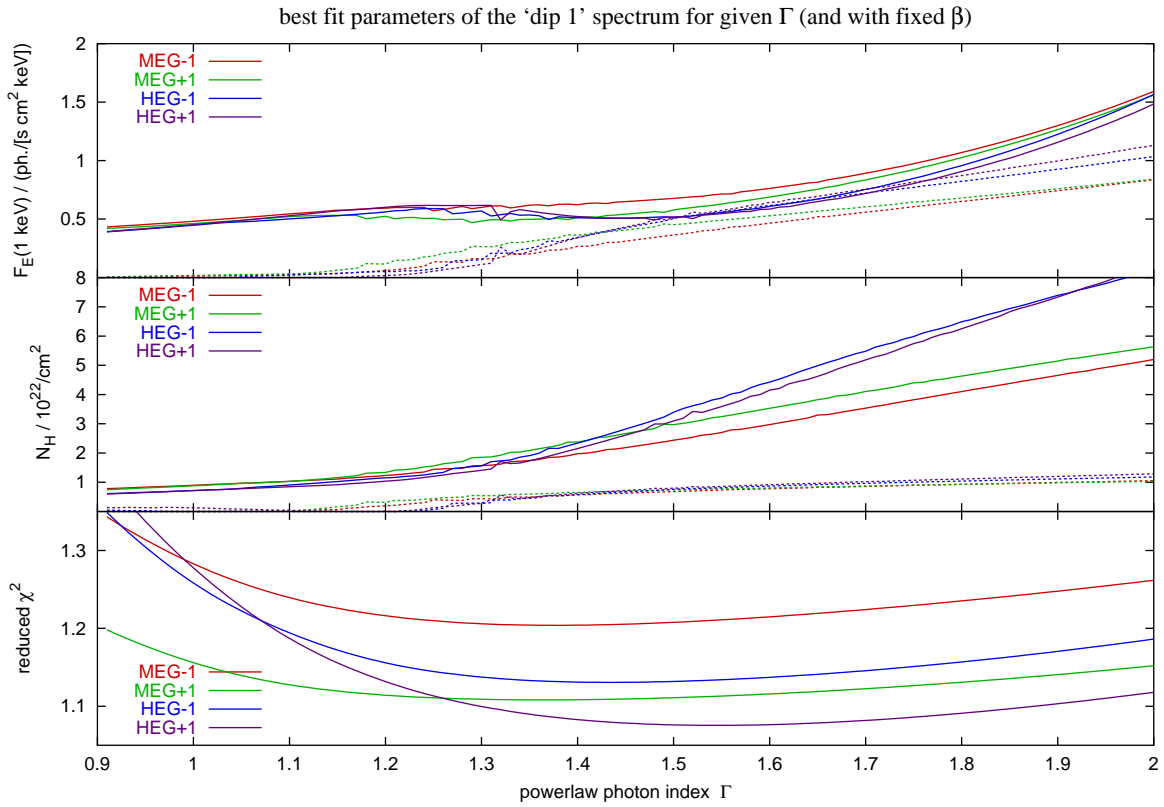


Figure A III.15: The ‘dip 1’ spectrum: Γ -dependence of the 2-comp. model’s fit parameters (rebinned to ≥ 30 counts/bin; [1 Å, 20 Å] range noticed).

The 'dip 1' spectrum: B) λ_2 -dependence (with pile-up scales thawed)

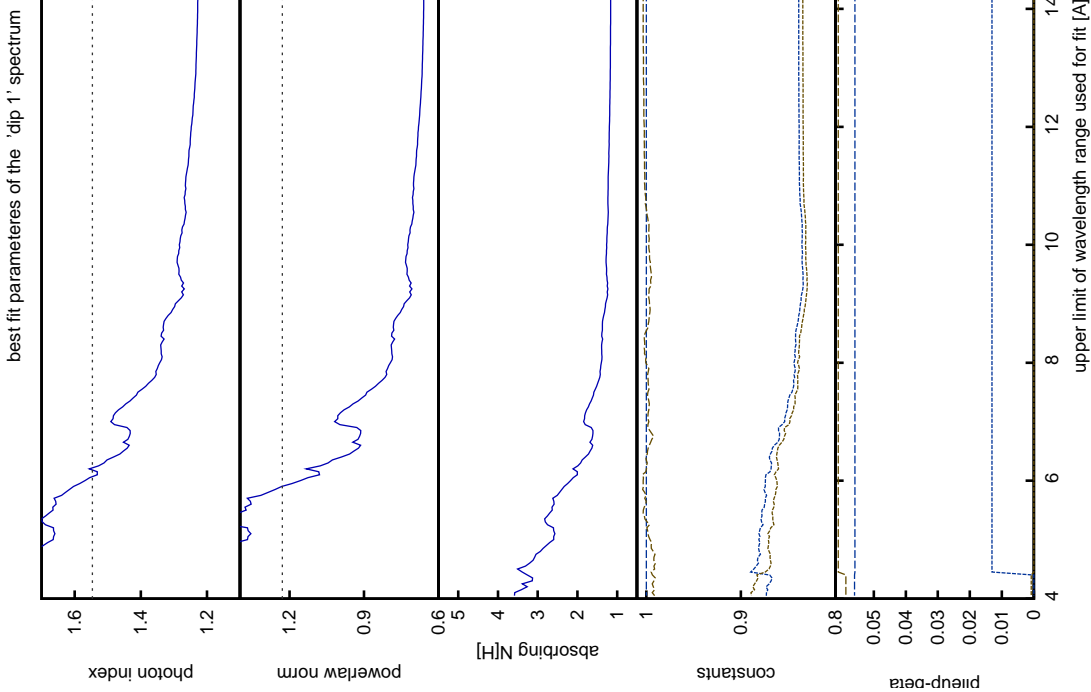


Figure A III.16: λ_2 -dependence of the 1-comp. model's fit parameters.

For these investigations, the wavelength range $[\lambda_1 = 1 \text{ Å}, \lambda_2]$ that was considered for the fitting was varied.

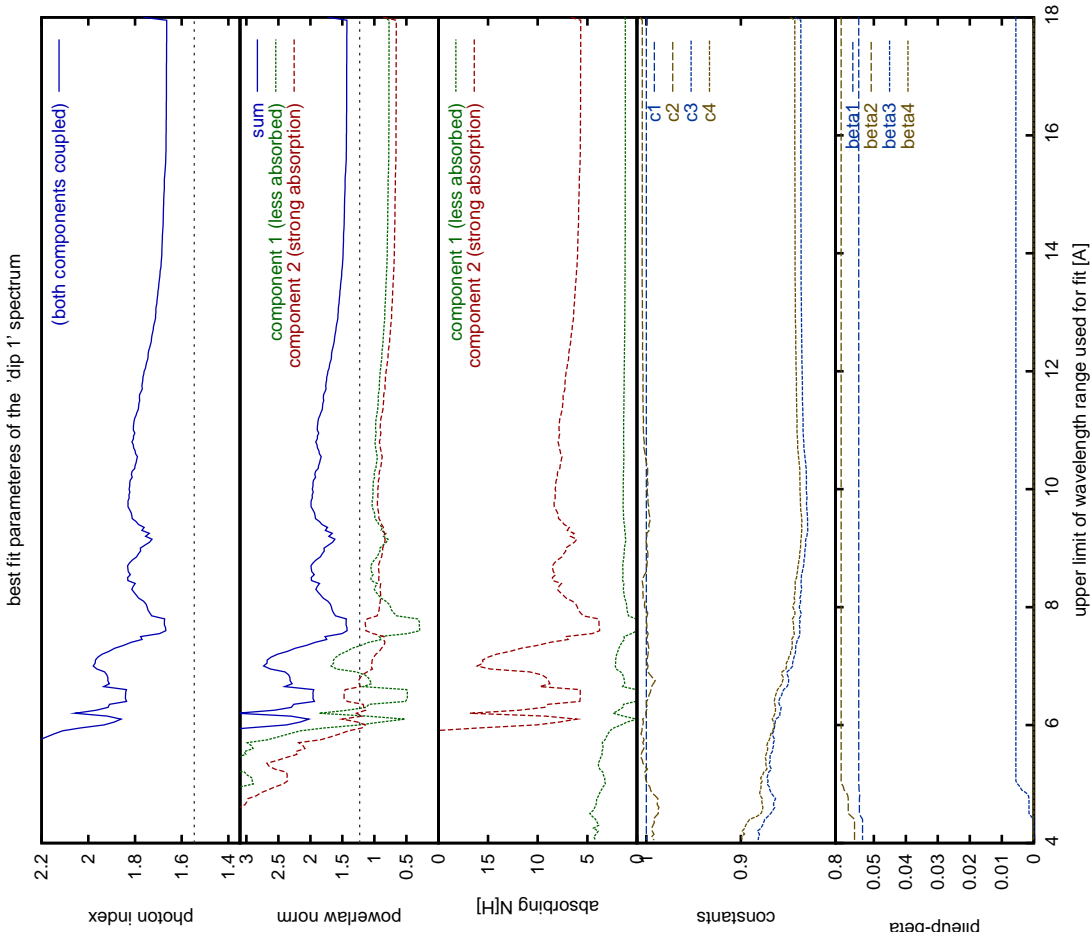


Figure A III.17: λ_2 -dependence of the 2-comp. model's fit parameters.

For these investigations, the wavelength range $[\lambda_1 = 1 \text{ Å}, \lambda_2]$ that was considered for the fitting was varied.

The ‘dip 1’ spectrum: B) λ_2 -dependence (with fixed pile-up scales)

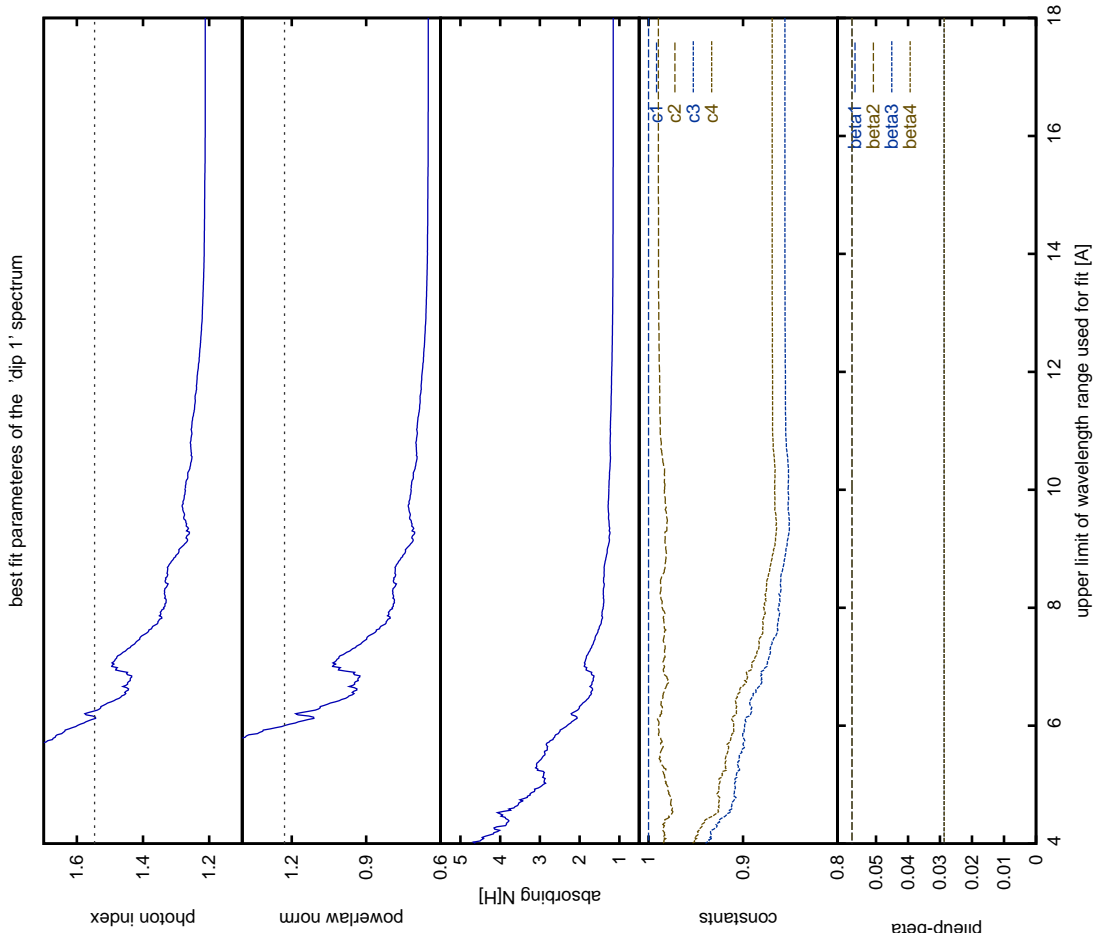


Figure A III.18: λ_2 -dependence of the 1-comp. model's fit par. (β fixed). For these investigations, the wavelength range $[\lambda_1 = 1 \text{ Å}, \lambda_2]$ that was considered for the fitting was varied. The pile-up scales β have been fixed to the canonical values.

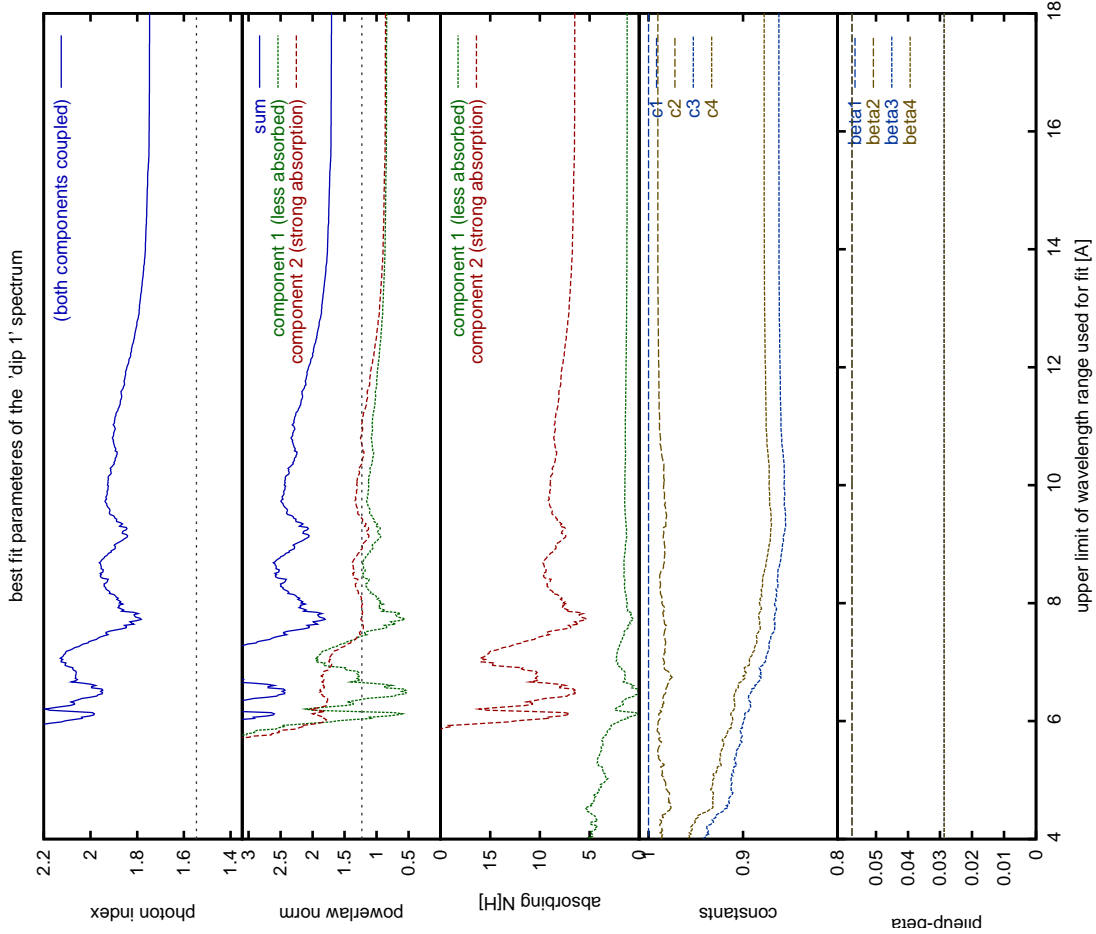


Figure A III.19: λ_2 -dependence of the 2-comp. model's fit par. (β fixed). For these investigations, the wavelength range $[\lambda_1 = 1 \text{ Å}, \lambda_2]$ that was considered for the fitting was varied. The pile-up scales β have been fixed to the canonical values.

The ‘dip 2’ spectrum: A) Γ -dependence

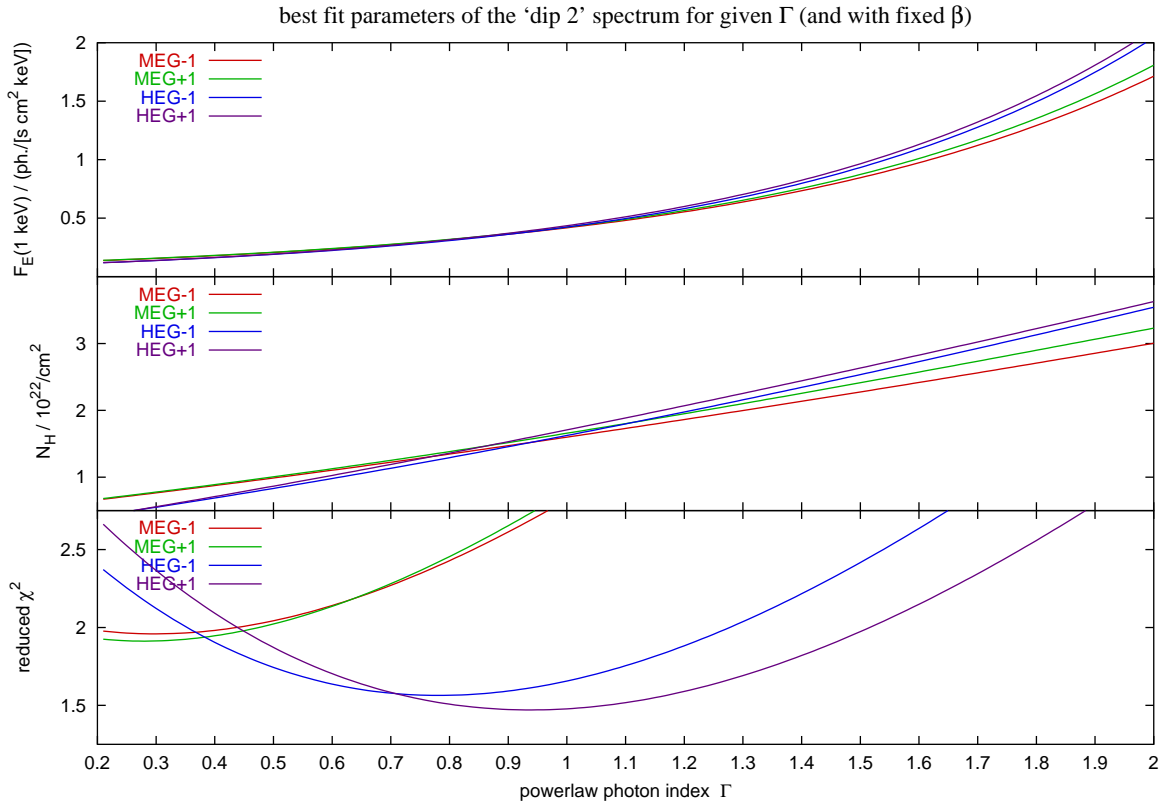


Figure A III.20: The ‘dip 2’ spectrum: Γ -dependence of the 1-comp. model’s fit parameters (rebinned to ≥ 30 counts/bin; [1 Å, 20 Å] range noticed).

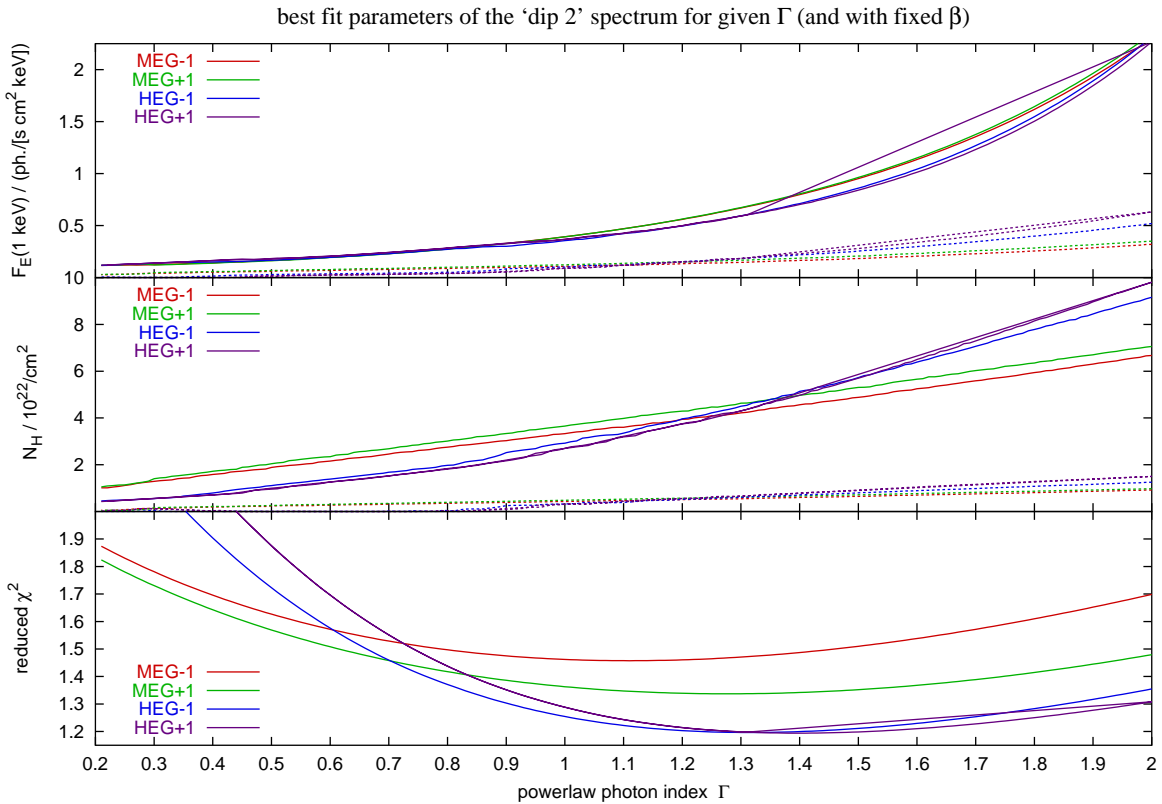


Figure A III.21: The ‘dip 2’ spectrum: Γ -dependence of the 2-comp. model’s fit parameters (rebinned to ≥ 30 counts/bin; [1 Å, 20 Å] range noticed).

The 'dip 2' spectrum: B) λ_2 -dependence (with pile-up scales thawed)

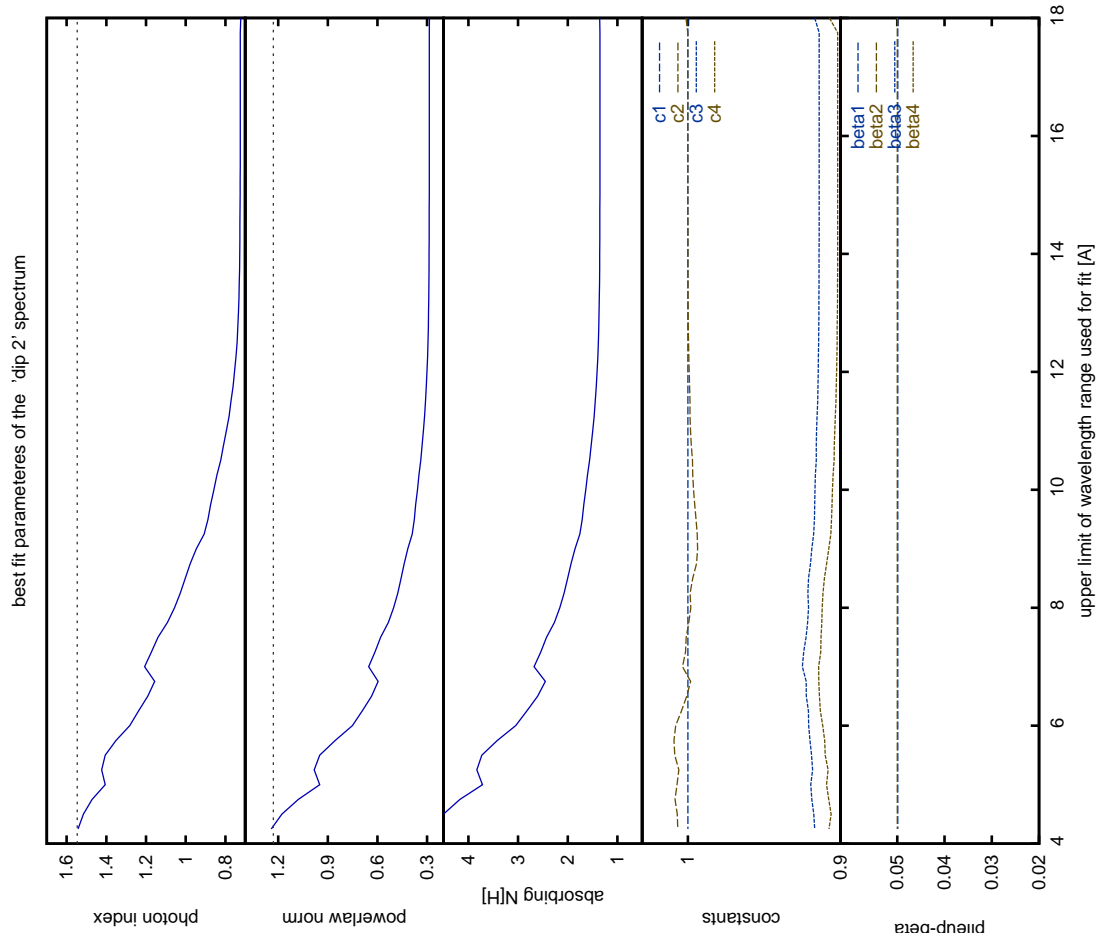


Figure AIII.22: λ_2 -dependence of the 1-comp. model's fit parameters.
For these investigations, the wavelength range $[\lambda_1 = 1 \text{ \AA}, \lambda_2]$ that was considered for the fitting was varied.

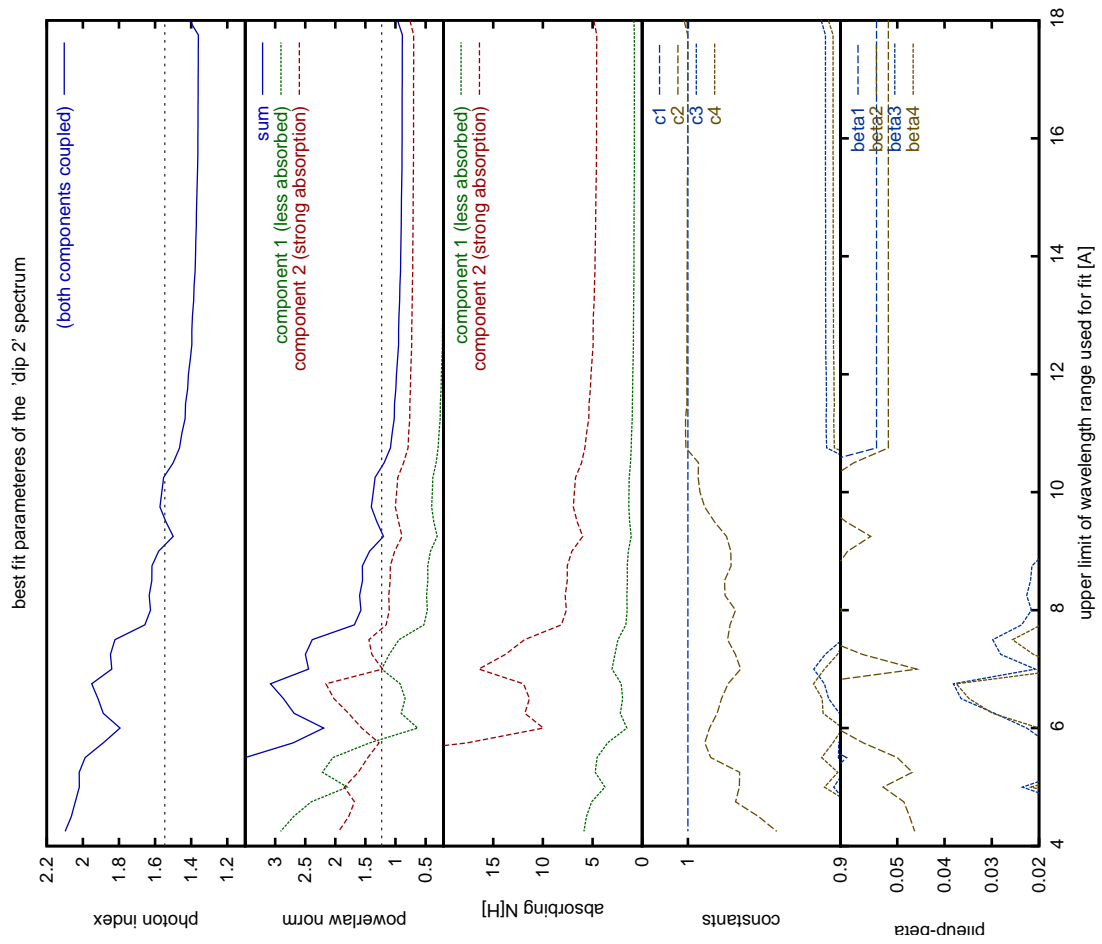


Figure AIII.23: λ_2 -dependence of the 2-comp. model's fit parameters.
For these investigations, the wavelength range $[\lambda_1 = 1 \text{ \AA}, \lambda_2]$ that was considered for the fitting was varied.

The 'dip 2' spectrum: B') λ_2 -dependence (with fixed pile-up scales)

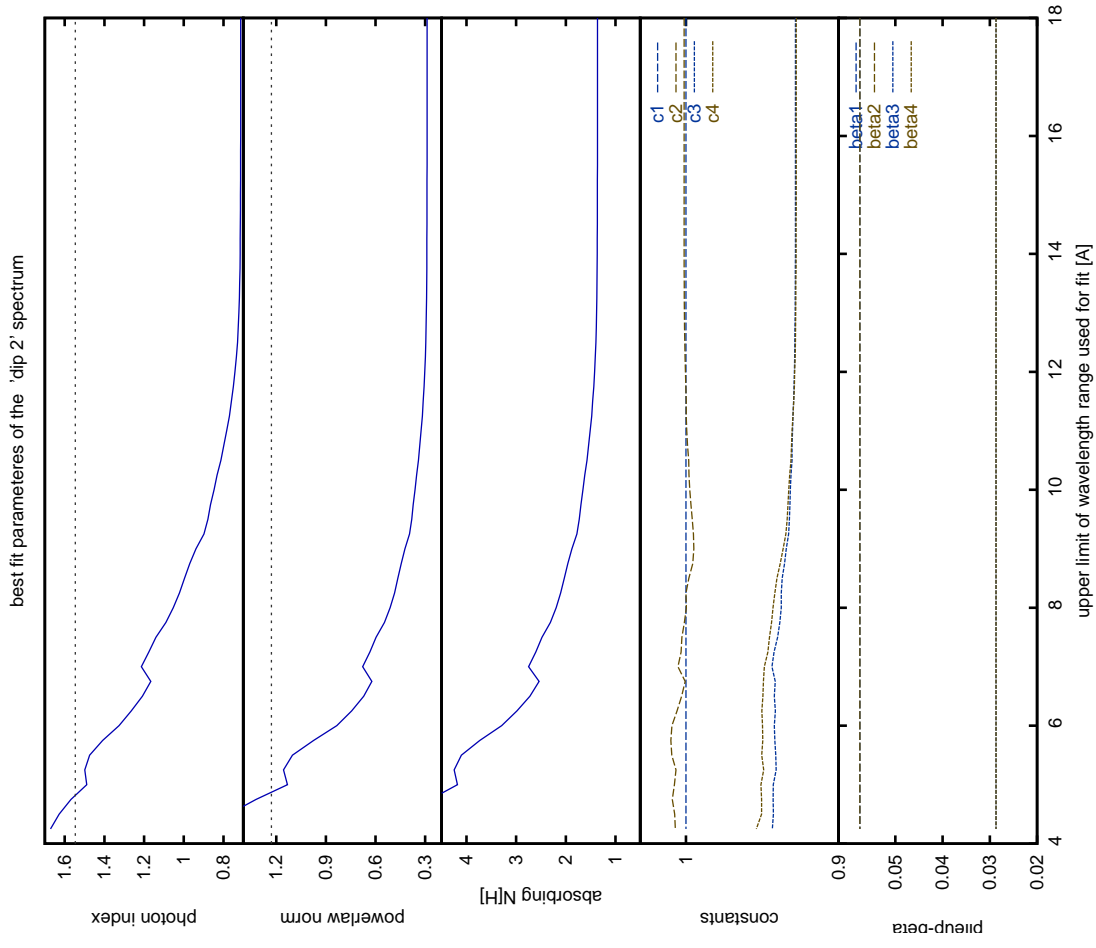


Figure A III.24: λ_2 -dependence of the 1-comp. model's fit par. (β fixed). For these investigations, the wavelength range [$\lambda_1 = 1 \text{ \AA}$, λ_2] that was considered for the fitting was varied. The pile-up scales β have been fixed to the canonical values.

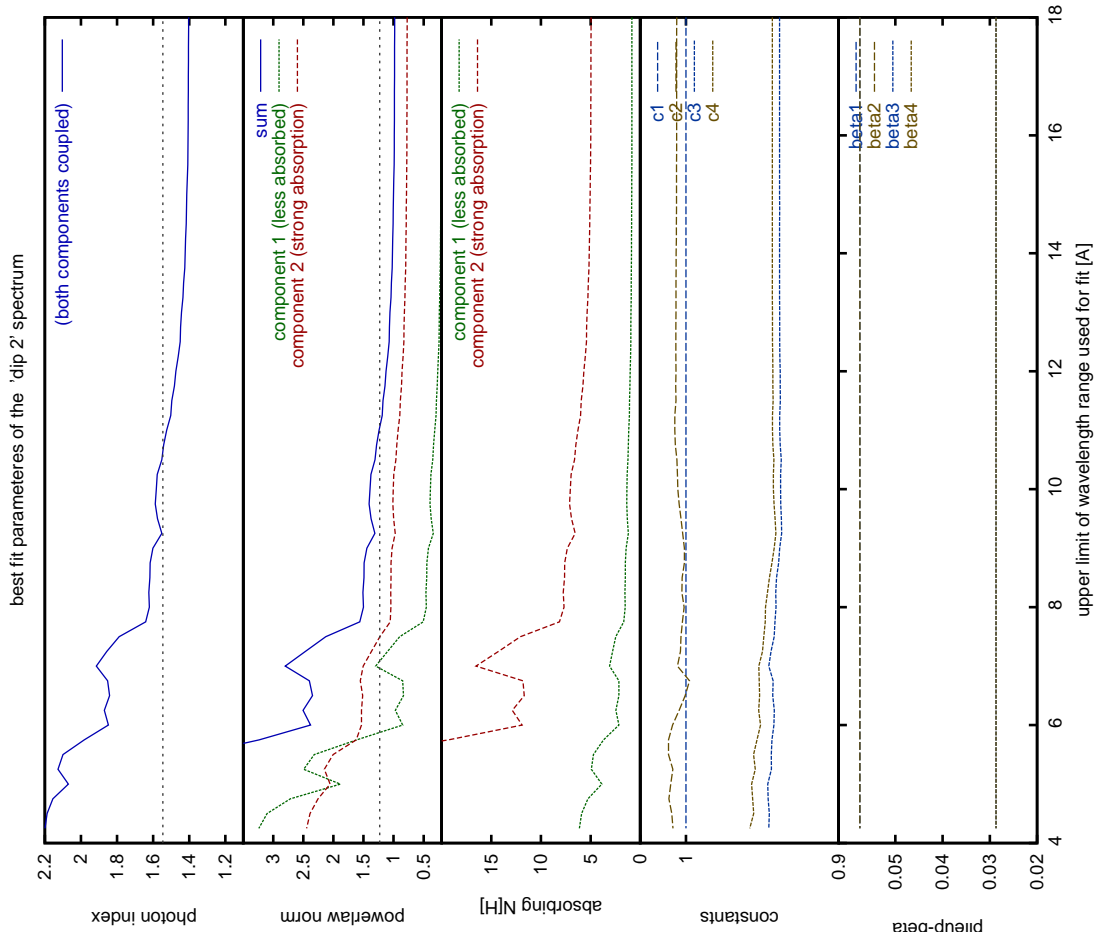


Figure A III.25: λ_2 -dependence of the 2-comp. model's fit par. (β fixed). For these investigations, the wavelength range [$\lambda_1 = 1 \text{ \AA}$, λ_2] that was considered for the fitting was varied. The pile-up scales β have been fixed to the canonical values.

III.4 Spectral analysis of the ‘dip’ spectrum

In section 4.3.3 (page 95), the absorption lines in the dip spectrum were investigated.

In the same way as in appendix III.2, first the list of all fitted lines is given (Table A III.2), and then the plots of the spectra are shown (Figs. A III.26a–A III.26h, pages 159–166). All further details are given on page 126.

Table A III.2: List of lines in the ‘dip’ spectrum – sorted by wavelength

λ [Å]	FWHM [mÅ]	EW [mÅ]	$\Delta\chi^2$	ion <i>i</i>	transition <i>j</i>	λ_0 [Å]	A_{ji} $[10^{12} \text{s}^{-1}]$	$\Delta\lambda/\lambda \cdot c$ [km/s]
1.4924 ^{+0.0026} _{-0.0032}	0.33 ^{+11.44} _{-0.33}	-3.50 ^{+1.78} _{-2.96}	10.5	(Fe XXVI	<u>1s</u> 3p	1.5024	75.2) ← -1981 ⁺⁵¹¹ ₋₆₄₈
				(Fe XXVI	<u>1s</u> 3p	1.5035	75.1) -2208 ⁺⁵¹⁰ ₋₆₄₈
1.5199 ^{+0.0058} _{-0.0070}	15.00 ^{+0.00} _{-4.46}	-6.26 ^{+2.44} _{-2.41}	18.1	(Ni XXVIII	<u>1s</u> 2p	1.5304	379) ← -2049 ⁺¹¹⁴⁴ ₋₁₃₇₇
				(Ni XXVIII	<u>1s</u> 2p	1.5356	378) -3055 ⁺¹¹⁴⁰ ₋₁₃₇₂
1.8521 ^{+0.0052} _{-0.0046}	9.01 ^{+11.42} _{-9.01}	-2.36 ^{+1.24} _{-1.30}	13.9	Fe XXV	<u>1s²</u> 1s2p	1.8504	503	← 280 ⁺⁸³⁹ ₋₇₄₈
1.9405 ^{+0.0049} _{-0.0032}	23.96 ^{+17.37} _{-8.89}	7.67 ^{+2.18} _{-1.81}	69.3	(Fe	Kα	1.937) ←	536 ⁺⁷⁵⁵ ₋₄₉₂
3.0461 ^{+0.0063} _{-0.0194}	4.40 ^{+41.32} _{-4.40}	-0.92 ^{+0.75} _{-1.04}	4.1	(Ca XX	<u>1s</u> 2p	3.0185	98.6) 2738 ⁺⁶²⁸ ₋₁₉₂₄
				(Ca XX	<u>1s</u> 2p	3.0239	98.5) 2196 ⁺⁶²⁷ ₋₁₉₂₀
3.3077 ^{+0.0068} _{-0.0156}	10.02 ^{+40.03} _{-10.02}	-1.46 ^{+0.92} _{-1.76}	7.8					
3.3545 ^{+0.0055} _{-0.0145}	0.00 ^{+76.27} _{-0.00}	-0.80 ^{+0.74} _{-0.69}	3.2	(Ar XVII	<u>1s²</u> 1s3p	3.3650	30.0) ← -939 ⁺⁴⁹³ ₋₁₂₉₀
3.7350 ^{+0.0072} _{-0.0056}	8.89 ^{+17.25} _{-8.89}	-1.46 ^{+0.90} _{-1.07}	7.8	Ar XVIII	<u>1s</u> 2p	3.7311	64.7	← 313 ⁺⁵⁷⁸ ₋₄₅₀
				Ar XVIII	<u>1s</u> 2p	3.7365	64.6	-121 ⁺⁵⁷⁸ ₋₄₅₀
3.9566 ^{+0.0051} _{-0.0035}	5.91 ^{+19.24} _{-5.91}	-2.42 ^{+0.96} _{-1.68}	24.0	(Ar XVII	<u>1s²</u> 1s2p	3.9491	109) ← 569 ⁺³⁸⁹ ₋₂₆₆
3.9940 ^{+0.0000} _{-0.0042}	0.37 ^{+7.84} _{-0.37}	-1.83 ^{+0.82} _{-0.76}	13.3	S XVI	<u>1s</u> 3p	3.9908	10.8	← 239 ⁺¹ ₋₃₁₆
				S XVI	<u>1s</u> 3p	3.9920	10.8	153 ⁺¹ ₋₃₁₆
4.3063 ^{+0.0200} _{-0.0200}	0.66 ^{+74.97} _{-0.66}	-1.41 ^{+0.94} _{-1.26}	6.0	S XV	<u>1s²</u> 1s3p	4.2990	18.3	← 511 ⁺¹³⁹⁵ ₋₁₃₉₅
4.7240 ^{+0.0057} _{-0.0061}	25.65 ^{+14.98} _{-12.44}	-4.91 ^{+1.74} _{-1.86}	29.0	S XVI	<u>1s</u> 2p	4.7274	40.4	← -215 ⁺³⁶⁰ ₋₃₈₆
				(S XVI	<u>1s</u> 2p	4.7328	40.3	-557 ⁺³⁶⁰ ₋₃₈₆
5.0375 ^{+0.0050} _{-0.0025}	0.00 ^{+20.22} _{-0.00}	-1.99 ^{+0.89} _{-1.16}	11.5	S XV	<u>1s²</u> 1s2p	5.0387	66.7	← -73 ⁺²⁹⁷ ₋₁₄₉
5.1325 ^{+0.0025} _{-0.0050}	0.00 ^{+23.18} _{-0.00}	-2.51 ^{+1.05} _{-2.07}	14.4	S XV	<u>1s²2p</u> (autoion.)	5.1293		187 ⁺¹⁴⁷ ₋₂₉₂
				(S XV	<u>1s²</u> 1s2s	5.1015	0.000) 1822 ⁺¹⁴⁸ ₋₂₉₄
5.1786 ^{+0.0052} _{-0.0051}	26.07 ^{+13.21} _{-8.46}	-6.38 ^{+1.89} _{-2.08}	36.6	(S XV	<u>1s²2p</u> (autoion.)	5.2090		-1751 ⁺²⁹⁹ ₋₂₉₂
5.2297 ^{+0.0020} _{-0.0020}	19.38 ^{+5.13} _{-4.34}	-10.98 ^{+1.74} _{-1.82}	153.3	(Si XIV	<u>1s</u> 3p	5.2168	6.32) ← 740 ⁺¹¹⁷ ₋₁₁₇
				(Si XIV	<u>1s</u> 3p	5.2180	6.31) 674 ⁺¹¹⁷ ₋₁₁₇
5.2747 ^{+0.0198} _{-0.0037}	18.51 ^{+35.57} _{-9.81}	-6.24 ^{+1.93} _{-6.39}	40.3	Si XIII	<u>1s²</u> 1s5p	5.2850	2.17	-587 ⁺¹¹²⁵ ₋₂₁₂
5.3180 ^{+0.0031} _{-0.0023}	1.30 ^{+14.16} _{-1.30}	-3.08 ^{+1.20} _{-1.53}	0.0					
5.4075 ^{+0.0053} _{-0.0052}	0.05 ^{+47.10} _{-0.05}	-1.58 ^{+1.21} _{-1.88}	4.5	Si XIII	<u>1s²</u> 1s4p	5.4045	4.30	← 167 ⁺²⁹² ₋₂₈₈
5.6875 ^{+0.0054} _{-0.0065}	20.66 ^{+22.18} _{-18.27}	-4.83 ^{+1.91} _{-2.43}	24.7	(Si XIII	<u>1s²</u> 1s3p	5.6805	10.4) ← 369 ⁺²⁸³ ₋₃₄₃
5.7050 ^{+0.0028} _{-0.0022}	0.36 ^{+12.83} _{-0.36}	4.53 ^{+1.51} _{-1.34}	29.8	(Ni XXV	<u>1s²2s²</u> 1s ² 2p ^{7d}	5.700	0.040) 233 ⁺¹⁴⁹ ₋₁₁₆
				(Ni XXV	<u>1s²2s²</u> 1s ² 2p ^{7s}	5.709	0.000	-207 ⁺¹⁴⁹ ₋₁₁₆
5.7935 ^{+0.0042} _{-0.0040}	1.66 ^{+16.02} _{-1.66}	2.08 ^{+1.28} _{-1.30}	7.2	(Ni XXVI	<u>1s²2s</u> 1s ² 2s ² p	5.800	1.33) -354 ⁺²¹⁶ ₋₂₀₅
				(Ni XXV	<u>1s²2s²p</u> 1s ² 2p ^{7p}	5.789	0.14	194 ⁺²¹⁶ ₋₂₀₅
				(Ni XXV	<u>1s²2s²p</u> 1s ² 2p ^{7p}	5.793	0.11	-12 ⁺²¹⁶ ₋₂₀₅
5.8153 ^{+0.0101} _{-0.0125}	18.84 ^{+27.86} _{-18.84}	-2.38 ^{+1.61} _{-1.90}	6.3	Ni XXVII	<u>1s2p</u> 1s5d	5.8177	2.4e+04	-122 ⁺⁵²¹ ₋₆₄₄
				Ni XXVI	<u>1s²2p</u> 1s ² 7d	5.8177	1.49	-122 ⁺⁵²¹ ₋₆₄₄
				Ni XXVI	<u>1s²2p</u> 1s ² 7d	5.8181	0.24	-141 ⁺⁵²¹ ₋₆₄₄
5.9097 ^{+0.0003} _{-0.0072}	0.00 ^{+16.16} _{-0.00}	-1.40 ^{+1.07} _{-1.04}	4.6	Ni XXVII	<u>1s2p</u> 1s5s	5.9064	0.40	170 ⁺¹⁴ ₋₃₆₇
				(Ni XXVII	<u>1s2p</u> 1s5d	5.8914	4.1e+04	932 ⁺¹⁴ ₋₃₆₈
				(Ni XXVII	<u>1s2p</u> 1s5d	5.8914	3.3e+03	932 ⁺¹⁴ ₋₃₆₈
				(Ni XXVII	<u>1s2p</u> 1s5d	5.8944	1.1e+03	779 ⁺¹⁴ ₋₃₆₈
				(Ni XXVII	<u>1s2p</u> 1s5d	5.8944	7.1e+03	779 ⁺¹⁴ ₋₃₆₈
6.0442 ^{+0.0048} _{-0.0045}	14.82 ^{+10.15} _{-8.86}	-3.22 ^{+1.24} _{-1.36}	19.9	(Al XIII	<u>1s</u> 3p	6.0526	4.70) ← -417 ⁺²⁴⁰ ₋₂₂₅
				(Al XIII	<u>1s</u> 3p	6.0537	4.69	-471 ⁺²⁴⁰ ₋₂₂₅
6.1814 ^{+0.0027} _{-0.0026}	24.59 ^{+6.87} _{-6.05}	-8.83 ^{+1.52} _{-1.59}	132.5	Si XIV	<u>1s</u> 2p	6.1804	23.7	← 46 ⁺¹³⁰ ₋₁₂₇
				(Si XIV	<u>1s</u> 2p	6.1858	23.6	-216 ⁺¹²⁹ ₋₁₂₇
6.3148 ^{+0.0070} _{-0.0061}	14.19 ^{+13.54} _{-14.19}	-2.35 ^{+1.23} _{-1.36}	10.3	Al XII	<u>1s²</u> 1s4p	6.3140	3.14	38 ⁺³³² ₋₂₉₁
				(Ni XXV	<u>1s²2p²</u> 1s ² 2p ^{6d}	6.3239	3.64	-430 ⁺³³² ₋₂₉₁
				(Ni XXV	<u>1s²2p²</u> 1s ² 2p ^{6d}	6.3175	1.91	-127 ⁺³³² ₋₂₉₁
6.4552 ^{+0.0039} _{-0.0052}	0.49 ^{+16.17} _{-0.49}	2.45 ^{+1.38} _{-1.17}	11.9	Ni XXV	<u>1s²2s²p</u> 1s ² 2p ^{5p}	6.453	1.88	93 ⁺¹⁸³ ₋₂₄₂
				Ni XXV	<u>1s²2s²p</u> 1s ² 2p ^{5p}	6.458	1.39	-163 ⁺¹⁸³ ₋₂₄₁
6.6461 ^{+0.0026} _{-0.0027}	11.50 ^{+7.78} _{-5.60}	-5.52 ^{+1.36} _{-1.58}	65.2	Si XIII	<u>1s²</u> 1s2p	6.6479	37.7	← -81 ⁺¹¹⁹ ₋₁₂₀

Table A III.2: List of lines in the ‘dip’ spectrum – sorted by wavelength (continued)

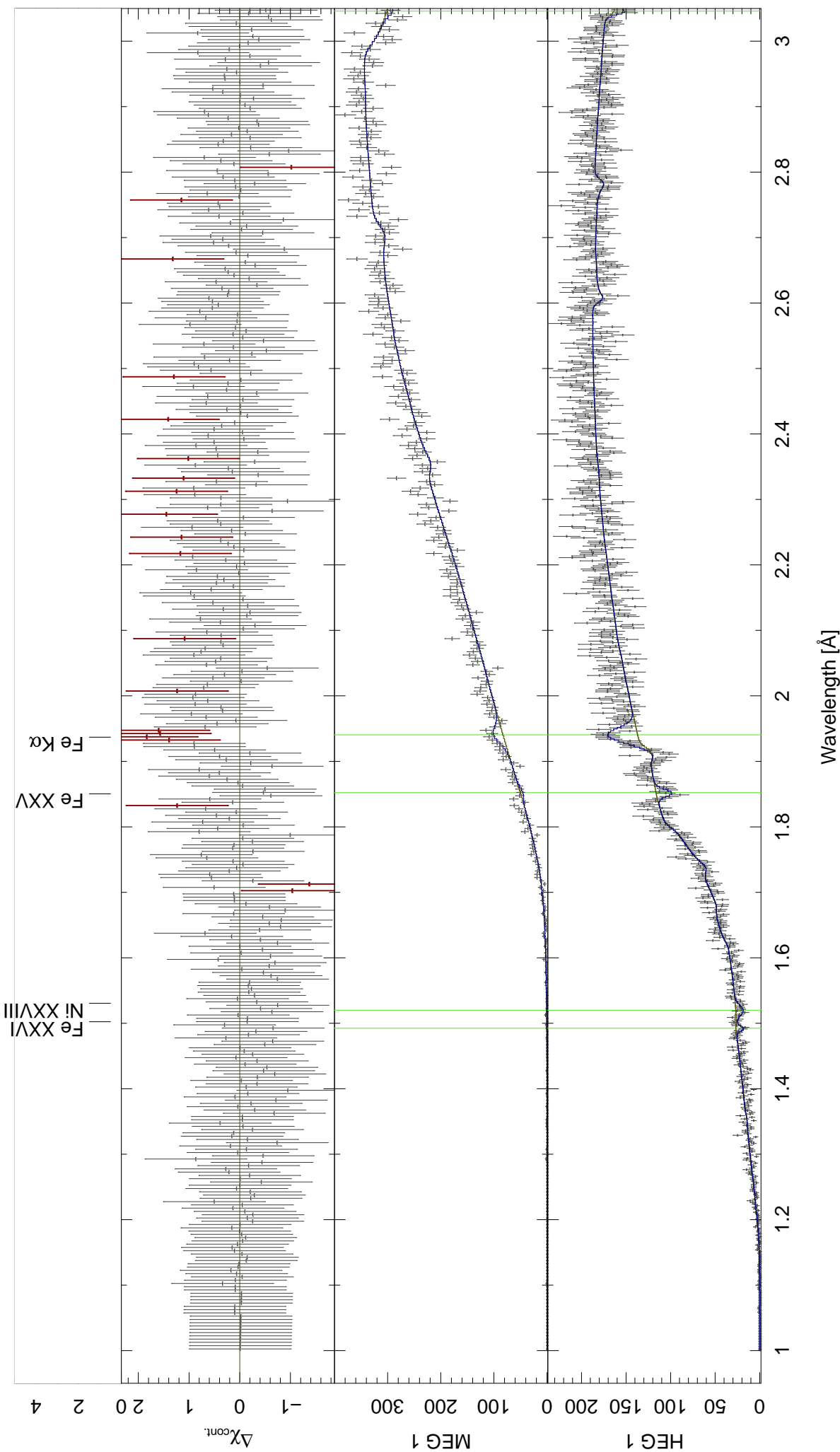
λ [Å]	FWHM [mÅ]	EW [mÅ]	$\Delta\chi^2$	ion <i>i</i>	transition <i>j</i>	λ_0 [Å] [10^{12}s^{-1}]	A_{ji}	$\Delta\lambda/\lambda \cdot c$ [km/s]	
6.7243 ^{+0.0009} _{-0.0045}	0.09 ^{+21.23} _{-0.09}	-1.96 ^{+0.98} _{-1.18}	10.6	(Mg XII Mg XII	<u>1s</u> <u>1s</u>	4p 4p	6.7378 6.7382	1.39) ← 1.39)	-598 ⁺⁴¹ ₋₂₀₂ -617 ⁺⁴¹ ₋₂₀₂
6.7426 ^{+0.0024} _{-0.0010}	1.02 ^{+6.56} _{-1.02}	6.88 ^{+1.35} _{-1.44}	79.0	(Si XIII Si XI	<u>1s</u> ² Kα	1s2s Kα	6.740: 6.8130	0.000) ←) ←	103 ⁺¹⁰⁶ ₋₄₅ -1158 ⁺⁸⁹ ₋₉₂
6.7867 ^{+0.0020} _{-0.0021}	17.89 ^{+5.97} _{-4.72}	-7.64 ^{+1.31} _{-1.41}	134.3	(Si X Si X	Kα Kα		6.8820) ←	-1239 ⁺⁶⁸ ₋₅₆
6.8536 ^{+0.0016} _{-0.0013}	9.96 ^{+4.04} _{-9.96}	-6.16 ^{+1.73} _{-1.00}	154.5	(Si IX Si IX	Kα Kα		6.8820) ←	-702 ⁺⁷⁰ ₋₇₁
6.8659 ^{+0.0016} _{-0.0016}	15.57 ^{+4.95} _{-3.60}	-7.81 ^{+1.17} _{-1.24}	178.4	(Si IX Si IX	Kα Kα		6.9470) ←	-1010 ⁺⁶⁰ ₋₅₈
6.9236 ^{+0.0014} _{-0.0013}	16.74 ^{+3.67} _{-3.74}	-10.09 ^{+1.28} _{-1.22}	274.7	(Si VIII Si VIII	Kα Kα		7.0070) ←	-302 ⁺¹⁰⁶ ₋₂
6.9400 ^{+0.0025} _{-0.0001}	0.02 ^{+8.26} _{-0.02}	-4.70 ^{+0.74} _{-0.67}	107.9	(Si VII Si VII	Kα Kα		7.0630) ←	-380 ⁺⁵⁸ ₋₅₂
6.9981 ^{+0.0013} _{-0.0012}	10.87 ^{+4.53} _{-4.30}	-8.26 ^{+1.26} _{-1.35}	207.6	(Mg XII Mg XII	<u>1s</u> <u>1s</u>	3p 3p	7.1058 7.1069	3.41 ← 3.41	95 ⁺¹⁹⁶ ₋₁₂₆ 47 ⁺¹⁹⁶ ₋₁₂₆
7.0550 ^{+0.0003} _{-0.0029}	0.07 ^{+7.53} _{-0.07}	-3.27 ^{+0.99} _{-0.90}	32.7	(Fe XXIV Fe XXIV	<u>1s</u> ² <u>2s</u>	1s ² 5p	7.1690	1.71	-539 ⁺¹⁰⁰⁵ ₋₁₀₈₉
7.1080 ^{+0.0047} _{-0.0030}	0.21 ^{+20.25} _{-0.21}	-2.05 ^{+0.99} _{-1.18}	11.3	(Fe XXIV Fe XXIV	<u>1s</u> ² <u>2s</u>	1s ² 5p	7.1690	1.69	-539 ⁺¹⁰⁰⁵ ₋₁₀₈₉
7.1561 ^{+0.0240} _{-0.0260}	0.01 ^{+50.42} _{-0.01}	-0.76 ^{+0.76} _{-1.46}	1.3	(Al XIII Al XIII	<u>1s</u> <u>1s</u>	2p 2p	7.1710 7.1764	17.6 17.6	-623 ⁺¹⁰⁰⁵ ₋₁₀₈₉ -848 ⁺¹⁰⁰⁴ ₋₁₀₈₈
				(Fe XXVI Fe XXVI	<u>2p</u> <u>2p</u>	4d 4d	7.1712 7.1748	9.27 1.54	-631 ⁺¹⁰⁰⁵ ₋₁₀₈₉ -781 ⁺¹⁰⁰⁵ ₋₁₀₈₈
7.1762 ^{+0.0038} _{-0.0062}	0.01 ^{+17.29} _{-0.01}	-1.40 ^{+1.03} _{-1.17}	4.9	(Al XIII Al XIII	<u>1s</u> <u>1s</u>	2p 2p	7.1710 7.1764	17.6 17.6	218 ⁺¹⁵⁷ ₋₂₅₉ -8 ⁺¹⁵⁷ ₋₂₅₉
7.4700 ^{+0.0025} _{-0.0000}	0.00 ^{+6.59} _{-0.00}	-3.23 ^{+0.97} _{-0.95}	28.2	(Mg XI Mg XI	<u>1s</u> ²	1s4p	7.4730	2.24) ←	-120 ⁺¹⁰⁰ ₋₀
7.7750 ^{+0.0171} _{-0.0097}	0.00 ^{+23.68} _{-19.88}	-2.08 ^{+2.45} _{-2.90}	0.0	(Al XII Al XII	<u>1s</u> ²	1s2p	7.7573	27.5) ←	684 ⁺⁶⁶² ₋₃₇₃
7.8024 ^{+0.0057} _{-0.0056}	25.11 ^{+13.65} _{-11.32}	6.32 ^{+2.28} _{-2.19}	27.4	(Al XII Al XII	<u>1s</u> ² <u>1s</u> ²	1s2p 1s2p	7.807: 7.803:	0.082 ← 0.000	-175 ⁺²¹⁷ ₋₂₁₄ -55 ⁺²¹⁷ ₋₂₁₄
7.8550 ^{+0.0040} _{-0.0038}	17.84 ^{+11.35} _{-8.58}	-5.79 ^{+1.73} _{-1.79}	40.5	(Mg XI Mg XI	<u>1s</u> ²	1s3p	7.8503	5.43) ←	180 ⁺¹⁵¹ ₋₁₄₆
7.8776 ^{+0.0224} _{-0.0176}	0.02 ^{+49.98} _{-0.02}	1.07 ^{+1.36} _{-1.07}	1.7	(Al XII Al XII	<u>1s</u> ²	1s2s	7.872: 7.872:	0.000 ←	210 ⁺⁸⁵² ₋₆₇₂
				(Ni XXII Ni XXIV	<u>2s</u> ² <u>p</u> ⁴ <u>1s</u> ² <u>2s</u> <u>2p</u> ²	2s2p ³ 5d 1s ² 2s2p4d	8.0494 7.9965	4.98) 4.47)	-884 ⁺⁵⁰⁵ ₋₅₇₉ 1094 ⁺⁵⁰⁸ ₋₅₈₃
8.0257 ^{+0.0136} _{-0.0155}	46.64 ^{+8.76} _{-38.22}	-5.00 ^{+3.13} _{-2.78}	13.0	(Ni XXIII Ni XXIV	<u>1s</u> ² <u>2s</u> ² <u>2p</u> ² <u>1s</u> ² <u>2s</u> <u>2p</u> ²	1s ² 2s2p2p4p 1s ² 2s2p4d	8.0400 8.0437	4.11) 4.10)	-533 ⁺⁵⁰⁵ ₋₅₇₉ -674 ⁺⁵⁰⁵ ₋₅₇₉
8.0706 ^{+0.0069} _{-0.0006}	0.00 ^{+17.80} _{-0.00}	2.70 ^{+1.48} _{-1.44}	9.8	(Ni XXIV Ni XXIV	<u>1s</u> ² <u>2s</u> <u>2p</u> ²	1s ² 2s2p4d	8.082: 8.082:	12.4)	-434 ⁺²⁵⁷ ₋₂₂
8.4220 ^{+0.0151} _{-0.0149}	42.69 ^{+0.00} _{-0.00}	-8.28 ^{+0.00} _{-0.00}	0.0	(Mg XII Mg XII	<u>1s</u> <u>1s</u>	2p 2p	8.4192 8.4246	12.8 ← 12.8	99 ⁺⁵³⁷ ₋₅₃₂ -93 ⁺⁵³⁷ ₋₅₃₂
				(Ni XXIII Ni XXIII	<u>1s</u> ² <u>2s</u> <u>2p</u> ³	1s ² 2s2p2p4d	8.4499	4.37)	-991 ⁺⁵³⁵ ₋₅₃₀
8.6551 ^{+0.0158} _{-0.0106}	74.76 ^{+0.59} _{-66.28}	-11.31 ^{+2.62} _{-3.80}	24.5	(Ni XX Ni XXIII	<u>2s</u> ² <u>2p</u> ⁵ <u>1s</u> ² <u>2s</u> <u>2p</u> ⁴	2s ² 2p ⁴ d 1s ² 2p ² 2p4d	8.6556 8.6564	2.81 3.33	-19 ⁺⁴⁶ ₋₃₆₈ -47 ⁺⁵⁴⁵ ₋₃₆₈
				(Ni XXI Ni XXVII	<u>1s</u> ² <u>2s</u> <u>2p</u> ³ <u>1s</u> ² <u>2s</u> <u>2p</u>	1s ² 2s2p ⁵ d 1s3d	8.6582 8.7069 1.7e+05	2.84)	-106 ⁺⁵⁴⁵ ₋₃₆₈ -1785 ⁺⁵⁴² ₋₃₆₆
				(Ni XXVII Ni XXVII	<u>1s</u> ² <u>2s</u> <u>2p</u> ³ <u>1s</u> ² <u>2s</u> <u>2p</u>	1s ² 2s2p ⁵ d 1s3d	8.7135 1.5e+04 8.6102 11.9))	-2008 ⁺⁵⁴² ₋₃₆₆ 1563 ⁺⁵⁴⁸ ₋₃₇₀
9.2311 ^{+0.0026} _{-0.0016}	7.16 ^{+5.39} _{-7.16}	13.39 ^{+3.29} _{-2.25}	72.8	(Mg XI Mg XI	<u>1s</u> ²	1s2p	9.231: 9.231:	0.034 ←	-3 ⁺⁸⁶ ₋₅₂
9.2860 ^{+0.0037} _{-0.0034}	21.55 ^{+10.54} _{-6.45}	-11.18 ^{+2.62} _{-3.12}	63.7	(Ni XX Ni XX	<u>2s</u> ² <u>p</u> ⁶ <u>2s</u> ² <u>2s</u> <u>2p</u> ²	2s2p ⁴ 4d 1s ² 2s2p4d	9.2618 9.2630	7.19) 5.69)	784 ⁺¹²⁰ ₋₁₁₀ 746 ⁺¹²⁰ ₋₁₁₀
9.3155 ^{+0.0029} _{-0.0029}	16.62 ^{+7.32} _{-6.37}	13.46 ^{+3.39} _{-3.25}	54.3	(Mg XI Mg XI	<u>1s</u> ²	1s2s	9.314: 9.314:	0.000	36 ⁺⁹⁴ ₋₉₃
9.3819 ^{+0.0019} _{-0.0021}	15.16 ^{+8.42} _{-4.97}	-13.22 ^{+2.29} _{-2.98}	140.6	(Fe XXII Fe XX	<u>1s</u> ² <u>2s</u> <u>2p</u> ² <u>2s</u> ² <u>p</u> ⁴	1s ² 2s2p4d 2p ² 2p ⁴ p	9.3824 9.3797	5.12 0.60)	-15 ⁺⁶² ₋₆₆ 71 ⁺⁶² ₋₆₆
9.4794 ^{+0.0043} _{-0.0131}	18.05 ^{+11.98} _{-8.94}	-8.69 ^{+2.62} _{-2.80}	39.0	(Fe XXI Ne X	<u>2s</u> ² <u>2p</u> ⁴ <u>1s</u> <u>1s</u>	2s ² 2p ² 5d 5p	9.3833 9.4807	0.44 0.34	-44 ⁺⁶² ₋₆₆ -48 ⁺¹³⁸ ₋₄₁₃
9.5006 ^{+0.0018} _{-0.0032}	8.34 ^{+8.00} _{-6.69}	-7.82 ^{+2.28} _{-2.21}	53.1	(Ni XX Ni XX	<u>2s</u> ² <u>2p</u> ⁵ <u>2s</u> ² <u>2p</u> ³	2s ² 2p ³ 4d 1s ² 2s2p ² 4d	9.4966 9.4966	10.3) 6.58)	124 ⁺⁵⁸ ₋₁₀₀ 124 ⁺⁵⁸ ₋₁₀₀
				(Fe XXI Ne X	<u>1s</u> ² <u>2s</u> <u>2p</u> ³	1s ² 2s2p ² 4d	9.4973	1.95)	103 ⁺⁵⁸ ₋₁₀₀

Table A III.2: List of lines in the ‘dip’ spectrum – sorted by wavelength (continued)

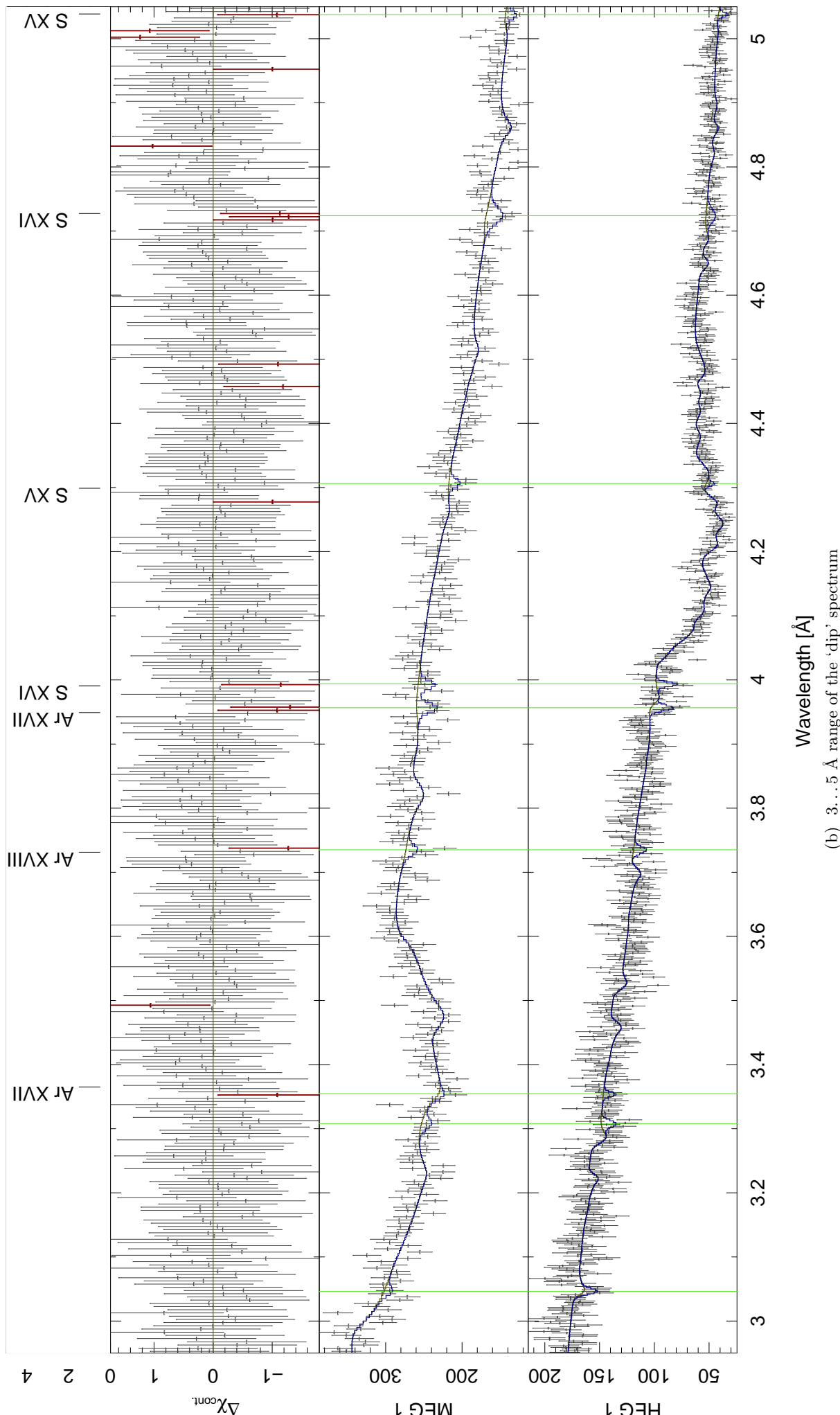
λ [Å]	FWHM [mÅ]	EW [mÅ]	$\Delta\chi^2$	ion <i>i</i>	transition <i>j</i>	λ_0 [Å]	A_{ji} $[10^{12}\text{s}^{-1}]$	$\Delta\lambda/\lambda \cdot c$ [km/s]
9.5167 ^{+0.0035} _{-0.0028}	11.68 ^{+8.57} _{-6.83}	-7.20 ^{+2.14} _{-2.45}	36.5	Fe XXI	$1s^2 2s2p^3$	$1s^2 2s2p2p4d$	9.5178	4.39
				(Fe XXI	$1s^2 2s2p^3$	$1s^2 2s2p2p4d$	9.5120	4.02)
				(Fe XXI	$1s^2 2s2p^3$	$1s^2 2s2p2p4d$	9.5213	3.29)
				Fe XXI	$1s^2 2s2p^3$	$1s^2 2s2p2p4d$	9.5146	2.45
				Fe XXI	$1s^2 2s2p^3$	$1s^2 2s2p2p4d$	9.5140	2.33
				(Fe XXI	$1s^2 2s2p^3$	$1s^2 2s2p2p4d$	9.5231	2.09)
				Ni XX	$2s2p^6$	$2s2p2p4d$	9.5196	6.21
				Ni XXV	$1s^2 2s2p$	$1s^2 2s3d$	9.6010	17.3
				(Fe XXI	$1s^2 2s2p^3$	$1s^2 2s2p4d$	9.6059	8.91)
				Fe XXI	$1s^2 2p^4$	$1s^2 2p3d$	9.5926	4.75
9.5963 ^{+0.0054} _{-0.0053}	26.43 ^{+13.15} _{-10.46}	-9.94 ^{+3.12} _{-3.35}	35.4	Fe XXI	$1s^2 2s2p^2$	$1s^2 2s2p4d$	9.5917	3.77
				(Fe XXI	$1s^2 2p^4$	$1s^2 2p3d$	9.5888	3.43)
				Ni XXV	$1s^2 2s2p$	$1s^2 2s3d$	9.6300	12.6
				Ni XX	$2s2p^6$	$2s2p2p3d$	9.6291	2.37
				(Fe XXI	$1s^2 2p^4$	$1s^2 2p3d$	9.6582	6.64)
9.6489 ^{+0.0041} _{-0.0039}	5.39 ^{+9.63} _{-5.39}	-5.06 ^{+1.88} _{-2.33}	19.1	(Fe XXI	$1s^2 2s2p^3$	$1s^2 2s2p4d$	9.6421	2.71)
				Fe XXI	$1s^2 2s2p^3$	$1s^2 2s2p2p4d$	9.6500	2.59
				(Fe XXI	$1s^2 2p^4$	$1s^2 2p3d$	9.6567	2.35)
				Fe XXVI	$2p$	$3d$	9.6745	29.1
9.6770 ^{+0.0103} _{-0.0102}	26.93 ^{+23.07} _{-18.05}	-5.89 ^{+3.20} _{-3.58}	10.4	(Ni XXV	$1s^2 2p^2$	$1s^2 2p3d$	9.6887	20.5)
				(Ni XXV	$1s^2 2p^2$	$1s^2 2p3d$	9.6913	15.2)
				(Fe XIX	$2s^2 2p^4$	$2s2p2p2p4p$	9.7061	0.015) ←
9.7116 ^{+0.0026} _{-0.0018}	0.10 ^{+12.34} _{-0.10}	-4.55 ^{+1.69} _{-1.90}	19.3	(Ne X	$1s$	$4p$	9.7080	0.67)
				(Ne X	$1s$	$4p$	9.7085	0.67)
				Fe XIX	$2s2p^5$	$2s2p2p3d$	9.7326	2.73
9.7275 ^{+0.0064} _{-0.0060}	19.64 ^{+19.64} _{-11.76}	-6.60 ^{+2.82} _{-3.19}	18.2	Fe XX	$2s^2 2p^3$	$2s2p2p4p$	9.7242	2.47
				Fe XX	$2s^2 2p^3$	$2s2p2p4p$	9.7269	2.42
				Fe XIX	$2s2p^5$	$2s2p2p3d$	9.7313	2.28
				Fe XIX	$2s^2 2p^4$	$2s^2 2p3d$	9.7327	1.45
				Ni XXV	$1s^2 2p^2$	$1s^2 2p3d$	9.7230	27.1
				(Ni XXIV	$1s^2 2s2p^2$	$1s^2 2s2p3d$	10.349	32.7)
				(Ni XXIV	$1s^2 2s2p^2$	$1s^2 2s2p3d$	10.329	20.8
10.3125 ^{+0.0199} _{-0.0125}	41.97 ^{+8.03} _{-25.80}	8.89 ^{+5.95} _{-6.30}	8.0	(Ni XXIV	$1s^2 2s2p^2$	$1s^2 2s2p3d$	10.297	19.4)
				(Ni XXIV	$1s^2 2s2p^2$	$1s^2 2s2p3d$	10.343	14.5)
				(Ni XXIV	$1s^2 2s2p^2$	$1s^2 2s2p3d$	10.331	14.2)
				Ni XXIV	$1s^2 2s2p^2$	$1s^2 2s2p3d$	10.4237	29.8
				(Ni XXIV	$1s^2 2s^2 2p$	$1s^2 2s3d$	10.4410	24.7)
10.4269 ^{+0.0131} _{-0.0149}	19.75 ^{+34.82} _{-19.75}	-5.14 ^{+3.85} _{-4.00}	5.3	(Ni XXIV	$1s^2 2s^2 2p$	$1s^2 2s3d$	10.4116	20.6)
				(Fe XVIII	$2s^2 2p^5$	$2s^2 2p4d$	10.5364	2.60) ←
				(Fe XVIII	$2s^2 2p^5$	$2s^2 2p2p5d$	10.5382	2.25)
10.5225 ^{+0.0075} _{-0.0051}	0.01 ^{+28.98} _{-0.01}	-4.12 ^{+2.53} _{-1.93}	6.8	(Fe XVIII	$2s^2 2p^5$	$2s^2 2p2p2p5d$	10.5442	1.22)
				(Fe XVIII	$2s^2 2p^5$	$2s^2 2p2p2p5d$	10.5442	1.22)
				(Fe XVIII	$2s^2 2p^5$	$2s^2 2p2p3d$	10.5640	1.58) ←
10.5525 ^{+0.0075} _{-0.0000}	0.00 ^{+14.78} _{-0.00}	-4.18 ^{+2.60} _{-2.77}	7.0	(Fe XVIII	$2s^2 2p^5$	$2s^2 2p2p4p$	10.5672	1.39)
				(Fe XVIII	$2s^2 2p^5$	$2s^2 2p2p3d$	10.5672	1.39)
				(Fe XVIII	$2s^2 2p^5$	$2s^2 2p2p4p$	10.5672	1.39)
10.5734 ^{+0.0064} _{-0.0060}	0.45 ^{+24.33} _{-0.45}	-5.06 ^{+2.72} _{-2.49}	9.6	(Fe XVIII	$2s^2 2p^5$	$2s^2 2p2p3d$	10.5640	1.58) ←
				(Fe XVIII	$2s^2 2p^5$	$2s^2 2p2p4p$	10.5672	1.39)
				Fe XIX	$2s^2 2p^4$	$2s^2 2p3d$	10.6414	5.20 ←
				(Fe XIX	$2s^2 2p^4$	$2s^2 2p3d$	10.6491	3.74)
10.6402 ^{+0.0054} _{-0.0037}	4.39 ^{+16.07} _{-4.39}	-6.04 ^{+2.70} _{-3.61}	13.6	Fe XIX	$2s^2 2p^4$	$2s^2 2p3d$	10.6407	1.24
				(Fe XIX	$2s^2 2p^4$	$2s^2 2p3d$	10.6295	4.78)
				(Fe XIX	$2s^2 2p^4$	$2s^2 2p3d$	10.6840	2.28) ←
				(Fe XIX	$2s^2 2p^4$	$2s^2 2p3d$	10.6798	0.84)
10.6897 ^{+0.0007} _{-0.0030}	0.09 ^{+8.30} _{-0.09}	-8.65 ^{+2.30} _{-2.29}	37.4	Ni XXIII	$1s^2 2p^4$	$1s^2 2p2p3d$	10.940	28.8
				Ni XXIII	$1s^2 2p^4$	$1s^2 2p2p3d$	10.928	26.4
				(Ni XXIII	$1s^2 2p^4$	$1s^2 2p2p3d$	10.920	11.7)
				Ni XXIII	$1s^2 2s2p^3$	$1s^2 2s2p3d$	10.947	8.41
				(Fe XIX	$2p^6$	$2p2p4d$	10.923	8.25
11.0010 ^{+0.0201} _{-0.0205}	0.00 ^{+50.42} _{-0.00}	-3.08 ^{+3.08} _{-3.45}	2.6					

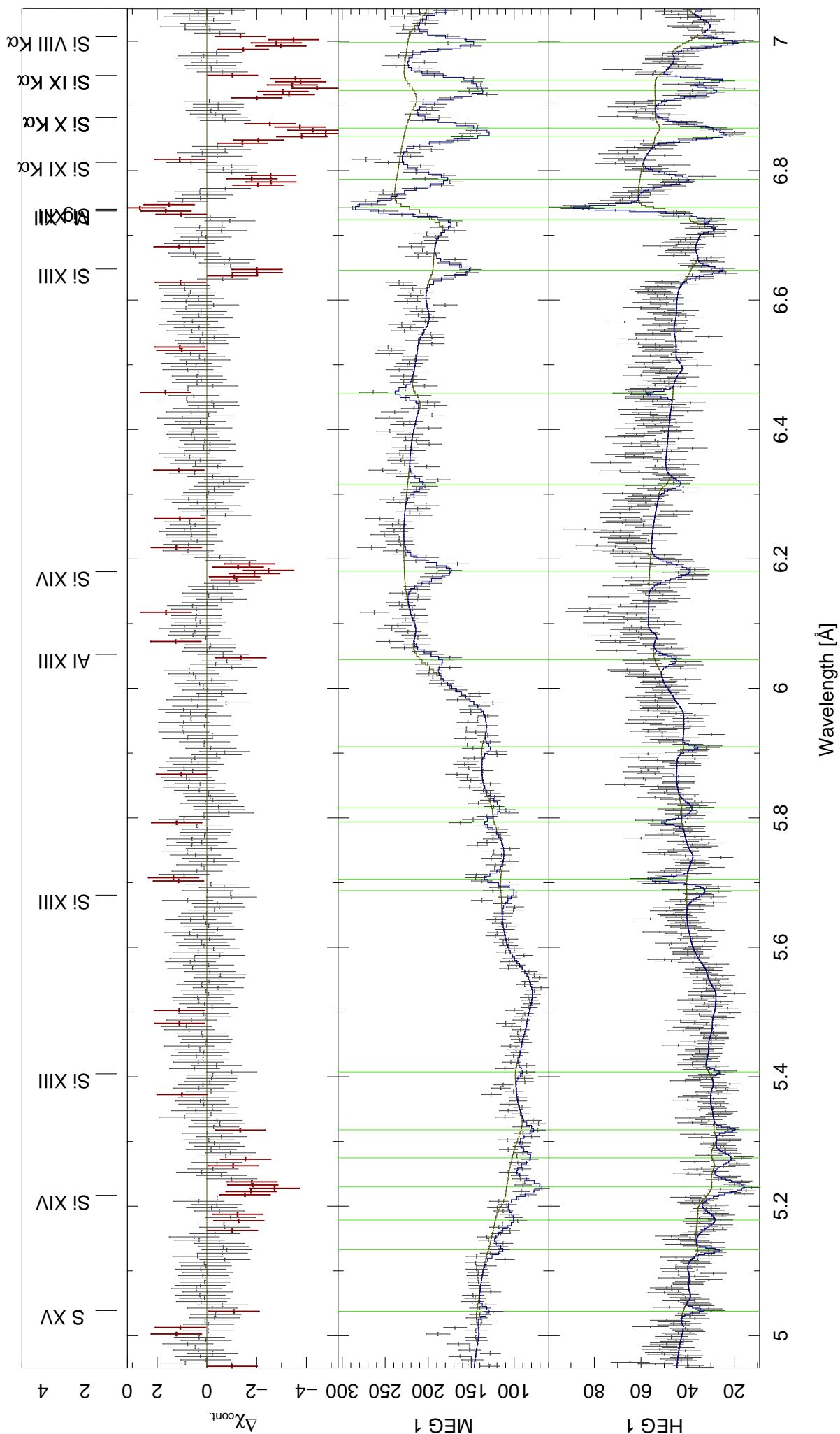
Table A III.2: List of lines in the ‘dip’ spectrum – sorted by wavelength (continued)

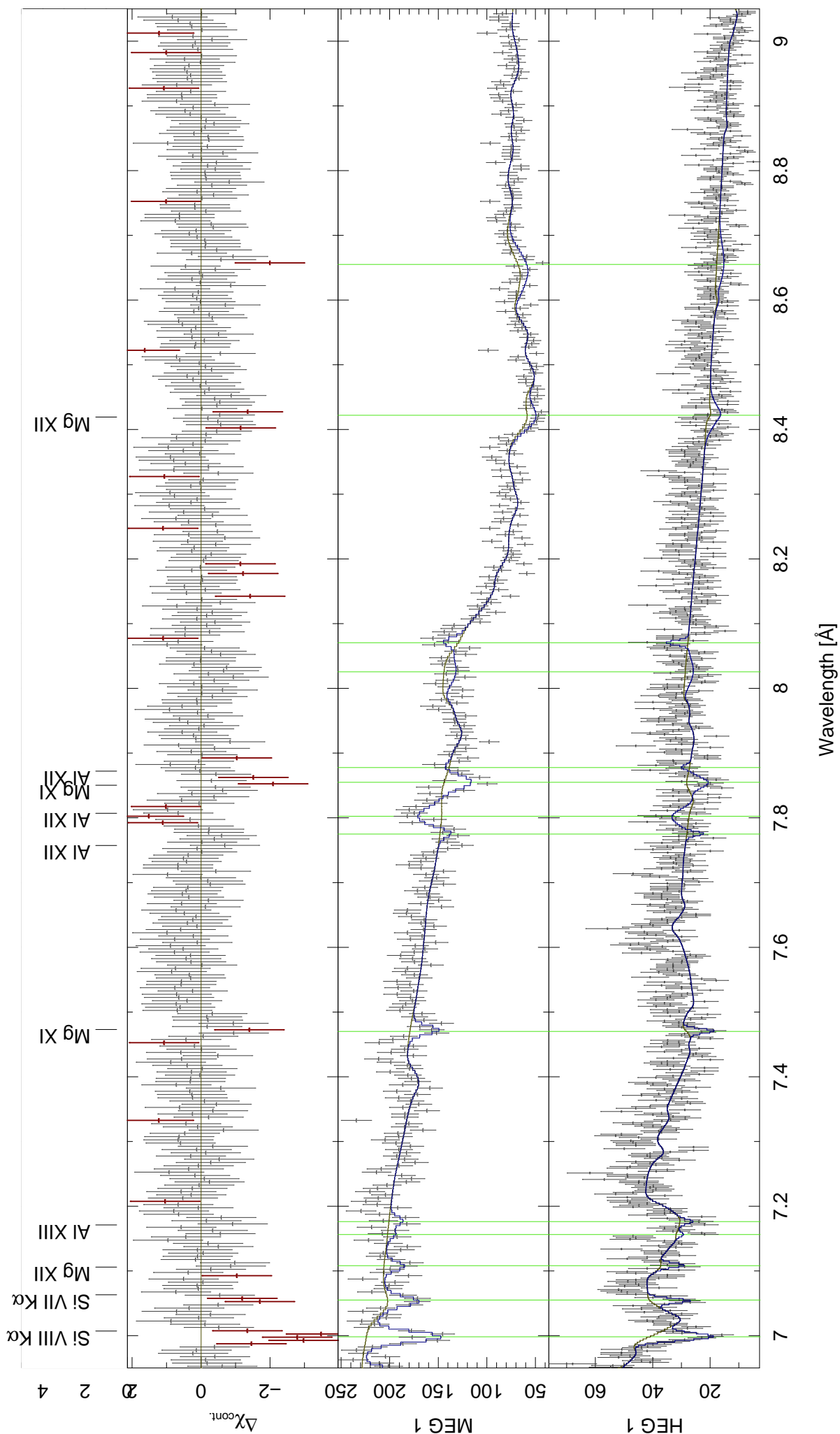
λ [Å]	FWHM [mÅ]	EW [mÅ]	$\Delta\chi^2$	ion <i>i</i>	transition <i>j</i>	λ_0 [Å] $\times 10^{12}$ s $^{-1}$	A_{ji}	$\Delta\lambda/\lambda \cdot c$ [km/s]	
11.0742 $^{+0.0008}_{-0.0092}$	0.01 $^{+24.08}_{-0.01}$	$-4.77^{+3.17}_{-3.15}$	6.1	(Ni XXIII	$1s^2 2p^4$	$1s^2 2p2p^2 3d$	11.0891	13.3)	-403 $^{+22}_{-249}$
				(Ni XXIII	$1s^2 2p^4$	$1s^2 2p2p^2 3d$	11.0951	12.9)	-565 $^{+22}_{-249}$
				Ni XXIII	$1s^2 2s2p^3$	$1s^2 2s2p^2 3d$	11.0722	12.6	55 $^{+22}_{-249}$
				(Ni XXIII	$1s^2 2s2p^3$	$1s^2 2s2p^2 3d$	11.0894	12.3)	-410 $^{+22}_{-249}$
11.0974 $^{+0.0026}_{-0.0073}$	24.37 $^{+20.55}_{-12.87}$	14.75 $^{+6.90}_{-5.94}$	16.7						
11.2051 $^{+0.0049}_{-0.0245}$	42.98 $^{+7.02}_{-30.24}$	11.34 $^{+7.39}_{-7.36}$	6.4						
11.5700 $^{+0.0125}_{-0.0200}$	12.13 $^{+38.30}_{-12.13}$	$-5.64^{+4.56}_{-6.27}$	4.2	(Ne IX	$\underline{1s^2}$	$1s3p$	11.5440	2.48)	675 $^{+324}_{-519}$
				Fe XVIII	$2s^2 2p^5$	$2s^2 2p^2 2p^2 4d$	11.5740	1.53	-104 $^{+323}_{-518}$
				Ni XXII	$2s2p^4$	$2s2p2p^2 3d$	11.5824	20.6	-320 $^{+323}_{-517}$
				Ni XXII	$2s2p^4$	$2s2p^3 3d$	11.5589	15.7	288 $^{+324}_{-519}$
12.0976 $^{+0.0135}_{-0.0095}$	28.00 $^{+19.20}_{-28.00}$	-15.63 $^{+8.63}_{-7.98}$	10.9	(Ne X	$\underline{1s}$	$2p$	12.1321	6.16)	-853 $^{+333}_{-235}$
				(Ne X	$\underline{1s}$	$2p$	12.1375	6.16)	-986 $^{+333}_{-234}$
12.4652 $^{+0.0098}_{-0.0005}$	0.06 $^{+13.28}_{-0.06}$	-14.04 $^{+5.65}_{-5.99}$	16.6	Fe XXI	$1s^2 2s2p^3$	$1s^2 2s2p^2 3d$	12.4656	26.9	-9 $^{+235}_{-12}$
				Fe XXI	$1s^2 2s2p^3$	$1s^2 2s2p^2 3d$	12.4726	9.00	-177 $^{+235}_{-12}$
				Fe XXI	$1s^2 2s2p^3$	$1s^2 2p2p^2 3p$	12.4675	5.82	-54 $^{+235}_{-12}$
12.8029 $^{+0.0177}_{-0.0223}$	0.15 $^{+49.85}_{-0.15}$	-3.94 $^{+3.94}_{-10.45}$	0.9	(Fe XX	$2s^2 2p^3$	$2s^2 2p2p3d$	12.8460	19.2)	-1006 $^{+413}_{-520}$
				(Fe XX	$2s^2 2p^3$	$2s^2 2p2p3d$	12.8240	17.1)	-493 $^{+414}_{-521}$
				Fe XXI	$1s^2 2p^4$	$1s^2 2p^3 3d$	12.7869	28.2	375 $^{+415}_{-523}$
13.5398 $^{+0.0058}_{-0.0049}$	31.33 $^{+12.61}_{-12.19}$	129.81 $^{+36.46}_{-35.78}$	39.0	(Ne IX	$\underline{1s^2}$	$1s2p$	13.550	0.000) \leftarrow	-231 $^{+128}_{-109}$
				(Ne IX	$\underline{1s^2}$	$1s2p$	13.553	0.006)	-294 $^{+128}_{-109}$
15.3289 $^{+0.0154}_{-0.0154}$	49.66 $^{+0.34}_{-29.20}$	138.96 $^{+68.53}_{-73.93}$	11.4	(Fe XVII	$2s^2 2p^6$	$2s^2 2p^5 3d$	15.261	5.87)	1334 $^{+302}_{-303}$
				Fe XIX	$2p^6$	$2p^2 2p^3 3s$	15.334	0.89	-99 $^{+301}_{-301}$
				(Fe XIX	$2s2p^5$	$2s2p2p^3 3s$	15.347	0.42)	-355 $^{+301}_{-301}$
				(Fe XIX	$2s2p^5$	$2s2p^2 2p^2 3s$	15.350	0.33)	-423 $^{+301}_{-301}$

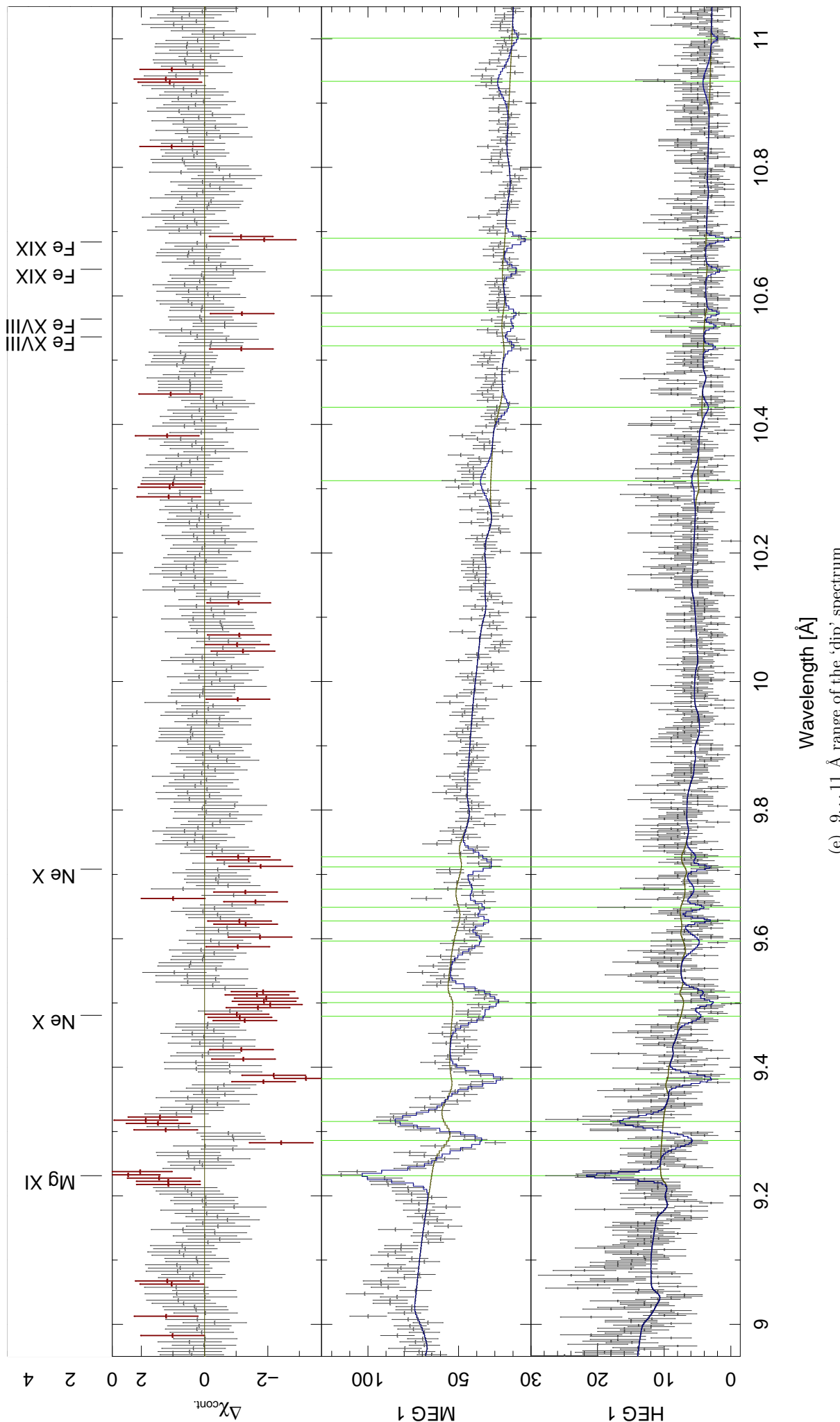


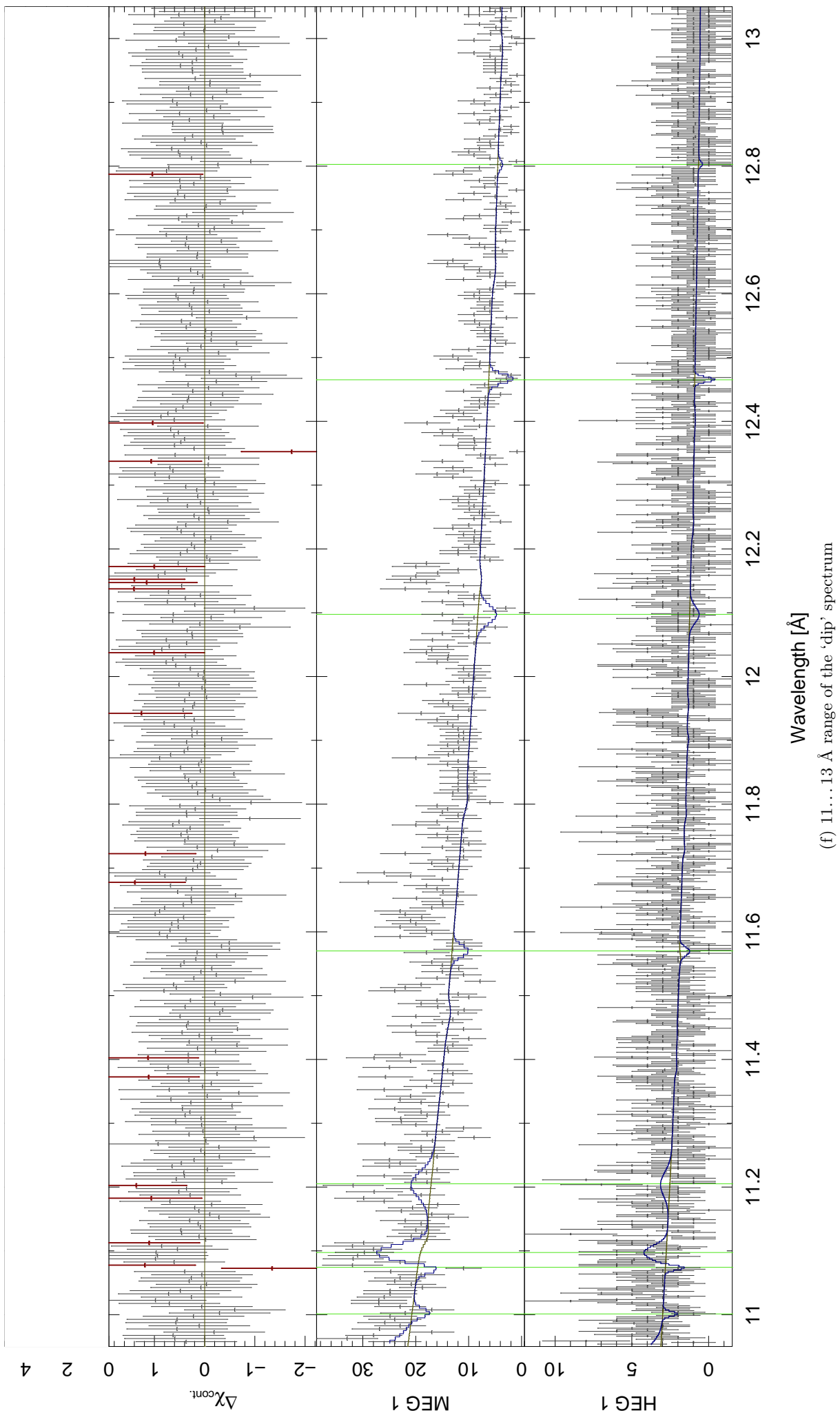
(a) 1...3 Å range of the 'dip' spectrum

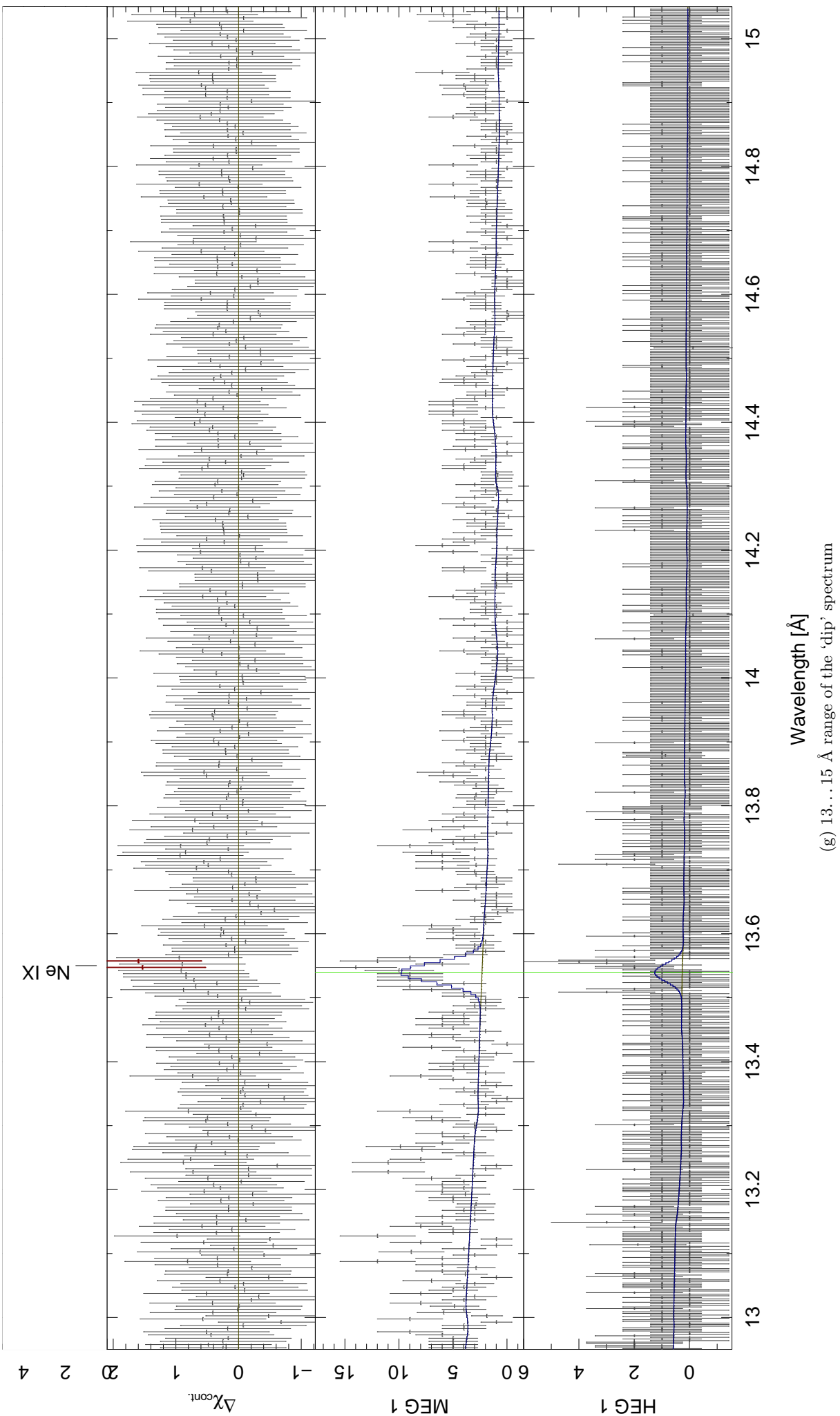












(g) 13..15 Å range of the ‘dip’ spectrum

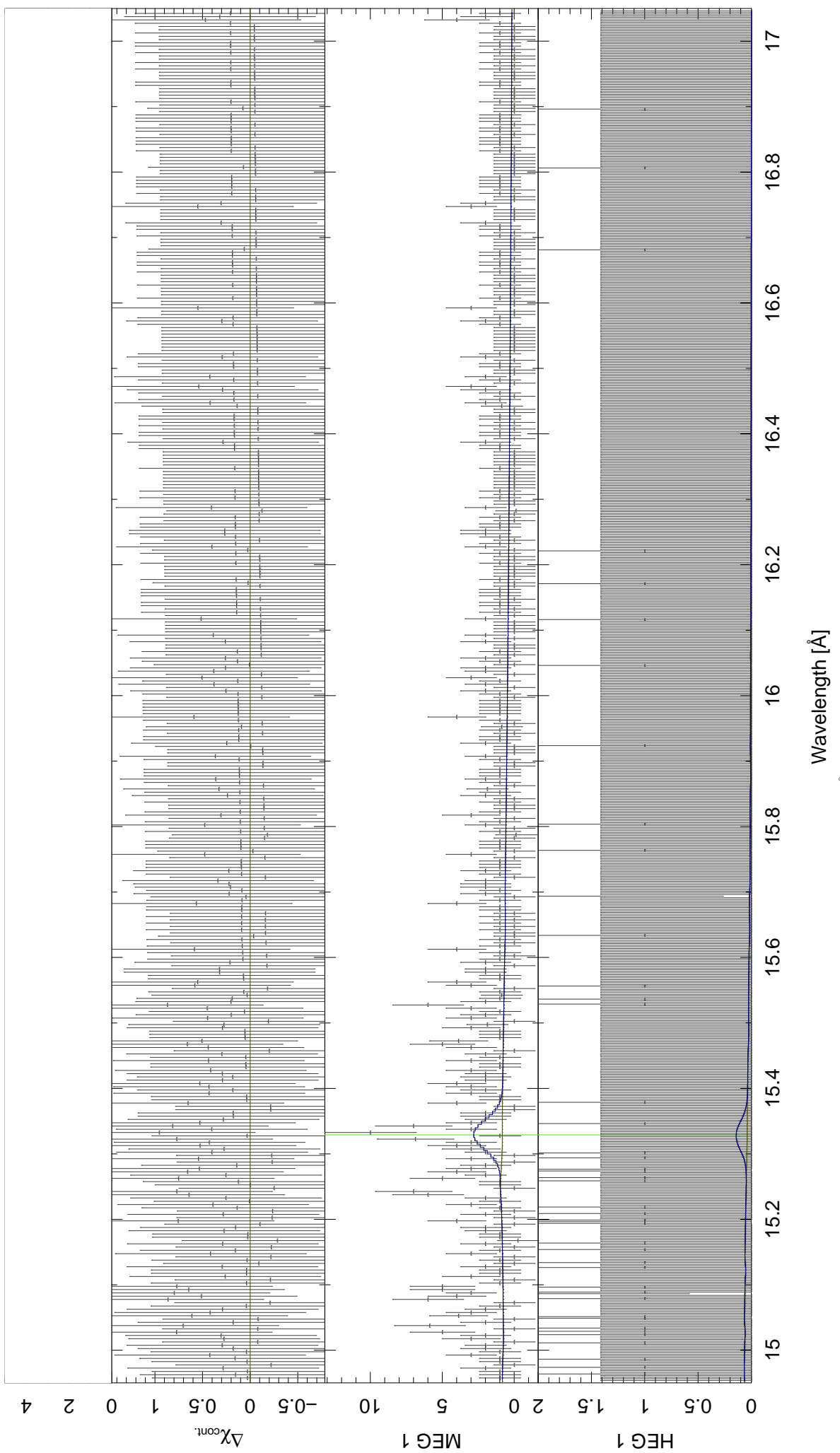


Figure A III.26: The fitted 'dip' spectrum, including all lines

Acknowledgments

First of all, I have to thank my advisor, Jörn Wilms, who introduced me in the exciting physics around black holes, such that I now share his enthusiasm of doing science with them. He has showed me many Linux-tricks and kindly asked me to give up some of my strange habits (concerning Perl, scripting, L^AT_EX, . . .), which has finally turned out to be a good idea. He has always had much confidence in me and my work, but he also had a sympathetic ear if I needed his advice or a critical discussion. His friendly nature contributed substantially to the nice and relaxed atmosphere at the whole institute, which encouraged the communication between the different groups and often made working a lot of fun. The professor – student relationship was thus more a collaboration, or even a friendship, which is a great honor for me. He unselfishly spent his flight voucher that made it possible for me, too, to visit our colleagues at the Massachusetts Institute of Technology in Boston. It was him who helped to establish contact to scientists (Peter Kretschmar, Andy Pollock) at the European Space Astronomy Center near Madrid, where I was finally permitted to perform an ESAC-traineeship to study the stellar wind in the Vela X-1 HMXB system with *XMM-Newton/RGS*.

I thank Katja Pottschmidt for reading my thesis so intensively. She found many misprints and gave useful comments. All errors still contained are solely due to my faults, of course.

Furthermore, I want to thank Adrienne Juett, whom I had the chance to meet when she spent a week in Bamberg to work on the high-resolution study of X-ray absorption by the interstellar medium. I took the profit to learn from her very much about reduction of *Chandra* data and she was so kind to answer me all my questions I had still later posed by email.

I also owe very much thanks to Mike Nowak, research scientist at the MKI/CXC, who has helped me with many technical problems with ISIS. He gave many comments on my strategy and was always willing for critical discussions. He has also organized part of our trip to Boston and, together with his wife Nirah, finally hosted us kindly for two days.

Moreover, I thank all the other scientists whom I met during my research visit at the MIT Kavli Institute for Astrophysics and Space Research (MKI), where I was hospitably received: John Houck, the developer of ISIS, who has always helped me with my questions; he either referred me to the appropriate functions, or added new features to ISIS – within at most two days. He also often had a look on my stupidly buggy code. Norbert Schulz showed me how the identification of absorption lines has to be done consistently. Andrew Young gave valuable comments about the curve of growth. Julia Lee (from Harvard) made the suggestion to fit complete line series.

I thank all my colleagues at the Remeis observatory, especially Heiko Hirsch and Stephan Geier, whose office I shared and with whom I have always had much fun, but also all the other ‘stellar astronomers’ from upper floor, namely Alfred Tillich, Christian Schmitt, Fernanda Nieva, Florian Schiller, Horst Drechsel, Markus Firnstein, Norbert Przybilla, Stefan Nesslinger and Uli Heber, as well as our sysadmin Rainer Sterzer and our helpful secretary Mrs. Day. I finally thank Dr. Karl Remeis (1837–1882), whose last will still guarantees the maintenance of the beautiful observatory in Bamberg, which is now our nice astronomical institute.

I thank all trainee students at the Remeis observatory, especially Clemens Bauer and Moritz Böck, for fruitful discussions on X-ray astronomy in general, Cygnus X-1 and ISIS.

I thank all my teachers, both from the university of Regensburg and from Erlangen-Nuremberg, who showed me how interesting physics is. I’d like to mention especially Andreas Schäfer from Regensburg, who encouraged me to accelerate the main courses in order to get faster into real research, which finally was a good decision, and who often helped me with organizational problems. I also will never forget all my fellow students from Regensburg, especially Christoph Lehner and Robert Lohmayer, with whom I have spent a very nice part of my study and who often spent their time together with me for critical discussions.

Last, but loved (not least at all!), I want to thank my darling Alexandra Hundschell. Although doing research is really fun, it will never be all in my life. I’m so glad that I may spend most of my spare time (which was sometimes rather sparse) with her; she supports me and my work (though it kept me sometimes away) and always gives me a lot of energy.

List of Figures

1.1	The penetration depth of electromagnetic waves in the Earth's atmosphere.	5
1.2	The Hertzsprung-Russell diagram.	7
1.3	The evolution of a compact binary. (after Postnov & Yungelson, 2006, Fig. 4)	8
1.4	Mass transfer via focused stellar wind (left) and Roche lobe overflow (right).	11
1.5	The 5 Lagrangian points.	11
1.6	Spectrum of LMC X-3, showing a transition from the hard to the state.	13
1.7	The constellation Cygnus with Cyg X-1	14
1.8	A velocity curve of HDE 226868, binned on the orbital phase.	15
1.9	The mass of the compact object for $f(M) = 0.252 \text{ M}_\odot$ and $M_\star = (16 \pm 2) \text{ M}_\odot$	16
1.10	Mass loss rate of Cyg X-1, modeled by Friend & Castor (1982, Fig. 4).	17
1.11	Unfolded spectra and residuals of Cyg X-1 in the hard and in the soft state.	18
1.12	Sketched geometry for the hard (top) and soft (bottom) state of Cyg X-1.	19
1.13	A jet blown ring around Cyg X-1 (cross) next to the H II region Sh2-101 (left).	19
1.14	Phase distribution of dips.	20
1.15	The <i>Chandra</i> spacecraft.	21
1.16	<i>Chandra</i> 's high resolution mirror assembly.	22
1.17	The Rowland geometry.	23
1.18	The High Energy Transmission Grating HETG.	24
1.19	The Science Instrument Module SIM and the High Resolution Camera HRC.	25
1.20	The ACIS CCD-chips: photography and sketch.	25
1.21	A readout streak.	26
1.22	<i>Chandra</i> 's Lissajous dither pattern: time-evolution of the focused target-position.	27
1.23	Fractional exposure of MEG+1 wavelength bins in a <i>Chandra</i> grating observation.	27
2.1	The photoionization cross section and the corresponding edges in the spectrum	29
2.2	Breaking of the degeneracy of the energy levels in multi-electron systems.	30
2.3	A simplified Grotrian diagram of He-like ions.	31
2.4	A curve of growth in the form W_λ/λ^2 vs. $N_i f_{ij}$	37
2.5	Curves of growth for S XVI Ly α in the form W_λ vs. $N_{\text{S XVI}}$	38
2.6	The response matrix of the xenon-gas Proportional Counter Array on <i>RXTE</i>	39
2.7	The probability density function $f_{\chi^2}^\nu$ of the χ^2 -distribution with $\nu = 1, 2, 3$ d. o. f..	41
2.8	The cumulative probability $F_{\chi^2}^\nu$ of the χ^2 -distribution with $\nu = 1, 2, 3$ d. o. f..	41
2.9	χ^2 contours for single parameter confidence levels.	42
3.1	Finding the zero-order position with HEG and MEG arm and readout streak.	45
3.2	Order sorting in a plot of energy vs. position along the MEG-arm.	45
3.3	The main data structures for spectral analysis in ISIS and their interactions.	47
3.4	68.3%, 90% and 99% 2-parameter confidence contours of a Gaussian's σ and E_λ	51
4.1	Detector-image of obs. ID 3814, color-coding the photon energies.	54
4.2	'Sky'-image of obs. ID 3814, color-coding the photon energies.	54
4.3	Default (red) and narrow (blue; excluding most of the halo) extraction regions.	54
4.4	Background count rate (lower panel) for different extraction regions:	54
4.5	Counts in the MEG and HEG spectra (including all events of obs. # 3814).	55
4.6	Light curve in the energy band of 0.5...7.2 keV.	56
4.7	Dips in the light curves of different energy bands and their ratio.	56
4.8	Definition of the 'non-dip' sub-spectra (see text).	57
4.9	RXTE/ASM light curve in 2003. The observation is marked by vertical lines.	58
4.10	The flux-corrected spectra and a photoabsorbed power law model.	59
4.11	As Fig. 4.10, but including the model for pile-up reduction.	59
4.12	Joint fit of the broad band continuum of Cyg X-1 with the 'non-dip' MEG-1	60
4.13	χ^2 -contours for column density and Doppler broadening in the S XVI line series.	81

4.14 Line profiles of the fitted series vs. wavelength in Å.	87
4.15 Definition of the ‘dip’ sub-spectra (see text).	88
4.16 The ‘non-dip’, ‘dip’, ‘dip 1’ and ‘dip 2’ flux-corrected spectra.	89
4.17 Normalized ‘non-dip’-spectrum (data/continuum-ratio) vs. wavelength in Å. .	106
4.18 Normalized ‘dip’-spectrum (data/continuum-ratio) vs. wavelength in Å. . .	107
5.1 ASM light curve of Cyg X-1 with indicators of the <i>Chandra</i> observation times.	109
5.2 Detector image of observation # 2415 (CC mode).	111
5.3 “Sky-image” of observation # 2415 (CC mode).	111
A III.1 Ratio of ‘non-dip 1’ and ‘non-dip’ flux-spectrum.	127
A III.2 Ratio of ‘non-dip 3’ and ‘non-dip’ flux-spectrum.	127
A III.3 Ratio of ‘dip 1’ and ‘dip’ flux-spectrum.	128
A III.4 Ratio of ‘dip 2’ and ‘dip’ flux-spectrum.	128
A III.5 Ratio of ‘dip 3’ and ‘dip’ flux-spectrum.	128
A III.6 The fitted ‘non-dip’ Cyg X-1 spectrum, including all lines.	144
A III.7 The ‘non-dip’ spectrum: Γ -dependence for both models’ fit parameteres . .	145
A III.8 The ‘non-dip’ spectrum: λ_2 -dependence of the 1-comp. model’s fit parameters.	146
A III.9 The ‘non-dip’ spectrum: λ_2 -dependence of the 2-comp. model’s fit parameters.	146
A III.10 The ‘dip’ spectrum: Γ -dependence of the 1-comp. model’s fit parameters .	147
A III.11 The ‘dip’ spectrum: Γ -dependence of the 2-comp. model’s fit parameters .	147
A III.12 The ‘dip’ spectrum: λ_2 -dependence of the 1-comp. model’s fit parameters.	148
A III.13 The ‘dip’ spectrum: λ_2 -dependence of the 2-comp. model’s fit parameters.	148
A III.14 The ‘dip 1’ spectrum: Γ -dependence of the 1-comp. model’s fit parameters	149
A III.15 The ‘dip 1’ spectrum: Γ -dependence of the 2-comp. model’s fit parameters	149
A III.16 The ‘dip 1’ spectrum: λ_2 -dependence of the 1-comp. model’s fit parameters.	150
A III.17 The ‘dip 1’ spectrum: λ_2 -dependence of the 2-comp. model’s fit parameters.	150
A III.18 The ‘dip 1’ spectrum: λ_2 -dependence of the 1-comp. model’s fit parameters.	151
A III.19 The ‘dip 1’ spectrum: λ_2 -dependence of the 2-comp. model’s fit parameters.	151
A III.20 The ‘dip 2’ spectrum: Γ -dependence of the 1-comp. model’s fit parameters	152
A III.21 The ‘dip 2’ spectrum: Γ -dependence of the 2-comp. model’s fit parameters	152
A III.22 The ‘dip 2’ spectrum: λ_2 -dependence of the 1-comp. model’s fit parameters.	153
A III.23 The ‘dip 2’ spectrum: λ_2 -dependence of the 2-comp. model’s fit parameters.	153
A III.24 The ‘dip 2’ spectrum: λ_2 -dependence of the 1-comp. model’s fit parameters.	154
A III.25 The ‘dip 2’ spectrum: λ_2 -dependence of the 2-comp. model’s fit parameters.	154
A III.26 The fitted ‘dip’ spectrum, including all lines	166

List of Tables

1.1	Parameters of stellar atmosphere and wind of HDE 226868 (Herrero et al., 1995)	15
1.2	Orbital elements of the binary HDE 226868 / Cyg X-1 (Gies & Bolton, 1982)	15
1.3	Recent ephemeris for HDE 226868 / Cyg X-1	15
2.1	Explicit functions of $F_{\chi^2}^\nu(\chi^2)$ and confidence-level defining values of $\Delta(\chi^2)$	42
4.1	Time of observation # 3814 in various formats	53
4.2	Events in the different orders of the spectra	55
4.3	Parameters of the ISIS model 4.3 describing the continuum in the ‘non-dip’ spectrum	60
4.4	List of lines in the ‘non-dip’ spectrum – sorted by χ^2 improvement (see text)	61
4.5	$\lambda/\text{\AA}$ of H-like ions’ absorption lines (as in Table A I.2) in the ‘non-dip’ spectrum	63
4.6	$\lambda/\text{\AA}$ of He-like ions’ triplets (as in Table A I.4) in the ‘non-dip’ spectrum:	63
4.7	$\lambda/\text{\AA}$ of He-like ions’ absorption lines (as in Table A I.5) in the ‘non-dip’ spectrum	63
4.8	$\lambda/\text{\AA}$ of Li-like ions’ absorption lines (as in Table A I.6) in the ‘non-dip’ spectrum	63
4.9	Further iron lines	65
4.10	List of lines in the ‘non-dip’ spectrum – sorted by ion	73
4.11	Fitresults for line series in the ‘non-dip’ spectrum	84
4.12	Detected column densities from the (neutral) absorption	84
4.13	fitted Γ for the one-component model 4.3 of the ‘non-dip’ spectrum	90
4.14	fitted Γ for the two-component model 4.6 of the ‘non-dip’ spectrum	91
4.15	fitted Γ for the one-component model 4.3 of the ‘dip’ spectrum	92
4.16	fitted Γ for the two-component model 4.6 of the ‘dip’ spectrum	92
4.17	fitted Γ for the one-component model 4.3 of the ‘dip 1’ spectrum	93
4.18	fitted Γ for the two-component model 4.3 of the ‘dip 1’ spectrum	93
4.19	fitted Γ for the one-component model 4.3 of the ‘dip 2’ spectrum	93
4.20	fitted Γ for the two-component model 4.6 of the ‘dip 2’ spectrum	93
4.21	Best fit parameters for the one / two absorbing component power law model.	94
4.22	List of lines in the ‘dip’ spectrum – sorted by χ^2 improvement (see Table 4.4)	95
4.23	$\lambda/\text{\AA}$ of H-like ions’ absorption lines (as in Table A I.2) in the ‘dip’ spectrum .	95
4.24	$\lambda/\text{\AA}$ of He-like ions’ triplets (as in Table A I.4) in the ‘dip’ spectrum:	96
4.25	$\lambda/\text{\AA}$ of He-like ions’ absorption lines (as in Table A I.5) in the ‘dip’ spectrum	96
4.26	$\lambda/\text{\AA}$ of Li-like ions’ absorption lines (as in Table A I.6) in the ‘dip’ spectrum .	96
4.27	Further iron lines	97
4.28	List of lines in the ‘dip’ spectrum – sorted by ion	103
5.1	<i>Chandra</i> observations of Cyg X-1 (all with the HETGS)	109
A I.1	Neutral K- and L-edge energies and relative abundances A_Z^{ISM}	117
A I.2	Wavelengths [in \AA] of H-like ions’ transitions from the ground state $1s$ (${}^2S_{1/2}$)	118
A I.3	Wavelengths [in \AA] of H-like ions’ transitions from the first excited state ($n = 2$)	118
A I.4	Wavelengths [in \AA] of He-like ions’ triplet transitions (from the $1s^2$ (1S_0) state)	118
A I.5	Wavelengths [in \AA] of He-like ions’ transitions from the $1s^2$ (1S_0) ground state	118
A I.6	Wavelengths [in \AA] of Li-like ions’ transitions from the ground state [$1s^2$] $2s$ (${}^2S_{1/2}$)	119
A I.7	Quantum states assigned to the first 25 level numbers in the ATOMDB	119
A I.8	Further iron lines	122
A II.1	Contents of a level 1-event file	122
A II.2	Contents of a aspect/PCAD file	123
A II.3	Contents of a parameter block file	123
A II.4	Contents of a bias file	123
A II.5	Contents of a filter file	123
A II.6	Contents of a mask file	123
A II.7	Contents of a bad pixel file	124

A II.8	Contents of a level 1.5-event file	124
A II.9	Contents of a light curve file	124
A II.10	Contents of a spectra (pha2) file	125
A II.11	Contents of a background (bkg2) file	125
A II.12	Contents of a grating redistribution matrix function (gRMF) file	125
A II.13	Contents of a grating ancillary response function (gARF) file	125
A III.1	List of lines in the ‘non-dip’ spectrum – sorted by wavelength	129
A III.2	List of lines in the ‘dip’ spectrum – sorted by wavelength	155

DECLARATION

Hereby I declare that I wrote this diploma thesis autonomously and that I have not used other resources than those quoted in this work.

ERKLÄRUNG

Hiermit erkläre ich, dass ich die Diplomarbeit selbstständig angefertigt und keine Hilfsmittel außer den in der Arbeit angegebenen benutzt habe.

Bamberg/Madrid, July 2007

(Manfred Hanke)

The references can be found at the end of the main part (before the appendix), on page 114.

Indeed, that's all.
Thanks for reading so far!

| Mh